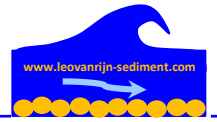




LONGMOR; LONGSHORE MODELLING AND APPLICATIONS

- 1. Introduction**
- 2. Description of LONGMOR-model**
 - 2.1 Basic equations**
 - 2.2 Numerical scheme**
 - 2.3 Sensitivity runs**
- 3. Application cases**
 - 3.1 Coastline changes south of IJmuiden, North-Holland, The Netherlands**
 - 3.2 Coastline changes at mega-nourishment of Sand-motor, South-Holland, The Netherlands**
 - 3.3 Coastline changes west of jetties of Port of Lagos, Nigeria**
 - 3.4 Coastline changes east of jetties of Port of Lagos in Nigeria**
 - 3.5 Detached breakwater at 450 m from the coast in Congo**
 - 3.6 Design of long groyne near Soulac sur Mer, France**
 - 3.7 Design Abu Qir western bay type beach**
- 4. References**



1. Introduction

This document describes various applications of the LONGMOR-model, which can be used to compute the coastline changes as function of time.

The LONGMOR-model is a numerical model (FORTRAN-code) which can compute the following parameters: water depth at the breaker line; wave height and wave incidence angle at the breaker line, sand transport in the breaker zone and corresponding coastline changes over time due to alongshore gradients of the sand transport rate in the breaker zone.

Typical problems that can be solved using the LONGMOR-model are:

1. accretion updrift of structure;
2. erosion down drift of structure;
3. accretion and erosion of mega-nourishment along beaches;
4. erosion of coastal extensions.

How to run LONGMOR-model

The LONGMOR-model can be run quite simply:

1. click on the Longmor2013-intel.exe file or longmor2025.exe; this opens the prompt-command line
2. type the name of the input file: name.inp, enter (latest input file 2025: AATEST1.inp)
3. the model runs and produce an output file: name.out; this file can be imported in EXCEL for plotting
4. if the model does run, see diagnose-file; this gives information where an input mistake is made (usually the table length does match the number data specified; if 8 wave data rows are specified then the table number is nt=8).
5. comments can be given to the right of *; enter new line, type *; old input data can be stored in input file by placing * before each data row; old input data is then always available.



Copy of input file (latest file: AATEST1.inp; LONGMOR2025), see below

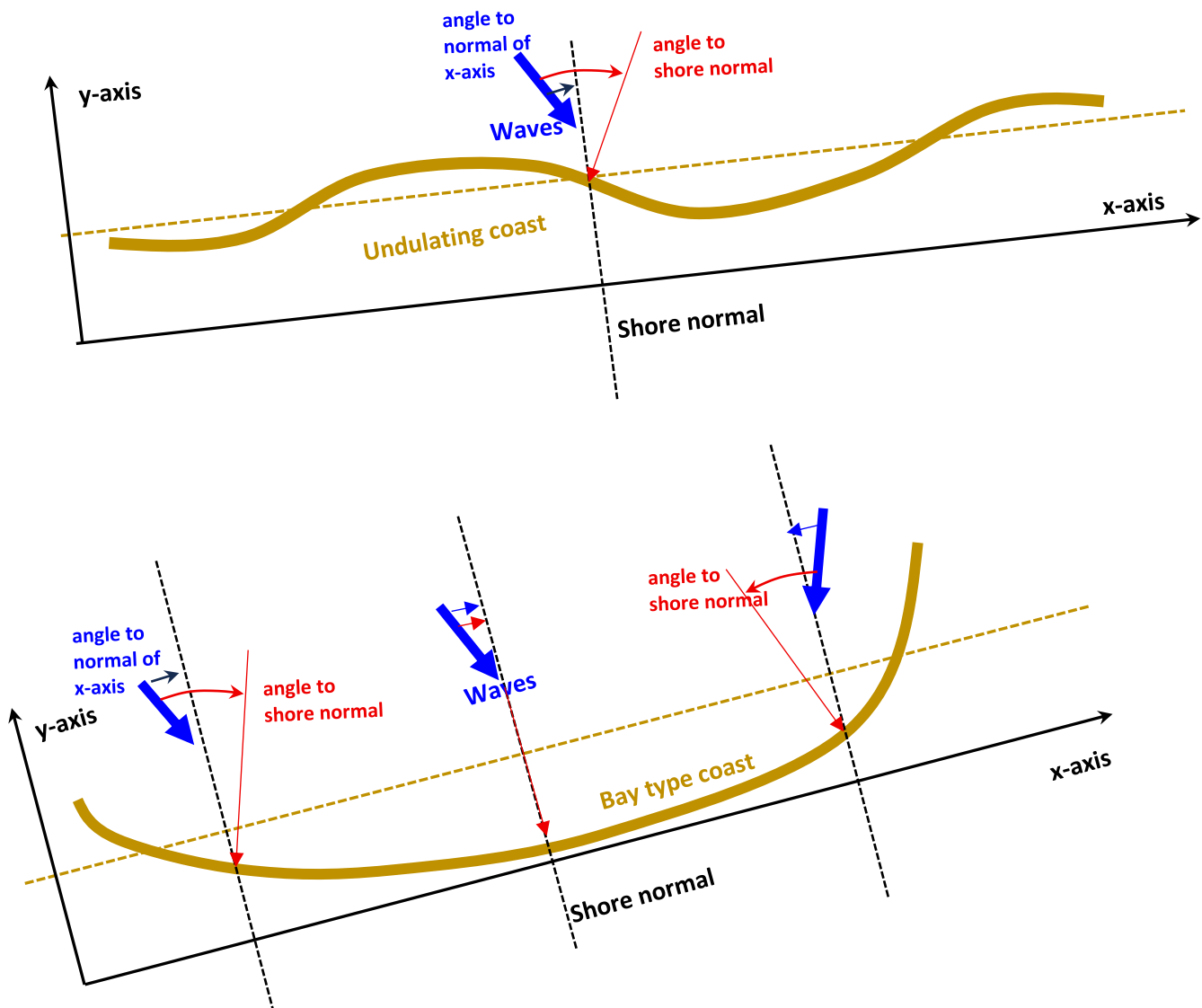
The input file the wave incidence angle defined to the **coast normal of the x-axis**.

The wave incidence angle to the **local shore normal** is computed by the model

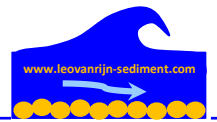
The model is mostly valid for an approximately straight coast.

In the case of an undulating coast or a bay type coast, the x-axis should be aligned as much as possible along the smoothed coastline or the coastline far away from the problem area (see Section 3.7).

The x-axis should be landward of the coast. The positive y-axis should be from the land to the sea.



Input file



```

* nx number of points of initial shoreline profile
15
* initial profile, number= nx
* (donot use two subsequent ys-values of 0.; use very small difference)
* x ys
0. 0.
160. 105.
335. 145.
475. 210.
565. 305.
680. 390.
830. 420.
935. 435.
1040. 435.
1195. 420.
1330. 370.
1500. 280.
1620. 210.
1725. 115.
1825. 0.
*
* hw, Ho,T, TETA are specified in mininum 2 and maximum 6 locations (nxp) along the shore
* hw=depth to MSL where Ho is defined (m)
* Ho=offshore wave height (m)
* T=wave period (s)
* Teta0=wave angle to x-axis
* nxp=number of x-positions where the wave parameters hw,Ho,T,Tetao
* are specified, minimum 2, maximum 6; if nxp=2 always at x=0 and
* ntt= number of time moments at which wave parameters are speciedied
* nxp (min 2, max 6) ntt (max 6)
6 3
* nxp x-positions
50. 475. 830. 1040. 1500. 1725.
*
* hw-parameter at ntt times
* t hw1, hw2, hw3, hw4, hw5, hw6
0. 6. 6. 6. 6. 6. 5.
100. 6. 6. 6. 6. 6. 5.
365. 6. 6. 6. 6. 6. 5.
* Wave height parameter at depth hw at ntt times
* t Ho1 Ho2 Ho3 Ho4 Ho5 Ho6
0. 0.5 0.6 0.6 0.6 0.6 0.5
100. 0.5 0.6 0.6 0.6 0.6 0.5
365. 0.5 0.6 0.6 0.6 0.6 0.5
* Wave period T parameter at depth hw at ntt times
* t T1 T2 T3 T4 T5 T6
0. 6. 6. 6. 6. 6. 6.
100. 6. 6. 6. 6. 6. 6.
365. 6. 6. 6. 6. 6. 6.
* Wave angle Tetao at depth hw to x-axis at ntt times
* t teta1 teta2 teta3 teta4 teta5 teta6
0. 10. -25. -25. -30. -65. -90.
100. 10. -25. -25. -30. -65. -90.
365. 10. -25. -25. -30. -65. -90.
*
* nt number of timetable values for correction coefficients ri
* nxr number x-values at which ri is defined
* nt nxr
2 8
* Correctioncoefficient r function of x,t
* (linear interpolation of ri between xi values and ti values)
* x1 x2 x3 x4 x5 x6 x7 x8
0. 150. 475. 830. 1040. 1500. 1725 1825.
* t(days)r1 r2 r3 r4 r5 r6 r7 r8
0. 0. -0.3 0.5 0.75 1. 1.0 1.0 0.7
365. 0. -0.3 0.5 0.75 1. 1.0 1.0 0.7
*
* sourceterm table nq values f(x,t)
* ntq number of time values of timetable sourceterms qcr (in m3/m/day; range of 0.1 to 0.5)of dredging or nourishment
* (linear interpolation of qcr between xi and ti values)
* nxq number of x-values at which qcr is defined
* ntq nxq
2 10
* x1 x2 x3 x4 x5 etc.
0. 300. 400. 500. 600. 700. 800. 900. 950. 2000.
* t qcr1 qcr2 qcr3 etc.
0. 0. 0. 0. 0. 0. 0. 0. 0. 0.
3600. 0. 0. 0. 0. 0. 0. 0. 0. 0.

```

2. Description of LONGMOR-model



2.1 Basic equations

2.1.1 Coastline changes

The LONGMOR1D-model (Van Rijn, 1998, 2002, 2005) is a coastline model based on the sediment balance equation for the littoral zone (roughly the surf zone) with alongshore length Δx , cross-shore length Δy_s and vertical layer thickness (h). The model computes coastline changes if the longshore transport rates are known.

Basically, the accretional and erosional processes along the coastline are the result of differences in onshore/offshore transport and gradients of longshore sand transport, induced by:

- changes of shoreline orientation (gradual or abrupt due to presence of bays and head-lands);
- changes of shoreface topography (local steep slopes, hollows, scarps, canyons);
- changes of wave-current conditions and mean sea level conditions;
- changes of sediment supply (sources like cliff erosion).

Coastline changes can be simply understood by considering the sediment continuity equation for the littoral zone (roughly the surf zone) with alongshore length Δx , cross-shore length Δy and vertical layer thickness (h), see **Figure 2.1.1**.

The sand volume balance reads:

$$h (\Delta y_s / \Delta t) + \Delta Q_{Ls} / \Delta x - q_s = 0 \quad (2.1)$$

with:

y = cross-shore coordinate, x = longshore coordinate,

y_s = shoreline position,

h = thickness of active littoral zone layer,

Q_{Ls} = longshore transport rate or littoral drift (bed-load plus suspended load transport in volume including pores per unit time, in m^3/s) and,

q_s = source, sink or cross-shore transport contribution (in m^2/s).

Basically, Equation (2.1) states that a coastal section erodes if more sand is carried away than supplied; vice versa coastal accretion occurs if there is a net supply. Coastline changes are linearly related to the assumed depth (h) of the active zone.

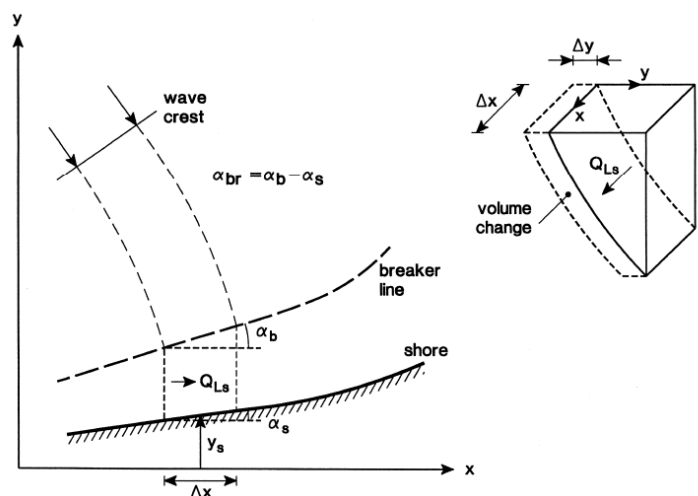
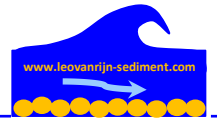


Figure 2.1.1 Definition sketch of shoreline configuration and sand balance volume

2.1.2 Longshore sediment transport



Most available LST-equations are valid for sandy beaches, mainly because only field data sets of sandy beaches have been used for calibration. Generally, the LST in the swash zone above the still water level is not included in the LST-equation for sandy beaches because it is a relatively small contribution compared to the LST in the wider sandy surf zone. At steep sloped gravel/shingle beaches which are mostly situated landward of the -3 m depth line (the seabed seaward of the -3 m line is mostly sand), the energy dissipation through wave breaking is concentrated over a much narrower zone than on a sand beach. Mostly, a single line of plunging breaking waves can be seen, even during storm events. The swash zone is mostly of similar width as the surf zone. This means that most of the transport of coarse materials occurs in a relatively narrow zone consisting of the inner surf zone and swash uprush zone which may extend up to +5 m during storm events. Another effect at steep beaches of gravel/shingle is that the refraction processes are confined to a narrow zone so that the waves arrive at the beach face with relatively large wave angles (Van Wellen et al., 2000). The swash uprush velocity is often much higher than the backwash due to infiltration processes along the coarse-grained beach.

LST in surf zone

Three longshore sand transport equations are available for computation of LST in the surf zone seaward of the MSL line.

The longshore sand transport of Van Rijn (2014) for the surf zone is described by:

$$Q_{LS} = 0.00018 p_s K_{surf} K_{swell} (1-\varepsilon)^{-1} g^{0.5} (\tan\beta_{surf})^{0.4} (d_{50})^{-0.6} (H_{s,br})^{3.1} \sin(2\alpha_{br}) \quad (2.2)$$

- Q_{LS} = total longshore sediment transport (in m³/s, incl. pores),
- ε = porosity (≈ 0.4), ρ_s = sediment density (kg/m³),
- d_{50} = median grain size (m),
- p_s = fraction of sediment in surf zone ($p_s=1$ for sand; $p_s=0-1$ for mixed beds of sand gravel/pebbles);
- $H_{s,br}$ = significant wave height at breaker line (m),
- θ_{br} = wave angle at breaker line,
- g = acceleration of gravity (m/s²),
- $\tan\beta_{surf}$ = slope in surf zone,
- K_{swell} = swell factor (see Equation 5),
- K = calibration factor (default=1).

Equation (2.2) can also be expressed, as:

$$Q_{LS} = 0.0006 p_s K_{surf} K_{swell} (1-\varepsilon)^{-1} (\tan\beta_{surf})^{0.4} (d_{50})^{-0.6} (H_{s,br})^{2.6} V_{eff,L} \quad (2.3)$$

$$V_{wave} = 0.3 (gH_{s,br})^{0.5} \sin(2\alpha_{br}) \quad (2.4)$$

with:

- $V_{eff,L} = [(V_{wave,L})^2 + (V_{tide,L})^2]^{0.5}$ = effective longshore velocity at mid surf zone (m/s) for tidal velocity and wave induced velocity in same direction (minus sign for opposing conditions);
- $V_{wave,L}$ = wave-induced longshore current velocity (m/s) averaged over the cross-section of the surf zone.
- $V_{tide,L}$ = longshore velocity in mid surf zone due to tidal forcing (=0 m/s for non-tidal cases; 0.1 m/s for micro-tidal, 0.3 m/s for meso-tidal and 0.5 m/s for macro-tidal cases).

Equation (2.1) does not account for the effect of the wave period on the longshore transport rate. However, low-period swell waves in the range of 1 to 2 m produce significantly larger transport rates compared to wind waves



of the same height ($H_{rms}=H$). This effect can to some extent be taken into account by using a correction factor to the longshore transport rate, if the percentage of swell waves (in terms of wave height) of the total wave height record is known.

Herein, it is proposed to use a swell factor, as follows:

$$K_{swell}=1.5(p_{swell}/100) + 1 (1-p_{swell}/100) = 0.015p_{swell} + (1-0.01p_{swell}) \quad (2.5)$$

with: p_{swell} = percentage of low-period swell wave heights of the total wave height record (about 10% to 20% for sea coasts and 20% to 30% for ocean coasts).

Some values are: $K_{swell}=1.05$ for $p_{swell}=10\%$; $K_{swell}=1.1$ for $p_{swell}=20\%$ and $K_{swell}=1.5$ for $p_{swell}=100\%$.

If swell is absent (or unknown), then $K_{swell}= 1$.

Using this approach, the longshore transport rate increases slightly with increasing percentage of swell. The swell factor is based on computations with grain sizes in the range of 0.2 to 50 mm.

The Kamphuis (1991) method is given by:

$$Q_{LS}=2.33 p_s K_{surf} [\rho_s/(\rho_s-\rho)] [(1-\varepsilon)\rho_s]^{-1} (T_p)^{1.5} (\tan\beta_{surf})^{0.75} (d_{50})^{-0.25} (H_{s,br})^2 [\sin(2\alpha_{br})]^{0.6} \quad (2.6)$$

with: Q_{LS} = longshore sediment (m^3/s , incl pores); $H_{s,br}$ =significant wave height at breaker line (m);

α_{br} =wave angle at breaker line ($^\circ$); d_{50} =median particle size in surf zone (m); $\tan \beta_{surf}$ =slope in surf zone; T_p = peak wave period; K_{surf} = calibration factor (default=1).

The longshore sand transport (Q_{LS}) of CERC (Shore Protection Manual 1984; Van Rijn, 1993):

$$Q_{LS}= 0.023 p_s K_{surf} g^{0.5} \gamma^{-0.5} (H_{s,br})^{2.5} \sin(2\alpha_{br}) \quad (2.7)$$

with: γ = breaker coefficient, H_{br} = significant wave height at breaker line and α_{br} = angle between breaker line and local shoreline; K_{surf} = calibration factor (default=1).

The longshore sand transport rate in the surf zone is defined in terms of parameters defined at the breaker line. Thus, the offshore wave climate has to be converted to a wave climate at the breaker line. **(The wave climate should be determined from measured or modeled data as close as possible to the shore!)**

Waves arriving from deeper water are transformed in shallow water according to the laws of energy flux conservation and refraction (Law of Snell) for gradually varying bathymetry, yielding (Van Rijn 2011);

$$\sin\alpha_{br}=(L_{br}/L_o) \sin\alpha_o \quad (2.8)$$

$$H_{br}= K_{r,br} K_{s,br} H_o \quad (2.9)$$

with $K_{r,br}$ = refraction coefficient at breaker line and $K_{s,br}$ = shoaling coefficient at breaker line.

The wave length is computed as: $L=L_o[1-\exp(-\alpha)]^{0.4}$ with $L_o=1.56T^2$ =wave length in deep water and $\alpha=[2\pi h/L_o]^{1.25}$.

For gradually varying bathymetry these values are:

$$K_{r,br}=(\cos\alpha_o/\cos\alpha_{br})^{0.5} \text{ and } K_{s,br}=(n_o c_o/n_{br} c_{br})^{0.5} \quad (2.10)$$

with c = wave propagation velocity, n = coefficient, α = wave angle, index br= at breaker line and index o= at deep water.



The wave height at the breaker line $H_{br} = \gamma h_{br}$ can be computed if the breaker depth h_{br} and the breaker coefficient γ (0.6-0.8) are known. Generally, this procedure requires iterative computations.

The breaker depth is given by (Van Rijn 2011, 2014):

$$h_{br} = ((H_{s,o}^2 c_o \cos \alpha_o) / (1.8 \gamma^2 g^{0.5}))^{0.4} \quad \text{and } H_{s,br} = \gamma_{br} h_{br} \quad \text{if } h_{br} < h_s \quad (2.11a)$$

$$h_{br} = h_s \quad \text{and } H_{s,br} = \gamma_{br} h_s \quad \text{if } h_{br} > h_s \quad (2.11b)$$

with:

$$c_o = L_o / T_p;$$

h_s = water depth defined at the location between surf zone with breaking waves and outer zone with non-breaking waves; h_s can be set to a large value (10 m) for sandy beaches; $h_s = h_{coarse}$ = separation depth (range of 1 to 3 m) between the sand bed and the coarse bed for coarse grained beaches, see **Figure 2.1.2**.

Equation (2.11b) means continuous breaking in the surf zone between h_{br} and MSL.

Mostly, the bed slope in the surf zone with a milder slope is smaller than in the swash zone.

The wave breaking coefficient in the surf zone with a milder slope ($\tan \beta_{surf}$) is in the range of $\gamma_{br} = 0.6-0.8$ for $h_s \approx 3$ m (spilling breaking waves).

The wave breaking coefficient in the swash zone with a steeper slope ($\tan \beta_{swash}$) is in the range of $\gamma_{br} = 0.8-1$ for $h_s = 1$ m (plunging breaking waves).

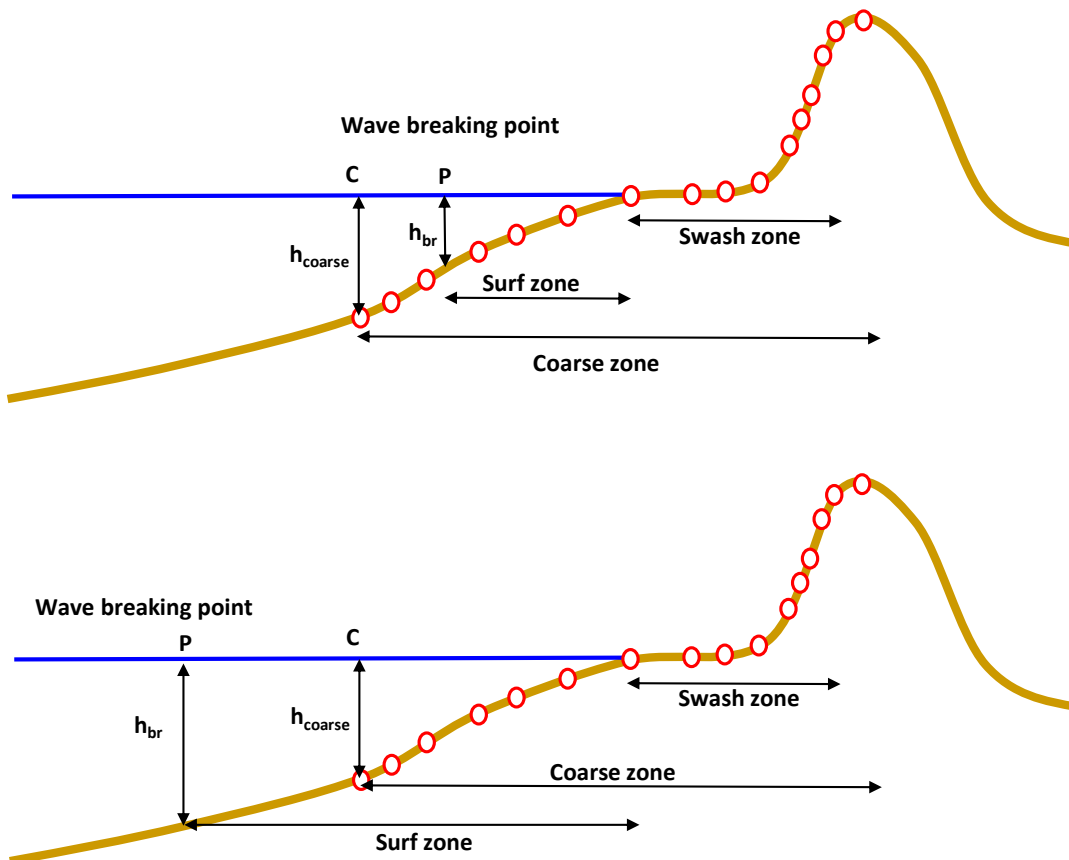


Figure 2.1.2 Definition sketch of swash, surf and coarse zone for coarse-grained beach



Effect of high wave angles to shore normal

The longshore transport rate along a specific coastal section depends on the angle α_o between the shoreline and the deep-water wave direction. If the shoreline orientation varies and the wave direction is constant, the longshore transport rate can be expressed as a function of α_o . This curve (including refraction and shoaling effects) is shown for a specific case in **Figure 2.1.3**. The transport rate is maximum for a shoreline orientation of about $\alpha_o = 40^\circ$ to 45° (depending on refraction effects) and zero for angles of 0° (wave crests parallel to coast) and 90° (wave crests normal to coasts). The longshore transport will be in opposite direction (negative Q_{LS}) for $\alpha_o < 0^\circ$. The longshore transport can also be expressed as a function of the shoreline angle α_s ($\alpha_s = \alpha_n - \alpha_o$, $\alpha_n =$ constant if wave direction is constant and shoreline is varying) with respect to the x-axis. In the case of a wave climate with various wave classes, directions and probabilities of occurrence the net longshore transport rate can be expressed as a function of shoreline orientation.

Equation (1) is valid for wave-induced longshore transport in the absence of tide- or wind- driven currents. The effect of quasi-steady currents superimposed on the wave-induced longshore current will result in a vertical shift of the transport curve in **Figure 2.1.3**.

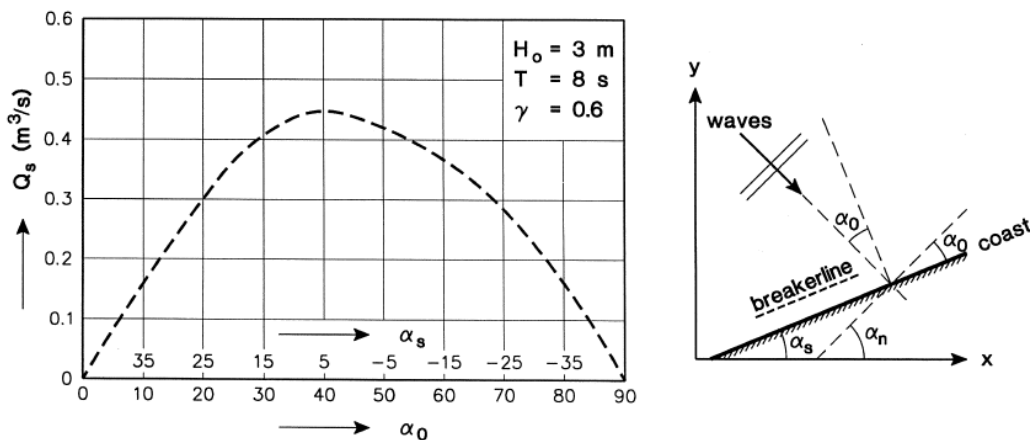


Figure 2.1.3 Longshore transport rate as a function of shoreline orientation
(α_o = angle between deep-water wave direction and shoreline)
(α_s = angle between shoreline and x-axis)

Effect of long submerged breakwater

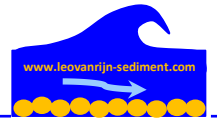
When a submerged/emerged breakwater is present in the surf zone (input parameters are water depth to MSL at toe of structure, water depth to MSL above the crest of the structure, distance of structure to coastline), two cases can be distinguished:

- low waves which break at the structure and the transmitted wave breaks landward of the structure; LST only in the surf zone landward of the structure;
- high waves, which break seaward of the submerged breakwater and transmitted wave breaks landward of the structure; LST in the surf zone seaward of the structure and also in the surf zone landward of the structure.

Case A

- wave length, wave speed and wave angle are computed at the seaward toe of the structure;
- the shoaling and refraction coefficients are computed at the seaward toe of the structure;
- the wave height at the seaward toe ($H_{s,toe}$) of the structure is computed;
- the wave transmission coefficient is computed (Figure 2.1):

$$R_c/H_{s,toe} < -3 \quad \text{then } K_T = 1 \text{ (no structure),}$$



$$-3 < R_c/H_{s,toe} < -1 \quad \text{then } K_T = -\max[1, -0.1(R_c/H_{s,toe}) + 0.7],$$

$$-1 < R_c/H_{s,toe} > 1 \quad \text{then } K_T = \min[1, -0.35(R_c/H_{s,toe}) + 0.45];$$

- the transmitted wave height is computed ($H_{s,transmitted} = K_T H_{s,toe}$);
- the water depth and the wave height at the breaker line in the lee of the structure are computed;
- the wave length, the wave angle at the breaker line in the lee of the structure are computed;
- the LST_{lee} landward of the breaker line in the lee of the structure is computed.

Case B

- compute LST assuming that no structure is present: LST_{ns} ;
- compute length of surf zone to water line assuming no structure: $L_{surfzone\ ns} = h_{br} / \tan \beta_{surf}$ with h_{br} = water depth at breaker line;
- compute LST in surf zone seaward of structure: $LST_{seaward} = (L_{sc} / L_{surfzone\ ns}) LST_{ns}$ with L_{sc} = distance of structure to water line (input);
- compute LST_{lee} in lee of surf zone as in Case A;
- compute total $LST_{total} = LST_{seaward} + LST_{lee}$.

The alongshore sand transport (LST) is substantially reduced when a submerged breakwater is present.

Figure 2.1.4 shows the effect of a submerged breakwater at depth of 7 m on the annual LST in the case of a severe wave climate (exposed coast with $H_{s,o}$ between 1 and 6 m). The crest level is varied between -7 m (below the water surface) and +1 m (above the surface). The ratio of the LST with and without a submerged breakwater is plotted as function of the ratio of the water depth above the crest of the structure and the water depth without the structure. The LST is reduced to 25% of the original value (without structure) for a submerged crest level at -0.7 m (relative $0.7/7=0.1$, on horizontal axis). The LST is minor when the crest of the breakwater is above the water surface (emerged structure). Thus, the crest of the submerged breakwater should be as high as possible to reduce the longshore sand transport at the beach as much as possible.

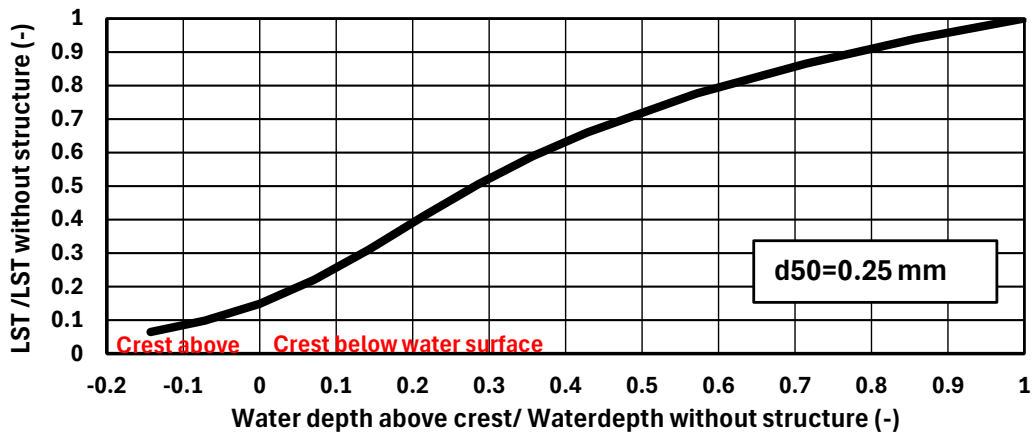


Figure 27 Relative LST as function of relative water depth above crest (depth at structure=7 m)

LST in swash zone

The LST-equation of Van Rijn has been extended to include the LST in the swash zone landward of the water line. The swash zone is a zone with intermittent (bed load type) transport of coarse sediments as result of the normal or oblique wave-induced uprush and downwash of water depending on the height and direction of the incident waves. Coarse particles are carried as bed load transport upward and downward in a zig-zag type of movement



along the beach face. This gives a parabolic type of distribution across the swash zone from a maximum value at the toe of the swash zone and an approximately zero value at the uprush point.

The model has been calibrated using field data (gravel/shingle of 12 mm) from 1) Pevensey Beach, UK; 2) Shoreham Beach, UK and 3) pebble nourishment Magdalen Island Beach, St Lawrence Bay, Canada..

The model input is time series (1 to 3 hours) of H_s , T_p and direction to north and tidal water level to mean sea level at some depth offshore or nearshore (-6 m depth line). This can be output of a wave model (SWAN or other). This file can be copied into the LST-excel model.

The swash zone is a zone with intermittent transport of coarse sediments as a result of the normal or oblique wave-induced uprush and downwash of water depending on the height and direction of the incident waves.

The LST in the (thin) swash zone is assumed to consist of bed load transport with a parabolic type of distribution across the swash zone from a maximum value at the toe of the swash zone and a zero value at the uprush point.

The mean thickness of the (thin) swash layer is set to $h_{swash}=3d_{50}$.

Using this approach, the LST (m^3/s) in the swash zone is given by:

$$Q_{b,swash} = 0.7 K_{swash} L_{swash} q_{b,swash,toe} \sin(2\alpha_{br}) \quad (2.12a)$$

$$L_{swash} = [R_s^2 + (R_s / \tan \beta_{swash})^2]^{0.5} \quad (2.12b)$$

$$R_s = 0.4 \tanh(4.3 \zeta_o) H_{s,o} \quad \text{for } \zeta_o < 0.5 \quad (2.12c)$$

$$R_s = 0.6 (\zeta_o)^{0.4} H_{s,o} \quad \text{for } \zeta_o \geq 0.5 \quad (2.12d)$$

$$\zeta_o = \tan \beta_{swash} (H_{s,o} / L_{s,o})^{-0.5} \quad (2.12e)$$

with: L_{swash} =length of swash along the beach (m); R_s =runup level (m) exceeded by 33% of the waves above still water level (Van Rijn et al., 2025); ζ_o =surf similarity parameter (-); $H_{s,o}$ =significant wave height at deep water (m); $L_{s,o}$ =significant wave length at deep water (m); $q_{b,swash,toe}$ =volumetric bed load transport vector of coarse materials at still water level (m^2/s); α_{br} = angle at wave breaker line ($^\circ$); β_{swash} =slope angle of beach-swash zone($^\circ$); K_{swash} =calibration coefficient (default=1; range 0.5-1.5).

The bed load transport equation of Van Rijn (2007a) is used which reads as:

$$q_{b,swash,toe} = 0.015 \alpha_b v_{swash} h_{swash} (d_{50}/h_{swash})^{1.2} (M_e)^{1.5} \quad (2.13a)$$

Using: $h_{swash}=3 d_{50}$, it follows that:

$$q_{b,swash,toe} = 0.012 \alpha_b v_{swash} d_{50} (M_e)^{1.5} \quad (2.13b)$$

$$v_{swash} = \alpha_{sw} 1.25 [\tan(\beta_{swash}) g H_{s,br}]^{0.5} \quad (2.13c)$$

$$M_e = (v_{swash} - v_{cr}) / ((s-1) g d_{50})^{0.5} \quad (2.13d)$$

with: v_{swash} =effective swash velocity vector at still water level (m/s); α_{sw} =correction coefficient (default 1); v_{cr} =critical swash velocity (m/s) at initiation of motion (input parameter: $v_{cr}=0.95$ m/s for $d_{50}=0.01$ m; $v_{cr}=1.15$ m/s for $d_{50}=0.02$ m; $v_{cr}=1.25$ m/s for $d_{50}=0.04$ m); M_e = mobility parameter (-); $s=\rho_s/\rho_w$ = relative density (-); α_b =calibration coefficient bed load transport (default=1). It is noted that oscillatory swash velocity is represented by a continuous effective swash velocity, which is lower than the peak swash velocity of the oscillatory velocity.

The longshore transport of gravel/shingle in the swash zone can also be expressed as:

$$Q_{b,swash,toe} = M_{grains} v_{swash} = N_{grains} M_{1grain} v_{swash} = N_{grains} (\pi/6) (d_{50})^3 \rho_s v_{swash} \quad (2.14a)$$

$$N_{grains} = q_{b,swash,toe} / [(\pi/6) (d_{50})^3 \rho_s v_{swash}] \quad (2.14b)$$

$$P_{grains} = (N_{grains} / N_{grains \text{ per } m^2}) \times 100\% = [q_{b,swash,toe} / \{N_{grains \text{ per } m^2} (\pi/6) (d_{50})^3 \rho_s v_{swash}\}] \times 100\% \quad (2.14c)$$

with: M_{grains} =mass of moving grains (kg); M_{1grain} =mass of 1 grain (kg); N_{grains} =number of moving grains (-); d_{50} =median grain size (m); P_{grains} = percentage of moving grains per m^2 (%); $N_{grains \text{ per } m^2}$ = maximum number of grains in close packing per m^2 ($\cong 10,000$ for $d_{50}=0.01$; 2,500 for $d_{50}=0.02$ m; 625 for $d_{50}=0.04$ m).



Computed LST value based on Equations (2.13) and (2.14) are shown in **Figure 2.1.5**. The grain sizes and critical velocities are $d_{50}=0.01$, $v_{cr}=0.95$ m/s; $d_{50}=0.02$ m, $v_{cr}=1.15$ m/s and $d_{50}=0.04$ m, $v_{cr}=1.25$ m/s. The bed load transport is approximately the same for all three grain sizes with maximum value of about 13 kg/m/s for $v_{swash}=3$ m/s (Van Rijn 2007a). The percentage of moving grains per m^2 is highest (maximum 25% for $v_{swash}=3$ m/s) for $d_{50}=0.01$ m and lowest for $d_{50}=0.04$ m (maximum 7%).

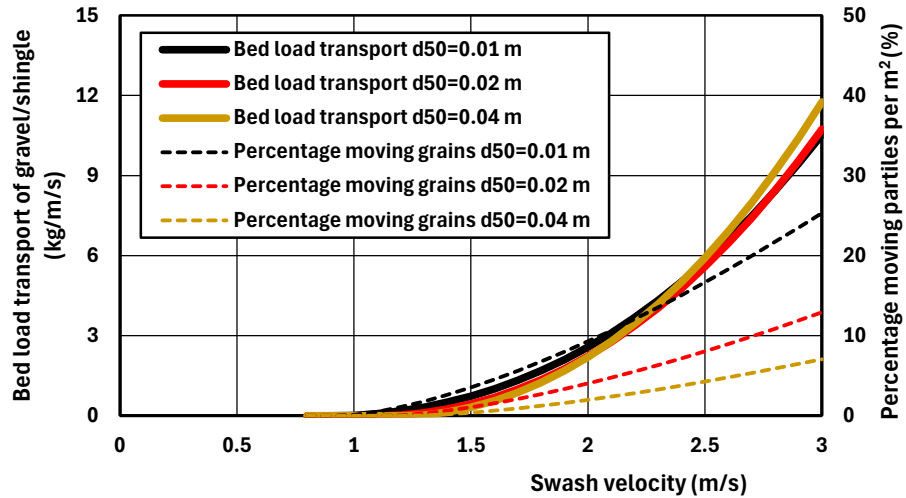


Figure 2.1.5 Bed load transport (left axis) and percentage of moving grains per m^2 (right axis) as function of swash velocity

2.1.3 Model validation for coarse-grained beaches

To justify that the LST-equation of Van Rijn (2014) produces realistic results for steep coarse-grained (gravel/pebble) beaches, the computed LST-values have been compared to measured values for three cases: 1) Pevensey Beach, UK; 2) Shoreham Beach, UK and 3) Magdalen Island Beach, St. Lawrence Bay, Canada.

Pevensey Beach, UK

The measured net LST was derived from beach changes at the terminal groyne at Cooden during storm Ciaran on 2 November 2023. The water level and wave characteristics of storm Ciaran are shown in **Figure 2.1.6**. The most remarkable observations are: i) the wave heights at Hastings buoy and Pevensey buoy are almost the same (3 to 4 m) in the beginning of the storm event (0 to 5 hours), but the value at Hastings buoy in very deep water (43 m) grows further to a maximum value of 5.8 m, while the value at Pevensey buoy remains constant at about 4 m between 5 and 9 hours due to limited depth and the wave height decreases slowly at both locations after 9 hours due to waning of the storm; ii) the maximum wave height at Pevensey is about 40% higher than the significant wave height at Pevensey ($H_{max} \cong 1.4 H_{s,o}$); iii) the total duration of waves > 2 m (> 3 m) is about 30 hours (24 hours) at Pevensey buoy; and iii) the wave direction gradually increases from 180° to 235° (from south to south-west).

Field observations showed an accumulation of sediment on the downdrift side (east) of the terminal groyne (GC32) at Cooden (surveys on 1 November and on 3 November 2023; interval=48 hours). Based on these observations from east of the groyne it was possible to calculate the change in volume for this area resulting in a net accumulation of about $1760 m^3$ over a period of 48 hours between pre- and post surveys, mainly due to longshore transport of shingle. Most likely, this is an under-estimation of the true LST to east, because i) the accumulation of sediment just updrift (west) of the terminal groyne is not taken into account and ii) sediment will have moved beyond the range of the survey east (> 90 m) of the groyne. Therefore, the measured LST



passing the location Cooden is herein assumed to be about $2500 \pm 500 \text{ m}^3$ to east over a period of 48 hours during storm Ciaran.

The LST-model of Van Rijn (2014) is run with the following input data: offshore water depth is 13.5 m to MSL (\cong OD); beach slope of 1 to 10; wave breaking coefficient of 0.6; friction coefficient is 0.85; single diameter is $d_{50}=0.012 \text{ m}$ (12 mm); critical velocity for initiation of motion $v_{cr}=1 \text{ m/s}$; p_{coarse} in surf zone=1; $h_{coarse}=3 \text{ m}$; shore normal angle to north= 350° ; calibration coefficient of LST is $K=1$ (default). The LST-model predicts a value of 2715 m^3 to east for storm Ciaran with peak duration of 48 hours, which is somewhat higher (10%) than the measured value of 2500 m^3 , see Figure 2.1.7. Given all uncertainties involved, the agreement between observed and computed values at the eastern Cooden boundary is quite reasonable.

The computed total LST at location Cooden is 2715 m^3 which consist of $LST_{surf\ zone}=2280 \text{ m}^3$ and $LST_{swash\ zone}=435 \text{ m}^3$. Thus the ratio LST_{swash}/LST_{total} is about 0.2 (20% of total LST). The highest wave event is after 4 hours: $H_{s,o}=4.2 \text{ m}$, $H_{s,br}=3.15 \text{ m}$, $T_p=9.5 \text{ s}$, water level= $+2.8 \text{ m OD}$ resulting in an effective swash velocity of about 2.2 m/s.

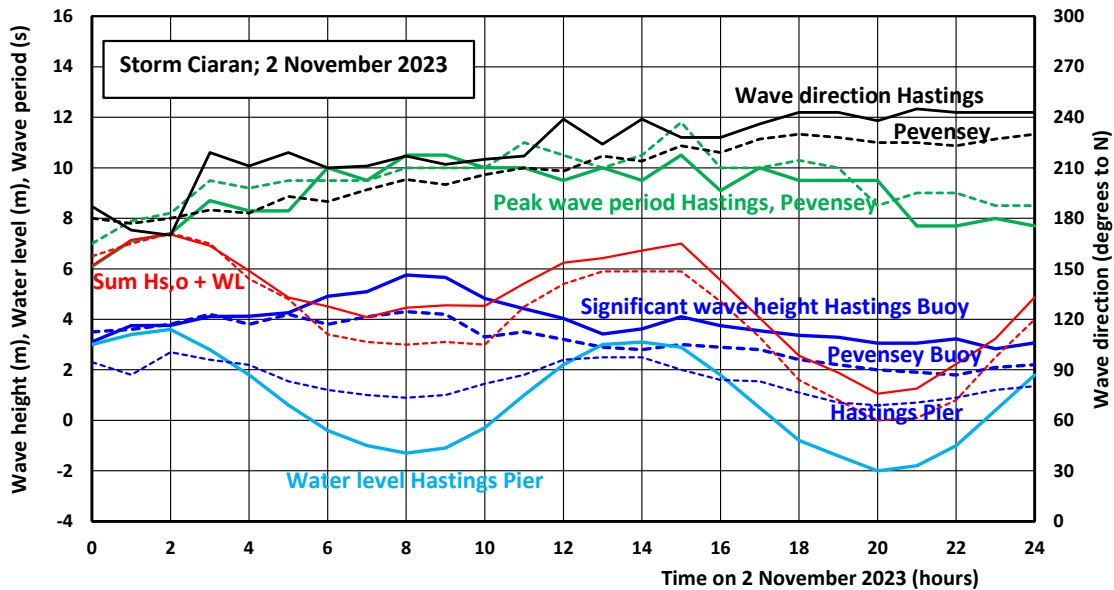


Figure 2.1.6 Wave and water level parameters at Hastings wave buoy, Hastings Pier and Pevensey wave buoy during storm Ciaran on Thursday 2 November 2023

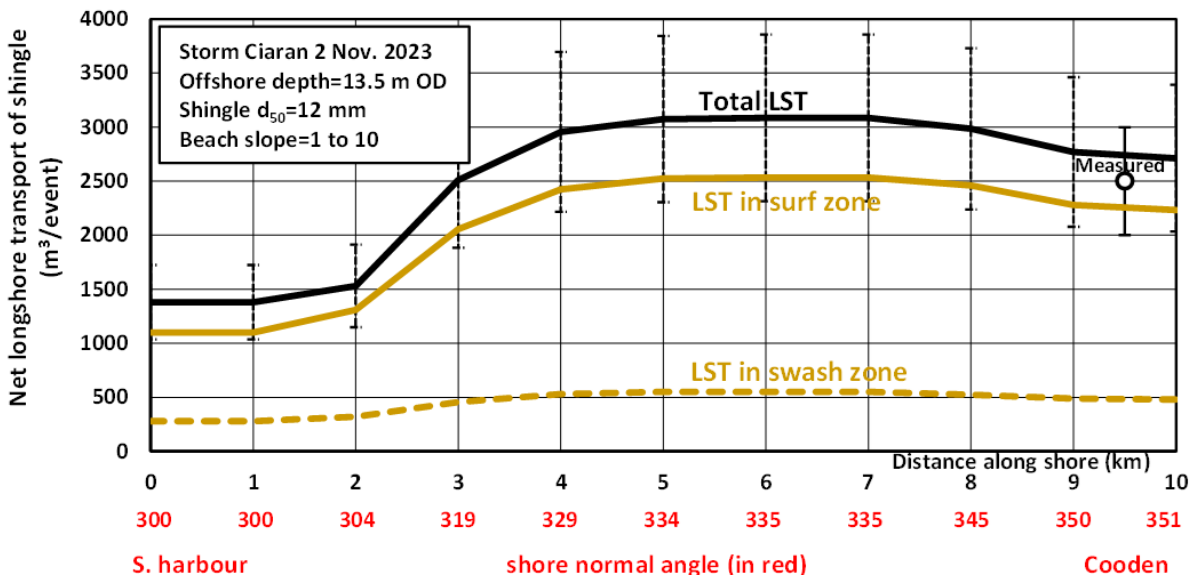




Figure 2.1.7 Computed LST along frontage during storm Ciaran on 2 November 2023

Shoreham Beach, UK

Measured values of net LST are also available for Shoreham beach along the English Channel (UK). This site is fairly close (about 40 km to the west) to Pevensy Beach, UK. The beach consists of shingle with $d_{50}=0.02$ m and $d_{90}=0.04$ m. The beach slope is 1 to 8.8 ($\tan\beta\cong 0.11$). The prevailing wave direction is from the southwest and south-southwest and the site is fully exposed to storm waves generated in the Atlantic Ocean and in the English Channel. The net annual LST in the period 1995 to 2000 is estimated to be about $17,500\pm 2,500$ m³/year (Van Wellen et al., 2000). The LST-model of Van Rijn (2014) has been used to compute the LST at Shoreham beach (UK). As Shoreham beach is fairly close to Pevensy beach, the wave buoy data of Pevensy bay of year 2004 are used.

The basic input data are: offshore water depth is 13.5 m to MSL (\cong OD); the shore normal (from sea to beach) is set to 5° to north. surf zone slope is set to 0.11; wave breaking coefficient is 0.6; friction coefficient for wave energy reduction due to bed friction is set to 0.85; single diameter is $d_{50}=0.02$ (20 mm); critical velocity for initiation of motion, $v_{cr}=1$ m/s; gravel separation depth is set to -3 m to MSL (sand seaward of -3 m and gravel landward of -3 m OD); fraction of coarse materials in surf zone $p_{coarse}=1$; calibration coefficient of LST is set to 1 (default value).

The computed net LST in the surf zone is 17,000 m³/year to east (18,800 to east and 1800 m³/year to west); the LST in the swash zone is 3600 m³/year to east (3800 m³/year to east and 200 m³/year to west). The total computed net LST is 20,600 m³/year to east, which is somewhat higher (about 20%) than the measured value of 17,500 m³/year to east.

Magdalen Island Beach, St Lawrence Bay, Canada

Magdalen Island is situated in St Lawrence Bay, Canada. South of the port of Cap-aux-Meules, a nourishment of very coarse materials ($d_{50}=0.04$ m; 40 mm) was constructed in August-September of 1922.

The tides are approximately between 1 m (Neap) and 2 m (Spring). The length of the nourishment is about 900 m and the slope in the swash zone above mean sea level (MSL) is 1 to 2.5. At the southwestern end of the site, a terminal groin is present to block the longshore transport of sediments. Post construction surveys shows the gradual development of an accretion area (about 3,000 m²) with a length of about 250 m updrift of the groin over a period of about 2.75 years after 1 October 2022. Most of the longshore transport was observed to take place in the swash zone. Based on analysis of cross-shore bed profile data between 17 May 2023 and 7 May 2024, the net LST at the updrift end of the accretion area is about 4600 ± 1100 m³ to SW over a period of 11.9 months. The net LST between 15 November 2023 and 7 May 2024 is about 3300 ± 300 m³ to SW over about 6 months (winter period). Hence, about 70% ($3300/4600 \times 100\%$) of the annual LST is in the winter period and about 30% in the summer period.

Wave energy enters from the Ocean (from direction of about 120° to N) into St Lawrence Bay through the opening between two major islands. Time series of tide and wave data (water level (η), significant wave height (H_s), peak wave period (T_p) and wave direction) are available from the MIKE21-model system for the period 1 January 2022 to 1 September 2024 (about 2.75 years). The dominant wave direction at a depth of -6 m in the middle of the nourishment site is about 105° N. About 98% of the waves are smaller than 1.5 m. About 2% of the waves are between 1.5 and 3.5 m. The dominant wave period is between 5 and 10 s.

The LST-model is run for the period 17 May 2023 to May 2024 with: modeled wave climate and water levels (hourly values) at offshore depth -6 m; coarse sediment $d_{50}=0.04$ m landward of -1 m depth line ($h_{coarse}=1$ m); fraction of coarse materials in the transition surf zone is assumed to be $p_{coarse}=0.5$; critical longshore velocity for initiation of motion $v_{cr}=1$ m/s; slope in swash zone $\tan\beta_{swash}=0.4$; slope in surf zone $\tan\beta_{surf}=0.3$; beach porosity $\varepsilon=0.4$ (bulk density=1600 kg/m³); fluid and sediment density 1025 and 2650 kg/m³; wave breaking coefficient $\gamma_{br}=0.9$; bed friction coefficient=1; calibration coefficient longshore transport in surf zone $K_{surf}=1$; calibration



coefficient swash velocity $K_{swash}=1$. The modeled wave climate was slightly shifted resulting in LST_{net} in surf zone = -250 m^3 to SW and LST_{net} in swash zone = -4250 m^3 to SW.

The total computed net LST is 4500 m^3 to SW, which is in good agreement with the measured value of $4600 \pm 1100 m^3$. It is clear that most (95%) of the LST takes place in the swash zone above MSL.

2.1.4 Definitions of directions in LONGMOR

- Longshore transport in positive x-direction is positive; this requires a positive wave angle to shore normal (**Figure 2.1.8**);
- Longshore transport in negative x-direction is negative; this requires a positive wave angle to shore normal.

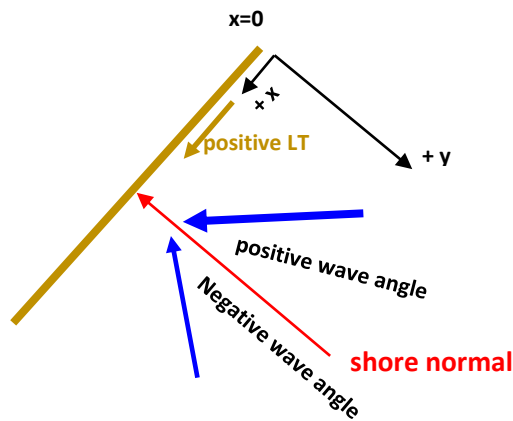


Figure 2.1.8 Definitions of positive and negative longshore transport rate

2.2 Numerical scheme

The mass balance equation (2.1) reads as:

$$h \Delta y_s / \Delta t + \Delta Q_{LS} / \Delta x - q_s = 0 \quad (2.15)$$

$$\Delta y_s = [\Delta x q_s - \Delta Q_{LS}] [\Delta t / (h \Delta x)]$$

with:

Δy_s = coastline change (m),

Δt = time step (s), Δx = space step (m),

h = thickness active layer (5 to 10 m),

q_s = source/sink term (nourishment or sand mining) per unit coastline (in $m^3/(ms)$),

Q_{LS} = longshore sand transport including pores (in m^3/s).

Deposition if $\Delta Q_{LS} / \Delta x < 0$ and if $q_s > 0$ (nourishment)

Erosion if $\Delta Q_{LS} / \Delta x > 0$ and if $q_s < 0$ (sand mining)

Equation (2.15) is solved by an explicit Lax-Wendorf scheme, as follows:.



$$y_{s,i \text{ new}} = y_{s,i, \text{old}} + \Delta y_{s,i} \quad (2.16)$$

with

$$\Delta y_{s,i} = [(q_s) (2\Delta x) - (Q_{SL,i+1, \text{old}} - Q_{SL,i-1, \text{old}})] [\Delta t / (2 h \Delta x)] + 0.5 \gamma [y_{s,i+1, \text{old}} + y_{s,i-1, \text{old}} - 2 y_{s,i, \text{old}}]$$

γ = smoothing parameter (0.0001 to 0.001; $\gamma = 0$ = no smoothing)

2.3 Sensitivity runs

The computation of the coastline using the LONGMOR-model is dependent on the applied wave climate and the wave order. Furthermore, the computation of the coastline position involves a smoothing parameter to suppress numerical oscillations of the computed coastlines. The coastline position is numerically computed from an explicit Lax-Wendroff scheme including a smoothing-parameter. The value of the smoothing parameter (in the range of 0.0001 to 0.001) has to be determined by trial and error.

Sensitivity runs have been made for a coastal extension of 1000 m perpendicular to the coast of North-Holland (The Netherlands) as shown in **Figure 2.3.1**. The applied offshore wave climate (9 conditions) is given in **Table 2.3.1**. This schematized wave climate represents annual-averaged conditions over a period of about 8 years (1980-1988; North-Holland) and produces a net longshore transport along the coast in northern direction (from left to right in **Figures 2.3.1, 2.3.2** and **2.3.2**). Positive wave angles yield longshore transport to the right.

To evaluate the effect of the wave order, the waves of **Table 2.3.1** have been applied in:

- positive-negative order; all waves with positive wave angles are taken first;
- negative-positive order (reversed order); all waves with negative wave angles are taken first;
- alternating order; waves with alternating positive and negative angles.

Time (days)	Significant wave height at deep water $H_{s,0}$ (m)	Peak wave period T_p (s)	Angle wave direction at deep water to coast normal (degrees)
0	1.5	4.9	58
44	1.5	4.9	58
44.1	1.8	5.4	28
87	1.8	5.4	28
87.1	2.75	6.6	28
102	2.75	6.6	28
102.1	2.0	5.7	-2
128	2.0	5.7	-2
128.1	1.8	5.4	-32
155	1.8	5.4	-32
155.1	1.6	5.1	-32
181	1.6	5.1	-32
181.1	3.0	6.9	-2
189	3.0	6.9	-2
189.1	3.2	7.2	-32
191	3.2	7.2	-32
191.1	0.5 m (no wind)	0.5	5.
365	0.5 m (no wind)	0.5	5.



Table 2.3.1 Schematized annual wave climate (9 conditions) of the North-Holland coast (1980-1988)

Figure 2.3.1 shows computed coastlines for a coastal extension of 1000 m and a net longshore transport of 500,000 m³/year based on waves in positive-negative order. Positive wave angles yield longshore transport to the right. The grid size is 50 m and the time step is 0.005 day (432 s). The numerical oscillations are relatively large if the smoothing = 0. The oscillations can be suppressed by using smoothing= 0.0005 and 0.001. The computed coastline is asymmetric, which is in agreement with the net longshore transport to the right. Using a smoothing= 0.0005, stable, but inaccurate results are obtained. The asymmetry of the computed coastline is suppressed.

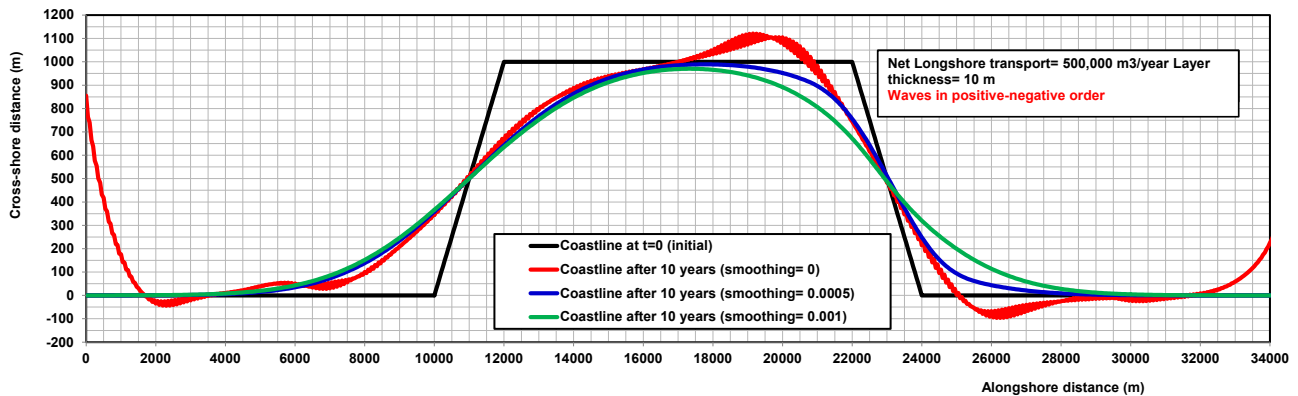


Figure 2.3.1 Coastlines; effect of wave order and smoothing parameter; positive-negative wave order

Figure 2.3.2 shows computed coastlines for a coastal extension of 1000 m and a net longshore transport of 500,000 m³/year based on waves in (reversed) negative-positive order. The numerical oscillations are relatively large if the smoothing = 0. The oscillations can be suppressed by using smoothing= 0.001. As a result, the computed erosion (total erosion area) increases by about 5%.

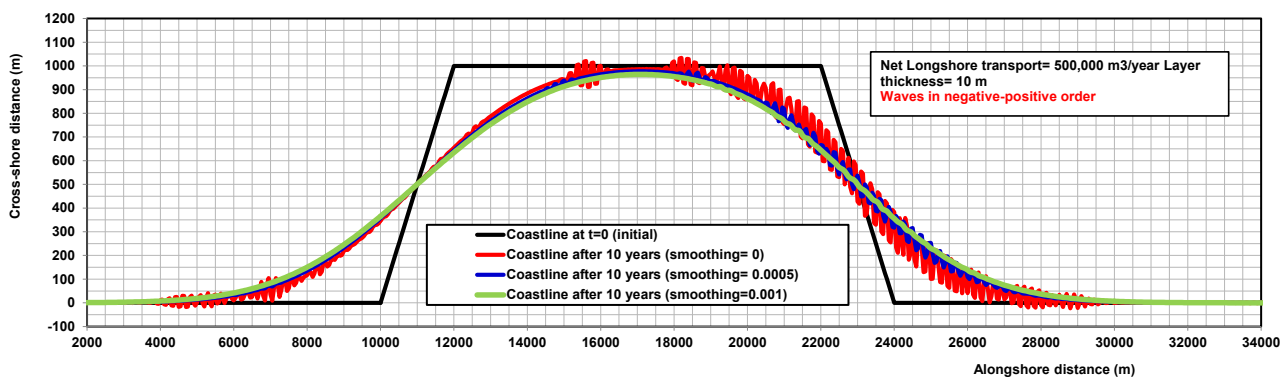


Figure 2.3.2 Coastlines; effect of wave order and smoothing parameter; negative-positive wave order

Figure 2.3.3 shows computed coastlines for a coastal extension of 1000 m and a net longshore transport of 500,000 m³/year based on waves in alternating order (alternating positive and negative wave angles). The numerical oscillations are absent for smoothing = 0. Minor instabilities are present at the boundary x=0, which can be suppressed by very minor smoothing =0.00003. Both coastlines lines are very close. The computed coastline after 10 years is slightly asymmetric.



These test computations show that for numerical stability it is best to apply a wave table with waves in alternating order (alternating positive and negative wave angles). The wave order slightly influences the accuracy of the long term coastline position (suppression of asymmetry). A smoothing parameter equal to 0.00003 introduces an erosion inaccuracy < 3%.

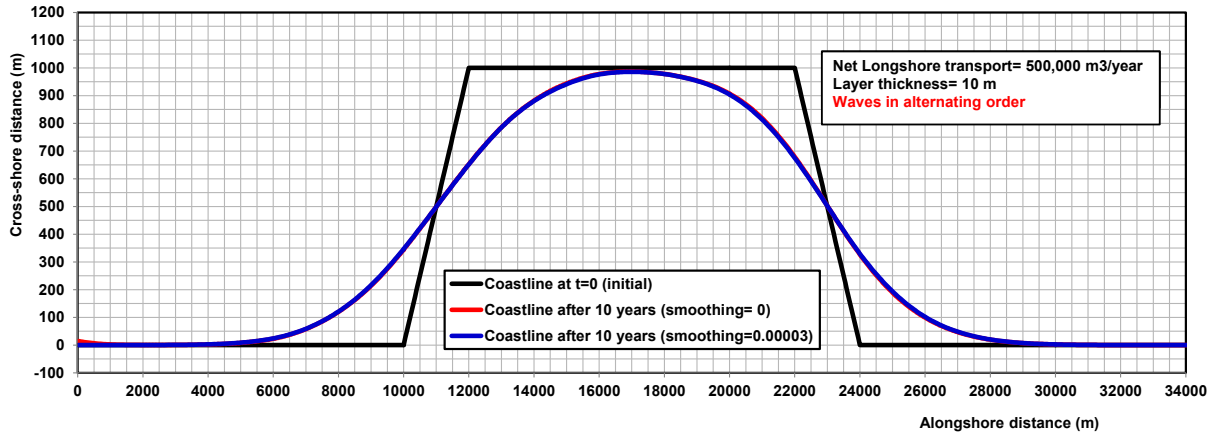


Figure 2.3.3 Coastlines; effect of wave order and smoothing parameter; alternating wave order



3. Application cases

3.1. Coastline changes south of IJmuiden, North-Holland, The Netherlands

The LONGMOR-model has been used to compute the coastline changes south of the harbor breakwaters at IJmuiden (**Figure 3.1.1**), The Netherlands.

The input parameters are:

- wave climate, see **Table 3.1.1** (only waves from south-west directions; data period 1979-2009);
- sediment properties: $d_{50}=0.0002$ m, $d_{90}=0.0003$ m;
- beach slope $\tan\beta =0.01$;
- breaking coefficient $\gamma=0.6$;
- effective tidal velocity=0.2 m/s (to north);
- grid size= 50 m; time step= 0.1 days; total time duration=40 years;
- initial coastline profile at 1965;
- shore normal at IJmuiden to North =104 degrees.

Significant wave height at deep water (m)	Wave period at deep water (s)	Wave direction at deep water to north (°)	Wave direction at deep water to coast normal (°)	Duration (days)
0.6	4.7	40	-64	11
0.6	4.7	95	-9	16
0.85	5.2	40	-64	29
0.85	5.2	95	-9	15
1.15	5.7	35	-69	23
1.32	5.7	90	-14	18
1.3	5.7	20	-84	1.5
1.7	5.7	45	-59	23
1.7	5.7	95	-9	9.4
1.9	7	45	-59	14.7
1.9	7	95	-9	7.6
2.5	7	45	-59	8.7
2.5	7	95	-9	4.6
2.9	8.4	45	-59	4.2
2.9	8.4	95	-9	2.8
3.2	8.4	45	-59	1.8
3.2	8.4	95	-9	1.6
3.6	8.4	45	-59	0.6
3.6	8.4	95	-9	1.0
4.5	9.3	45	-59	0.2
4.5	9.3	95	-9	0.5
5.0	9.3	45	-59	0.1
5.0	9.3	70	-34	0.1
5.5	10.2	95	-9	0.1
				total=194.5 days

Table 3.1.1 Wave climate IJmuiden, The Netherlands

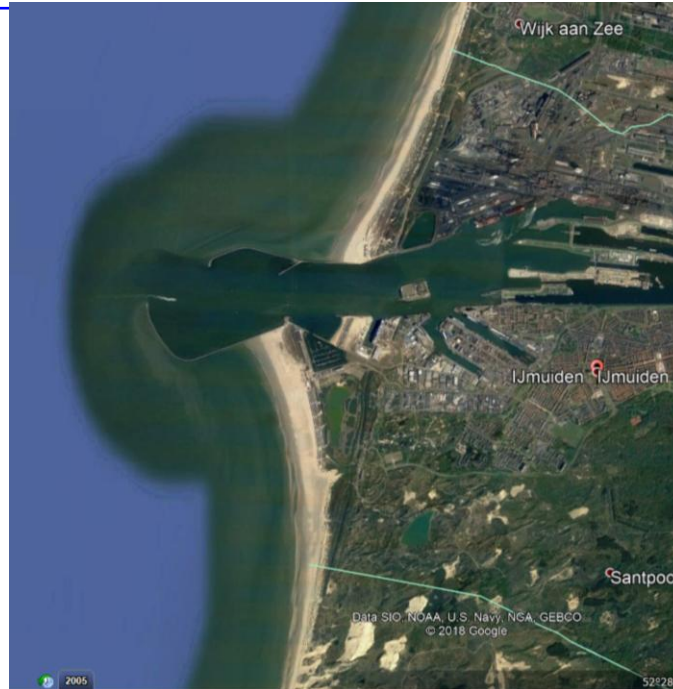


Figure 3.1.1 Coastal accretion south of IJmuiden, The Netherlands

Longshore transport Van Rijn (2014):

Two sediment diameters have been used $d_{50}=0.2$ mm and $d_{50}=0.25$ mm
Two calibration factors have been used $K=0.5$ and $K=1$.

Using $d_{50}=0.2$ mm and $K=1$ the measured coastline is overpredicted, see **Figure 3.1.2**.
The best results are obtained for $K = 0.5$.

Longshore transport Kamphuis (1991):

Using $d_{50}=0.2$ mm and $K=1$, the coastline is underpredicted, see **Figure 3.1.2**.

The annual longshore transport is (only waves from south-west based on **Table 3.1.1**):

Van Rijn	$d_{50}=0.2$ mm	$K=1$:	$Q_L=740000$ m ³ /year
		$K=0.5$:	$Q_L=370000$ m ³ /year
	$d_{50}=0.25$ mm	$K=1$:	$Q_L=600000$ m ³ /year
		$K=0.5$:	$Q_L=300000$ m ³ /year

Kamphuis	$d_{50}=0.2$ mm	$K=1$:	$Q_L=220000$ m ³ /year
----------	-----------------	---------	-----------------------------------

Based on this, the net longshore transport going to the North is of the order of 300,000 to 370.000 m³ per year.

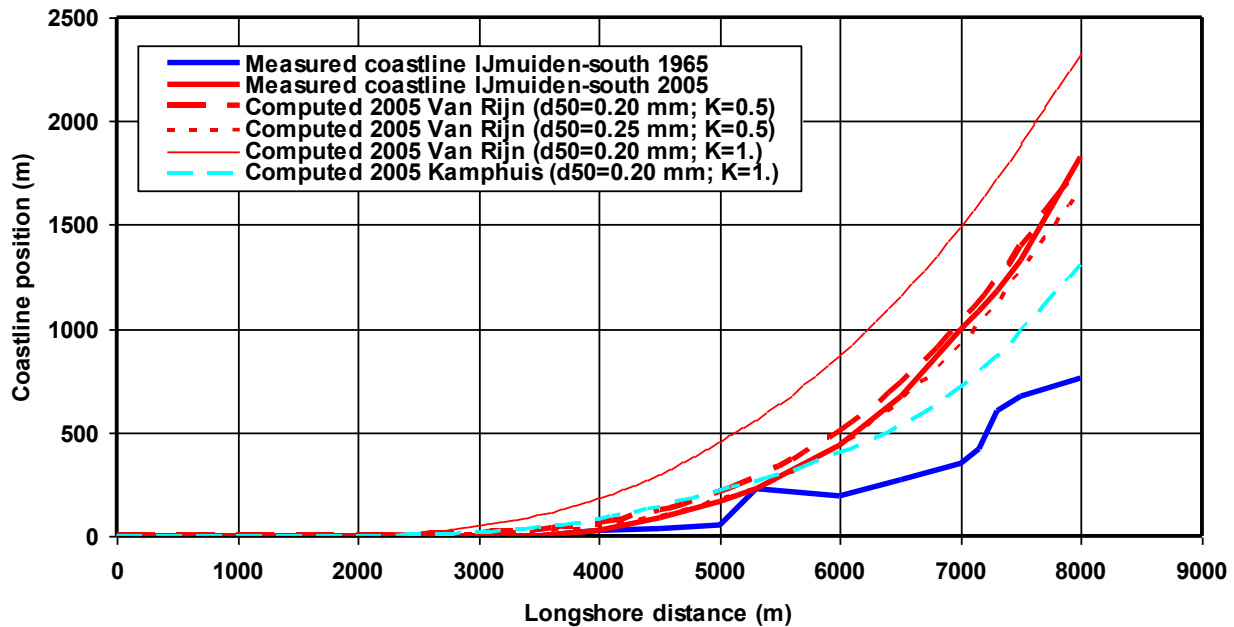


Figure 3.1.2 Measured and computed coastlines south of IJmuiden, The Netherlands

3.2 Coastline changes at mega-nourishment of Sand-motor, South-Holland, The Netherlands

The LONGMOR-model has been used to simulate the observed coastline changes and erosion volumes of the 'sand-motor' Case (Figure 3.2.1). This Case represents the dumping of a large volume of sand (about 20 million m^3) at coast south of The Hague in The Netherlands. The project is known as the sand motor. The net longshore transport of sand ($d_{50}=0.21$ mm) in the situation without 'sand-motor' is assumed to be about 200,000 m^3 /year based on earlier analysis results.

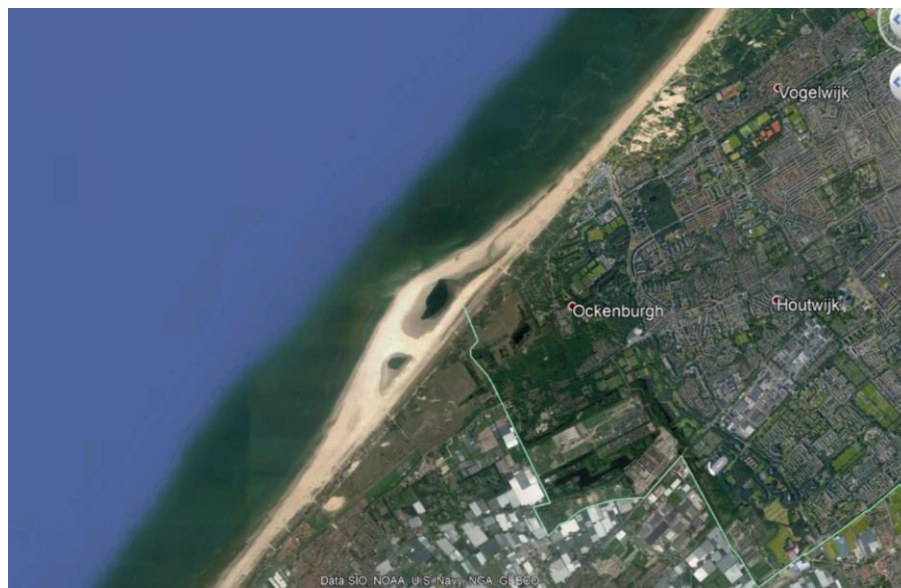


Figure 3.2.1 Coastal extension/mega-nourishment at the coast south of the Hague, The Netherlands



PARAMETER	Values
Grid size and length	50 m; 12.5 km
Timestep	0.002 day
Grid-‘smoothing’	0.00001
Sand d_{50} and d_{90}	0.21 mm; 0.5 mm
Slope surf zone 0 to -7 m NAP	1 to 100
Breaker coefficient	0.6
Wave order	Alternating (positive and negative angles)
Layer thickness of active zone	10 m (between -7 m and +3 m NAP)
Longshore transport formula	Van Rijn (2014)
File name	zandm1.inp; zandm2.inp

Table 3.2.1 Model settings LONGMOR for ‘sand-motor’, South-Holland

The model settings are given in **Table 3.2.1**. Three offshore wave climates have been used, see **Tables 3.2.2, 3.2.3, 3.2.4** and **3.2.5**. The most detailed wave climate consists of 34 wave conditions (wave angles between 60° and -60° to the normal line to the original coast) based on wave measurements in the period 1980-1988 at an offshore depth of 30 m. Onshore-directed waves > 0.5 m are only present during 108 days. The other climates consist of schematized wave conditions with 9 and 10 conditions.

The longshore sand transport equation of Van Rijn 2014 has been used.

Figure 3.2.2 shows the computed net longshore transport rates after 1 year using various wave climate conditions. The net longshore transport rate at the updrift boundary of the model is about $200,000 \text{ m}^3/\text{year}$. The LONGMOR-model has also been used in combination with a very simple wave climate consisting of four wave conditions. This wave climate was calibrated to give an erosion volume of about 1.1 million m^3 after 1 year (see **Figure 3.2.3**) and a net longshore transport of $200,000 \text{ m}^3/\text{year}$ at the updrift boundary. It is essential to include waves from almost normal directions to the coast, as these waves yield the largest erosion at the flanks of the coastal extension (nourishment).

The maximum transport gradient averaged over 1 year is approximately:

- 0.8 million m^3/year based on 10 wave conditions,
- 0.5 million m^3 based on the detailed wave climate with 34 conditions,
- 1.1 million m^3/year based on the calibrated wave climate with 9 conditions,
- 1.1 million m^3/year based on the simple wave climate with 4 conditions.

Sensitivity computations using other model settings yield a variation range of about $0.15 \text{ million m}^3/\text{year}$. The computed erosion volumes of 0.5, 0.8 and 1.1 million m^3 after 1 year are considerably smaller (factor 1.5 to 3) than the measured value of 1.5 million m^3 .

The computed coastline recession after 1 year based on wave climate with 9 conditions is shown in **Figure 3.2.2**. The computed average coastline recession between $x = 5300 \text{ m}$ and $x = 7000 \text{ m}$ is about 60 m. The average ‘measured’ coastline recession over the length of the central section ($x = 5300 \text{ m}$ to 7300 m ; layer thickness = 10 m) of the ‘sand-motor’ is $1.500,000 / (10 \times 2000) = 75 \text{ m}$ (green dotted line). The measured coastline after 1 year (coastline = waterline = 0 m NAP; green dashed line) is situated far more landward than the measured average recession line, which points to relatively large erosion near the waterline.

It is concluded that the 1D-LONGMOR-model can be used to compute the coastline changes, provided that some measured coastline data are available for calibration.

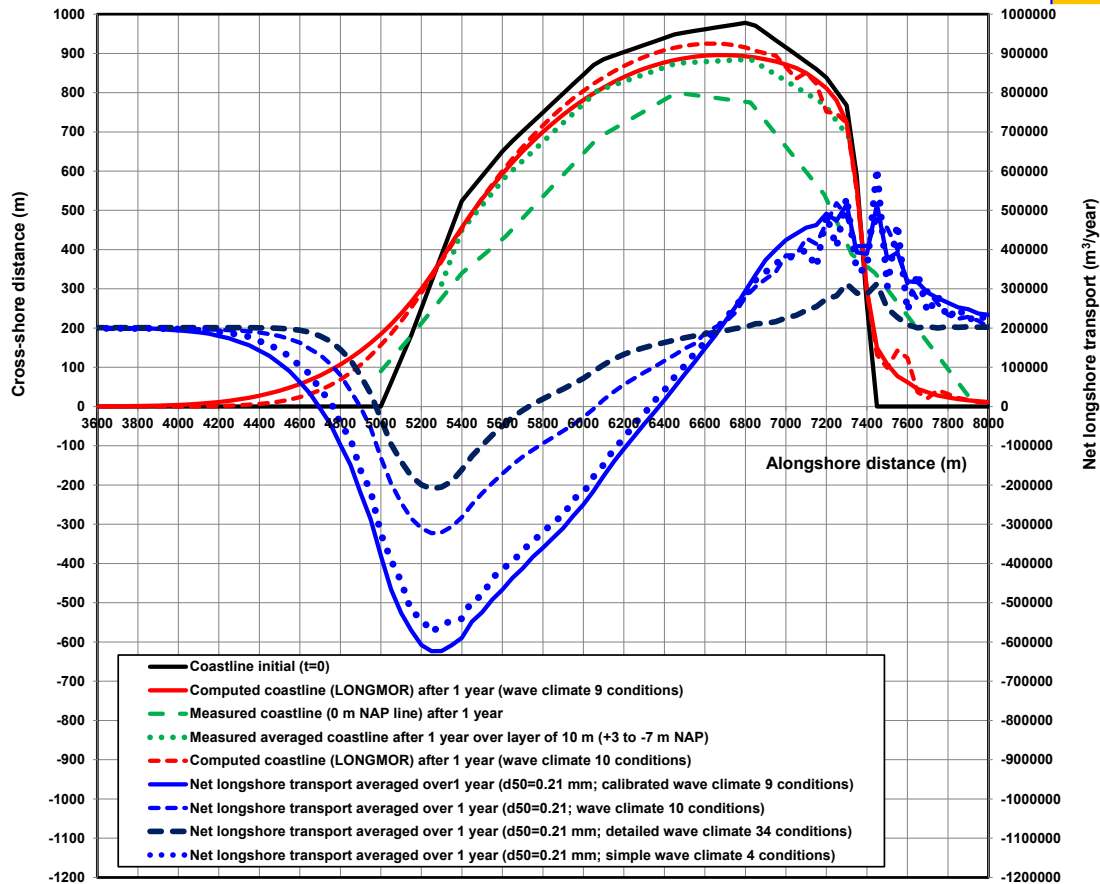


Figure 3.2.2 Computed longshore transport rates;
Computed and measured coastlines after 1 year, 'sandmotor', The Netherlands

Figure 3.2.3 shows the computed erosion volumes of the 1D-model based on four different wave climates. The measured initial erosion volumes after 0.5 and 1 year are significantly underestimated using a detailed wave climate with 34 conditions. These results show the strong effect of the wave climate on the 1D-model results. The 1D model underestimates the measured erosion volumes significantly using this detailed wave climate. The results of the 1D-model can only be improved by calibration of the wave climate (adjusting the wave angles and the durations) using measured erosion volumes.

The detailed DELFT3D-model yields an erosion volume of 3 million m³ after 3 years based on a wave climate with 10 conditions. The LONGMOR-model run with the same 10 wave conditions yields an erosion volume of about 2.5 million m³ after 3 years (30% less).

The discrepancies between the DELFT3D and the LONGMOR-results are caused by the following effects:

- different wave refraction seaward of the active surf zone (depth contours outside surf zone are almost stationary in Delft3D-model whereas they are rotating in LONGMOR-model similar as the coastline rotation);
- flow contraction resulting in an increase of the tide-driven velocities and transport rates (neglected in LONGMOR);
- wave focusing resulting in enhanced wave heights at both seaward corners (neglected in LONGMOR);
- erosion due to cross-shore transport gradients which may be relatively large during the initial years due to the presence of relatively steep beach profiles (neglected in LONGMOR).



The 1D-LONGMOR-model can be calibrated to better represent the measured values by adjusting the wave conditions slightly (9 conditions).

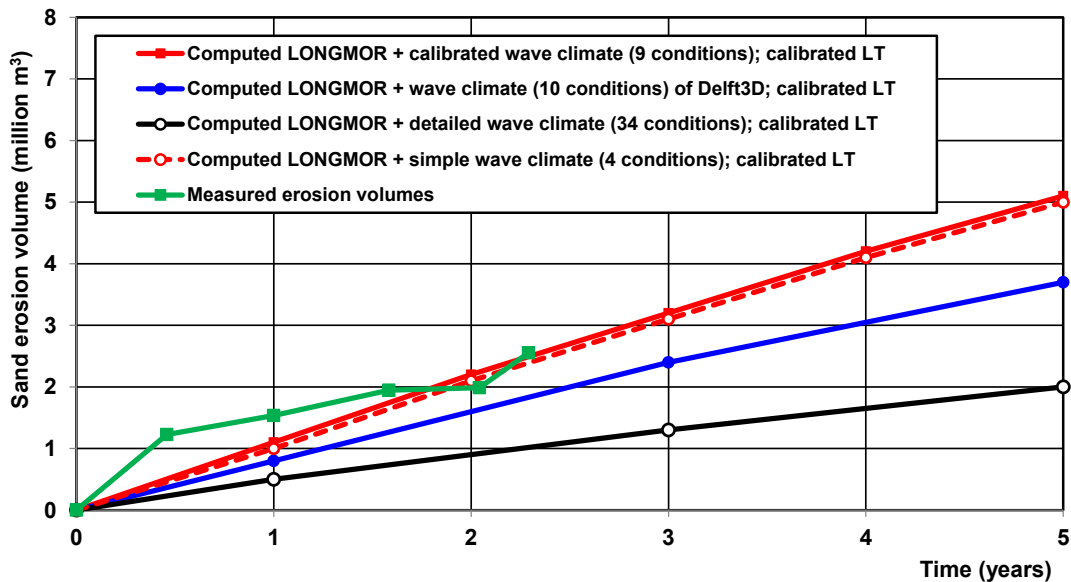
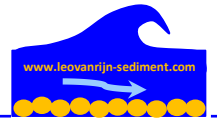


Figure 3.2.3 Measured and computed LONGMOR erosion volumes, sand-motor, The Netherlands

Time (days)	Significant wave height at deep water $H_{s,0}$ (m)	Peak wave period T_p (s)	Angle wave direction at deep water to coast normal (degrees)
0	1.08	5.2	58
71	1.08	5.2	58
71.1	2.43	6.9	56.6
82.	2.43	6.9	56.6
82.1	0.89	5.2	30.3
141.	0.89	5.2	30.3
141.1	2.64	7.2	30.4
149.	2.64	7.2	30.4
149.1	0.84	5.7	-1.5
212.	0.84	5.7	-1.5
212.1	0.72	5.2	-58.3
263.	0.72	5.2	-58.3
263.1	2.61	7.5	-1.6
270.	2.61	7.5	-1.6
270.1	0.82	5.9	-30.3
356.	0.82	5.9	-30.3
356.1	2.64	7.9	-25.4
364.	2.64	7.9	-25.4
364.1	2.24	7.0	-55
365.	2.24	7.0	-55

Table 3.2.2 Schematized annual wave climate (10 conditions) of the Dutch coast

Time (days)	Significant wave height at deep water $H_{s,0}$ (m)	Peak wave period T_p (s)	Angle wave direction at deep water to coast normal (degrees)
0	1.5	4.9	58



44	1.5	4.9	58
44.1	1.8	5.4	28
87	1.8	5.4	28
87.1	2.75	6.6	28
102	2.75	6.6	28
102.1	2.0	5.7	-2
128	2.0	5.7	-2
128.1	1.8	5.4	-32
155	1.8	5.4	-32
155.1	1.6	5.1	-32
181	1.6	5.1	-32
181.1	3.0	6.9	-2
189	3.0	6.9	-2
189.1	3.2	7.2	-32
191	3.2	7.2	-32
191.1	0.5 m (no wind)	0.5	5.
365	0.5 m (no wind)	0.5	5.

Table 3.2.3 Schematized annual wave climate (9 conditions) of the North-Holland coast (1980-1988)

Significant wave height H_s (m)	Peak wave period T_p (s)	Wave direction to shore normal θ (°)	Duration (days)	Significant wave height H_s (m)	Peak wave period T_p (s)	Wave direction to shore normal θ (°)	Duration (days)
0.75	5	-60	9.7	2.75	7	-60	0.3
		60	11.8			60	2.0
		30	9.1			30	2.0
		-30	8.9			-30	1.1
1.25	6	-60	6.2	3.25	8	-60	0.1
		60	10.4			60	0.9
		30	7.4			30	1.1
		-30	6.4			-30	0.4
1.75	7	-60	2.2	3.75	8	-60	0.04
		60	6.9			60	0.4
		30	5.3			30	0.9
		-30	3.5			-30	0.1
2.25	7	-60	0.4	4.25	9	60	0.2
		60	3.4			30	0.4
		30	3.4			-30	0.07
		-30	1.7	5.0	10	60	0.1
						30	0.4
						-30	0.1
Total			97 days				11 days
							108 days

Positive wave angle yields transport to north-east (dominant longshore transport direction)

Table 3.2.4 Detailed annual wave climate (34 conditions) of South-Holland coast 1980-1988, The Netherlands



Time (days)	Significant wave height at deep water $H_{s,o}$ (m)	Peak wave period T_p (s)	Angle wave direction at deep water to coast normal (degrees)
0	2.2	7.0	30
50.	2.2	7.0	30
50.1	2.0	6.0	-30
100.	2.0	6.0	-30
100.1	1.8	6.0	0.
130.	1.8	6.0	0.
130.1	0.5	4.0	0.
365.	0.5	4.0	0.

Table 3.2.5 Simple annual wave climate; 4 conditions; South-Holland coast 1980-1988, The Netherlands

3.3 Coastline changes west of jetties of Port of Lagos, Nigeria

The LONGMOR-model has been used to simulate the coastline changes over a period of 50 years (1960 to 2010) for the Lagos coast updrift of the western harbor breakwater, Nigeria (**Figure 3.3.1**).

The net longshore transport at the open coast far updrift of the harbor breakwater is estimated to be about $500,000 \pm 100,000 \text{ m}^3/\text{year}$ from West to East based on analysis of old maps and charts.

To simplify the wave climate, a single offshore wave height has been used. A single offshore wave height of $H_{s,o} = 3 \text{ m}$ with a wave incidence angle of 30° degrees and duration of 25 days per year yields a longshore transport of about $500,000 \text{ m}^3/\text{year}$ (Van Rijn 2014).

The model input data of the LONGMOR-model contains various uncertain parameters, as follows:

- parameters of net longshore transport of $500,000 \text{ m}^3/\text{year}$ (range of $400,000$ to $600,000 \text{ m}^3/\text{year}$);
- effective profile layer thickness (range of 8 m for short term computations to 12 m for long term computations); the layer thickness is the vertical distance between the sea bottom at the breaker line at about -7 m below MSL and the dune crest at +3m above MSL (MSL= Mean Sea Level);
- adjustment length scale of longshore transport (order of 5 km); alongshore distance over which the longshore transport reduces to zero close to the breakwater;
- bypassing rate of longshore transport at tip of harbor breakwater (10% to 30% of updrift value).



Figure 3.3.1 Lagos coast 2006, Nigeria

Figure 3.3.2 shows the computed coastline changes along the west coast for a period of 50 years (1960 to 2010). The net updrift longshore transport has been varied in the range of 400,000 to 600,000 m³/year. The layer thickness has been varied in the range of 10 to 12 m. The bypassing rate at the tip of the breakwater is set to 20% of the updrift value. The adjustment length is set to 5 km. Measured values of the coastline in 2010 are also shown. The LONGMOR-model produces very reasonable results for a net longshore transport of 400000 m³/year and layer thickness values of 10 to 12 m.

The assumption of a bypassing rate of 20% of the updrift value (100,000 m³/year) seems to be a very reasonable value. Bypassing of sand leads to deposition in the deeper entrance channel, which has to be removed by maintenance dredging. Around 2010, the western harbor breakwater has been extended with about 150 to 200 m to reduce the bypassing rate.

The cross-shore length scale of the accretion zone with respect to the original coast is about 300 m; the alongshore length scale of the accretion zone is about 9000 m. The ratio of the alongshore and cross-shore scales is about 9000/300 = 30.

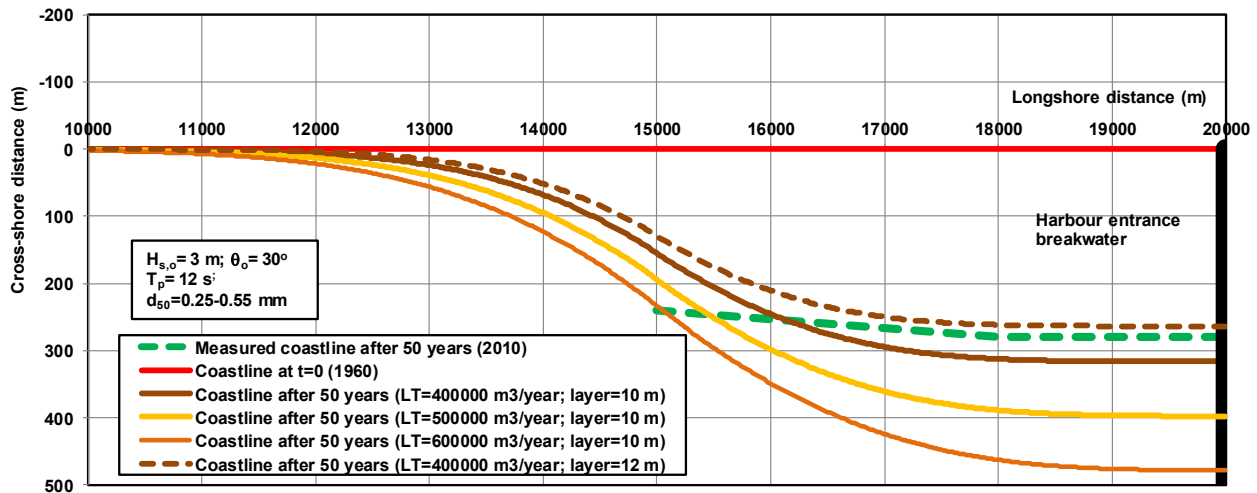


Figure 3.3.2 Computed and measured coastline changes on west side during period 1960 to 2010, Lagos, Nigeria



3.4 Coastline changes east of jetties of Port of Lagos in Nigeria

Approach

The coastline in the lee of a long breakwater with respect to the dominant wave direction is often suffering from erosion as result of the blocking of the longshore sand transport. An example case is the coast east of the long jetty of the Port of Lagos in Nigeria. The dominant wave direction is from the South-West.

The net annual longshore transport at the downdrift boundary should be known (input).

Most waves (about 80%) of the waves are coming from the South-West and are diffracted around the eastern breakwater of the harbor entrance, as can be seen in **Figure 3.4.1**. Wave diffraction is the lateral transfer (along the wave crest) of energy. Diffracted waves in the lee diffraction zone are smaller than the waves outside the diffraction zone. The beach of Kuramo waters has a length of about 1.6 km and the west beach end is at 2.3 km from the eastern harbor breakwater.

Two models have been used to determine the coastline changes in the lee of a breakwater:

- LONGMOR-model and;
- DWS-model (Diffracted Waves and Sand transport).

The LONGMOR-model is a state-of-the art coastline model based on longshore sand transport equations and computes the behavior of the coastline over time.

The DWS model is a simple spreadsheet model (Van Rijn 2015) to compute the wave heights, current velocities and alongshore sand transport rates along the breaker line in the wave diffraction zone of a long breakwater based on standard text-book equations of wave-diffraction processes. The computed wave heights are very close to the computed values of the very sophisticated SWAN wave-model.

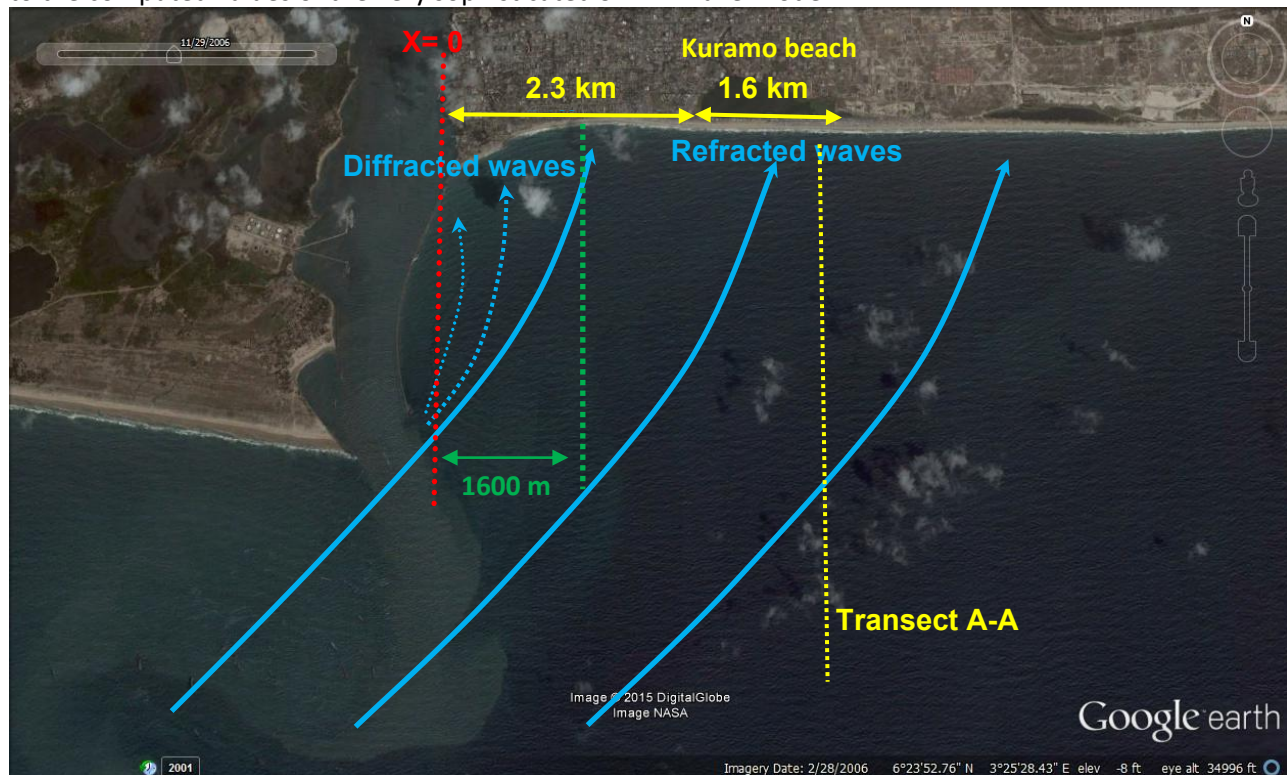


Figure 3.4.1 Wave patterns in lee zone of eastern harbor breakwater (before 2010); waves from South-West

Wave diffraction modelling



The DWS-model, which is based on the practical diffraction method of Kamphuis (1992), has been used to estimate the wave heights along the nearshore breaker line in the wave diffraction zone near Kuramo beach for a storm event with offshore wave height $H_{s,o} = 4$ m, $T_p = 15$ s and offshore wave angle of 30° from South-West (see **Table 3.4.1**). It is noted that this method is most valid for irregular directional waves and does not predict the (theoretical) wave height increase which may occur in the divergence zone.

Parameters	Storm 1	Storm 2	Storm 3
Offshore significant wave height (m)	2	3	4
Offshore wave angle to shore normal ($^\circ$)	30	30	30
Peak wave period (s)	10	12	15
Nearshore circulation current in surf zone towards breakwater (m/s)	-0.3	-0.4	-0.5
Tidal current velocity in surf zone far downdrift away from breakwater (m/s)	0.1	0.1	0.1
Offshore water depth (m)	100		
Water depth near tip of breakwater	7		
Distance of tip of breakwater from shoreline (m)	2800		
Distance of offshore location from shoreline (m)	20000		
Slope surf zone (tan)	0.015		
Breaker coefficient γ_{br} (-)	0.6		
Friction factor f_w (-)	0.01		

Table 3.4.1 Input data DWS-model; no land reclamation; waves from South-West

Figure 3.4.2 shows the computed significant wave heights and wave angles at the breaker line of Kuramo beach and surrounding coastlines for the situation without land reclamation based on the DWS-model; the wave breaking coefficient is $\gamma_{br} = 0.6$. The origin $x=0$ is the red line through the tip of the eastern breakwater, see **Figure 3.4.1**. The longshore current velocity is also shown (+ to East; - = to West). The breaker line is at about 6.5 m depth for offshore waves of $H_{s,o} = 4$ m.

The beach of Kuramo waters is between $x=2.3$ and 3.9 km from the entrance breakwater, see **Figure 3.4.1**. The wave diffraction zone with reduced wave heights has an alongshore length of about 3 km. Outside the wave diffraction zone ($x > 3000$ m), the wave height is approximately constant. The wave height at $x=0$ is about 65% of the wave height outside the wave diffraction zone. The wave angles at the breaker line are about 10° (waves almost normal to the shore). Bottom friction is rather important as the swell waves are relatively long waves propagating from deep water of 100 m over a distance of about 20 km to the shore (large friction distance).

The wave height at the west end of Kuramo beach is about 90% of the far east wave height.

The wave height at the east end of Kuramo beach is about equal to the far east wave height.

The longshore current velocity is negative (towards the breakwater; to the West) with a value of about -0.5 m/s close to the breakwater and positive further away from the breakwater. The transition from negative to positive velocity occurs at about 1300 to 1500 m from the harbor breakwater. The transition location marks the location of maximum erosion (which is about 1600 m from the harbor breakwater). The longshore current velocity based on the DWS-model increases gradually to about 0.7 m/s faraway from Kuramo beach for offshore waves of 3 to 4 m.

The wave height at the west end of Kuramo Waters beach is slightly smaller than at the east end of the beach. Similarly, the longshore current velocity increases slightly along Kuramo beach.

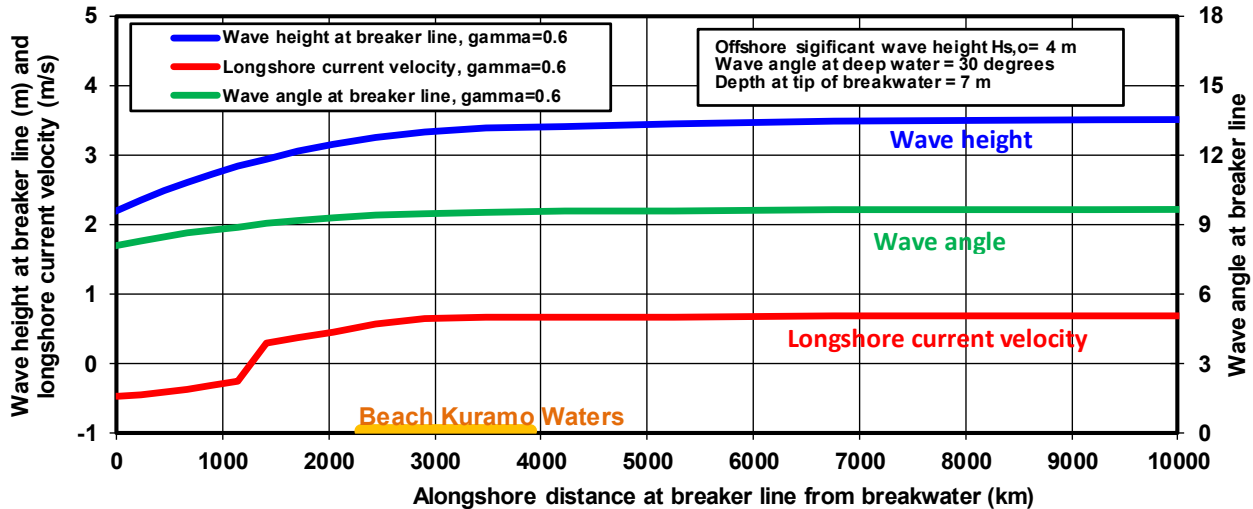


Figure 3.4.2 Wave height and wave angle along the breaker line in the lee area of a breakwater; DWS-model; $H_{s,o} = 4$ m from South-West; $\gamma_{br} = 0.6$; (+ to East; - to West)

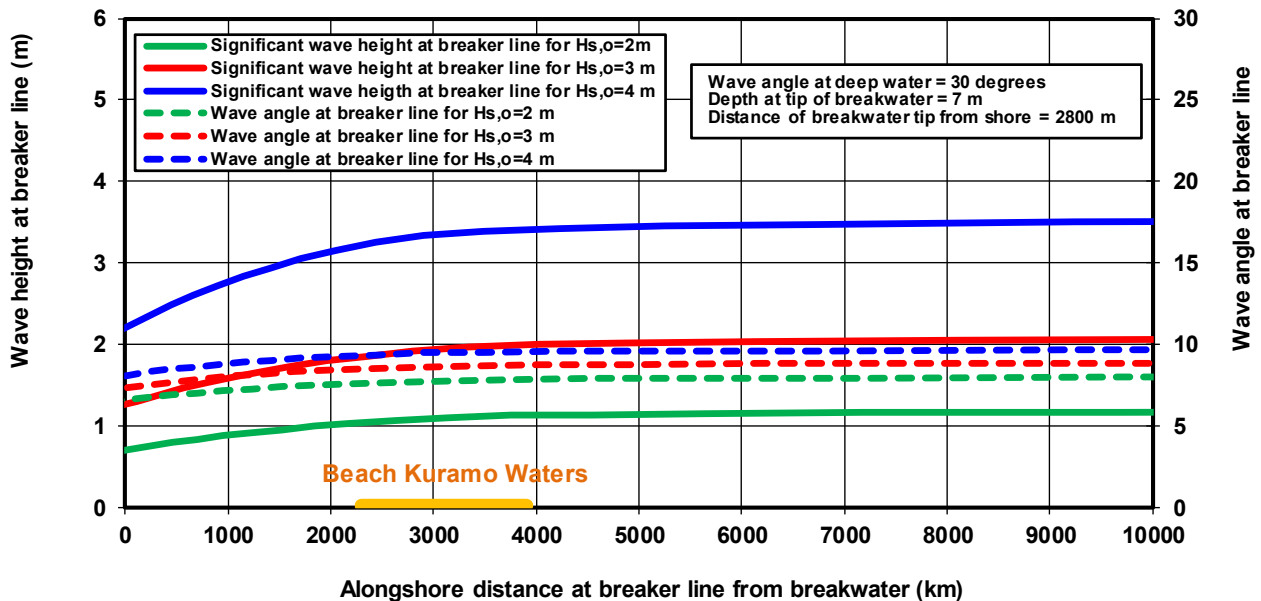


Figure 3.4.3 Wave height and wave angle along the breaker line near Kuramo beach; DWS-model; $H_{s,o} = 2, 3$ and 4 m from South-West; $\gamma_{br} = 0.6$

Table 3.4.2 shows the wave heights at depth lines of 7 and 5 m for Kuramo West and East based on the DWS-model (with $\gamma_{br}=0.6$) and the SWAN-model. The SWAN-model results are best and show that the largest waves (red and green values) occur at Kuramo West due to wave focusing in the region of the protruding harbor entrance. The SWAN wave height is relatively small at Kuramo East for $H_{s,o}=3$ m due to wave refraction effects resulting in a dip in the wave height distribution. The transition zone from relatively small waves in the diffraction zone to the larger waves outside the diffraction zone has an alongshore length scale of about 2 km for the SWAN-model and 3 km for the DWS-model.



Depth (m)	Offshore: $H_{s,o}=3$ m; $T_p=12$ s; angle= 30° (210° N)				Offshore: $H_{s,o}=4$ m; $T_p=15$ s; angle= 30° (210° N)			
	Kuramo West		Kuramo East		Kuramo West		Kuramo East	
	DWS	SWAN 2D	DWS	SWAN 2D	DWS	SWAN 2D	DWS	SWAN 2D
7	2.3	2.6	2.6	2.2	3.3	3.2	3.7	3.1
5	2.2	2.6	2.5	2.2	2.7	3.1	3.0	3.0

Table 3.4.2 Significant wave height (in m) at Kuramo West and East; waves from South-West

Figure 3.4.4 shows the plan view with the wave and current parameters at the beach of Kuramo Waters for a storm event with $H_{s,o} = 4$ m based on DWS-model. The wave height at the breaker line varies from $H_{s,br} = 2.2$ m at $x=0$ m to $H_{s,br} = 3.4$ m outside the diffraction zone ($x > 3$ km). Near the breakwater, the longshore current is towards the structure. At Kuramo beach, the longshore current velocity increases from 0.55 m/s to 0.7 m/s in eastward direction.

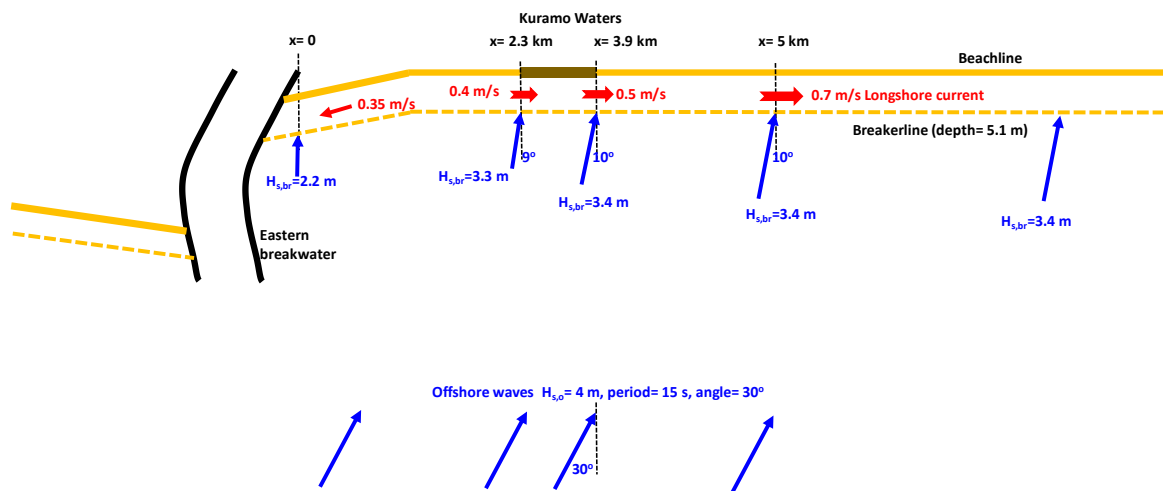


Figure 3.4.4 Plan view for wave conditions in lee of breakwater; $H_{s,o} = 4$ m from South-West ($\gamma_{br} = 0.6$); DWS-model

Longshore transport variations and coastline changes

To simplify the wave climate, a single offshore wave height has been used to run the LONGMOR-model.

The net longshore transport in eastern direction is about 650,000 m³/year based on historical coastline changes for the East coast.

A single offshore wave height of $H_{s,o} = 1.5$ m with duration of 210 to 230 days per year yields a longshore transport of 650,000 m³/year.

Similarly, a single wave height of $H_{s,o} = 3$ m yields with duration of 28 to 30 days per year also yields a longshore transport of about 650,000 m³/year.

The LONGMOR-model has been calibrated to produce the correct distribution of the longshore transport rate at Kuramo beach and surrounding coast, as computed by the more detailed DWS-model.

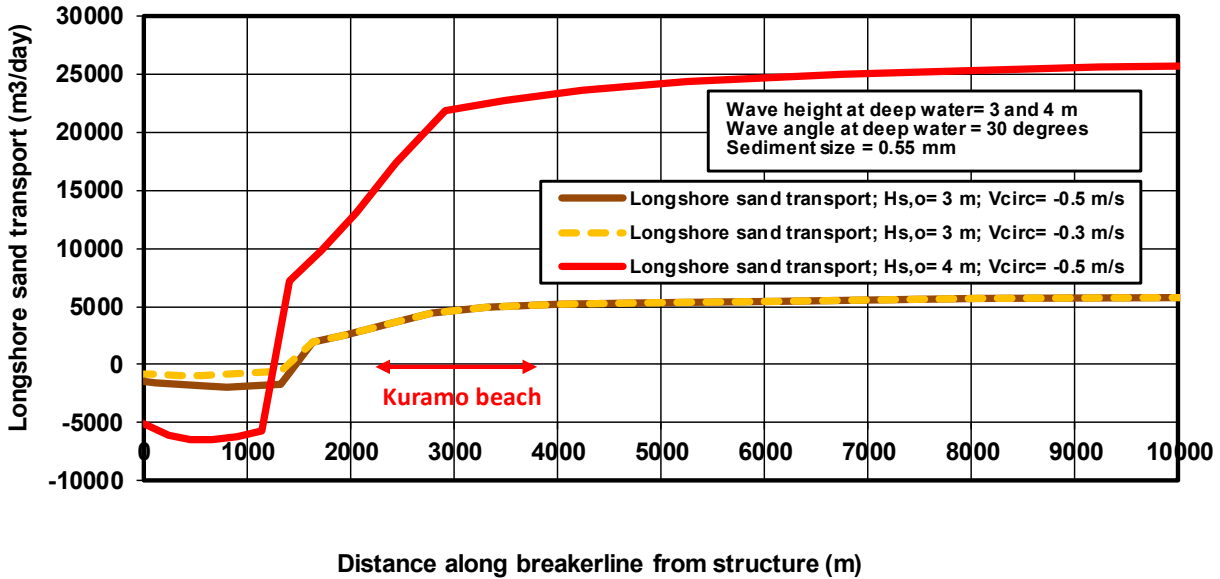


Figure 3.4.5 Longshore transport along Kuramo beach and surrounding coastlines (DWS-model); $d_{50} = 0.55 \text{ mm}$, $H_{s,o} = 3$ and 4 m from South-West

Figure 3.4.5 shows the computed longshore transport of the DWS-model for $H_{s,o} = 3$ and 4 m , offshore angle = 30° (waves from South-West), $d_{50} = 0.55 \text{ mm}$ and slope = 0.015 . Far away (East) from the harbor entrance channel, the longshore transport is about $6100 \text{ m}^3/\text{day}$ for offshore waves of 3 m . Using a duration of 106 days, the net longshore transport is $650,000 \text{ m}^3$ per year.

Figure 3.4.6 shows the computed coastline of the LONGMOR-model after 5 years (2005 to 2010) for a wave climate with one wave height of $H_{s,o} = 3 \text{ m}$ and duration representing 5 years. The input data are given in **Table 3.4.3**. Two computations have been made, as follows:

- high estimate of the net annual longshore transport $LT_{\text{net}} = 650,000 \text{ m}^3/\text{year}$ (at the far end $x = 15 \text{ km}$ east of the harbor breakwater);
- low estimate of the net annual longshore transport $LT_{\text{net}} = 300,000 \text{ m}^3/\text{year}$ (at the far end $x = 15 \text{ km}$ east of the harbor breakwater).

The high estimate of the net LT yields coastal recession rates of 40 to 50 m after 5 years or 8 to 10 m per year at Kuramo beach, which are much too high compared with the measured data of 2 to 3 m per year.

Therefore, another computation has been made for a low estimate of the LT resulting in a recession rate of 3 to 5 m per year. The location of maximum erosion is at about 1800 to 2000 m from the harbor breakwater. The alongshore scale of the coastal erosion on the east coast is of the order of 10 km, see **Figure 3.4.6**. It is noted that the region of maximum erosion will gradually shift eastwards with the construction progress of the Lagos Wall (after 2010).

The net annual longshore transport rate to simulate the coastal recession rates at Kuramo beach before the construction of the land reclamation correctly is of the order of $300,000 \text{ m}^3/\text{year}$, which is considerably less than the value of about 500,000 to 900,000 m^3/year derived from the long term historical coastline recession rates of the East coast. Most likely, the present recession rates are smaller than the older recession rates due to the presence of local coastal defense structures (revetments and short groins are present) and local beach nourishment schemes.

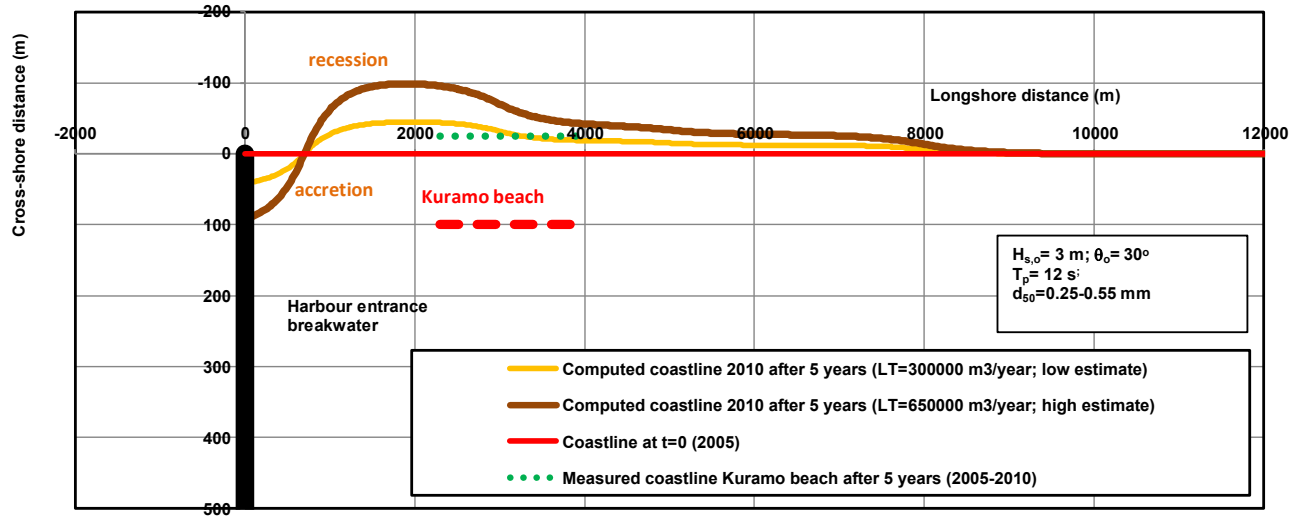


Figure 3.4.6 Coastline along Kuramo beach and surrounding coastlines (LONGMOR-model); $d_{50} = 0.25-0.55$ mm, $H_{s,o} = 3$ m from South-West

PARAMETER	VALUES
Offshore significant wave height	3 m
Offshore wave angle	30°
Peak wave period	12 s
Grid size and traject length	20 m; 15000 m
Time step and grid-'smoothing'	0.01 day; 0.01-0.5
Sand d_{50} , d_{90}	0.25-0.55 mm; 1 mm
Slope beach-surf zone 0 tot -5 m MSL	1 to 65 (tan slope=0.015)
Breaker coefficient	0.8
Layer thickness of active zone	10 m (between -8 m and +2 m MSL)
Longshore transport formula; Calibration coefficient	Van Rijn 2014; 0.45 to 1
Angle of coastnormal to North	0 degrees
Tidal currents in surf zone	$V_{flood}=0$ m/s; $V_{ebb}=0$ m/s (no effect if both values are equal)
Beach nourishment volumes	0
Input files	NigerW.inp: west coast Niger1.inp: east coast 1.4 years (Jan 2010-May 2011) Niger12.inp: east coast 2 years (May 2011-March 2013)

Table 3.4.3 Input data of LONGMOR-model; Kuramo beach.



3.5 Detached breakwater at 450 m from the coast in Congo

Introduction

This case refers to the design of loading facility along the coast of West-Afrika (Congo). A detached breakwater is planned to be constructed about 465 m from the shore. Between the shore and breakwater, a berthing zone will be created, see **Figure 3.5.1**.

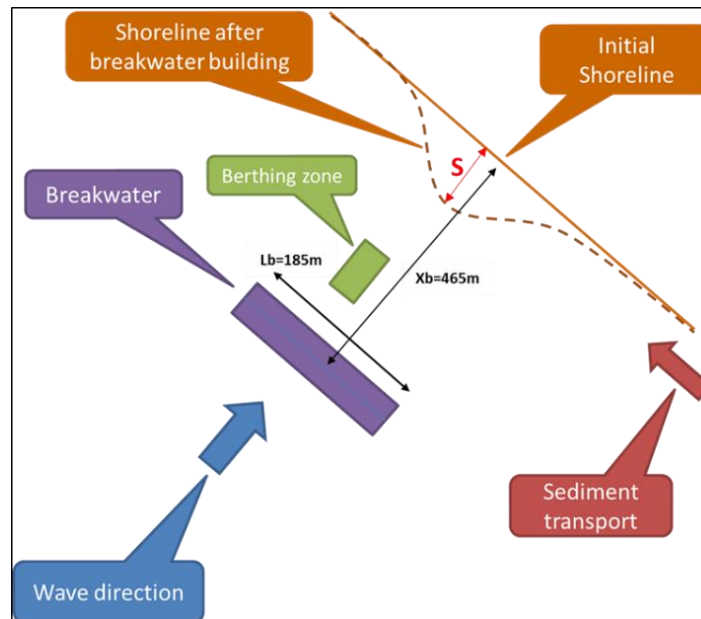


Figure 3.5.1 Single detached breakwater

Wave and flow patterns

The DELFT3D-flow model and the SWAN-wave model have been used to compute the wave and flow patterns and coastline changes in the lee of a (single) detached breakwater. The length of the breakwater (parallel to the coast) is about 200 m. The distance between the breakwater and the coast is about 450 m. The water depth at the position of the breakwater is about -6 m (to mean sea level). The beach slope is 1 to 7; the surf zone slope is 1 to 20 to -6 m depth line and the sea bottom slope is 1 to 200 beyond the -6 m depth line. The beach and seabed consist of sand with $d_{50}=0.3$ mm and $d_{90}=0.6$ mm. The representative offshore significant wave height is $H_{s,o}=1.25$ m with $T_p=12$ s and a wave angle of 10° with respect to the coast normal (which makes an angle of 40° with the North, see **Figure 3.5.2**). The net longshore transport is about $100,000$ m³/year based on Littoral.xls.

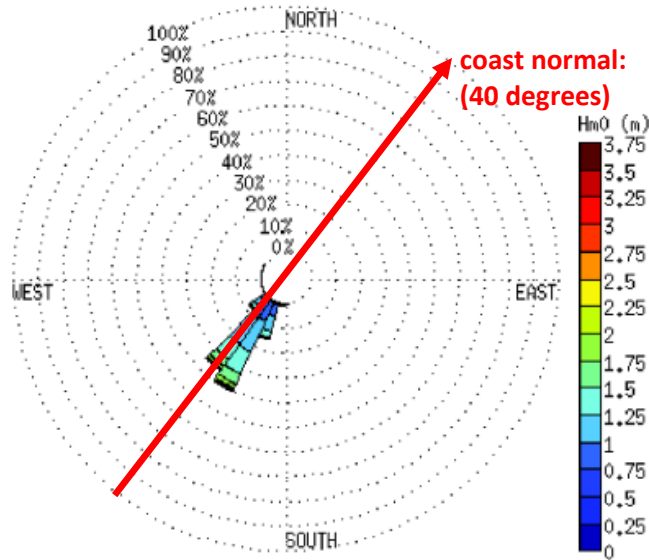


Figure 3.5.2 Wave rose and coast normal

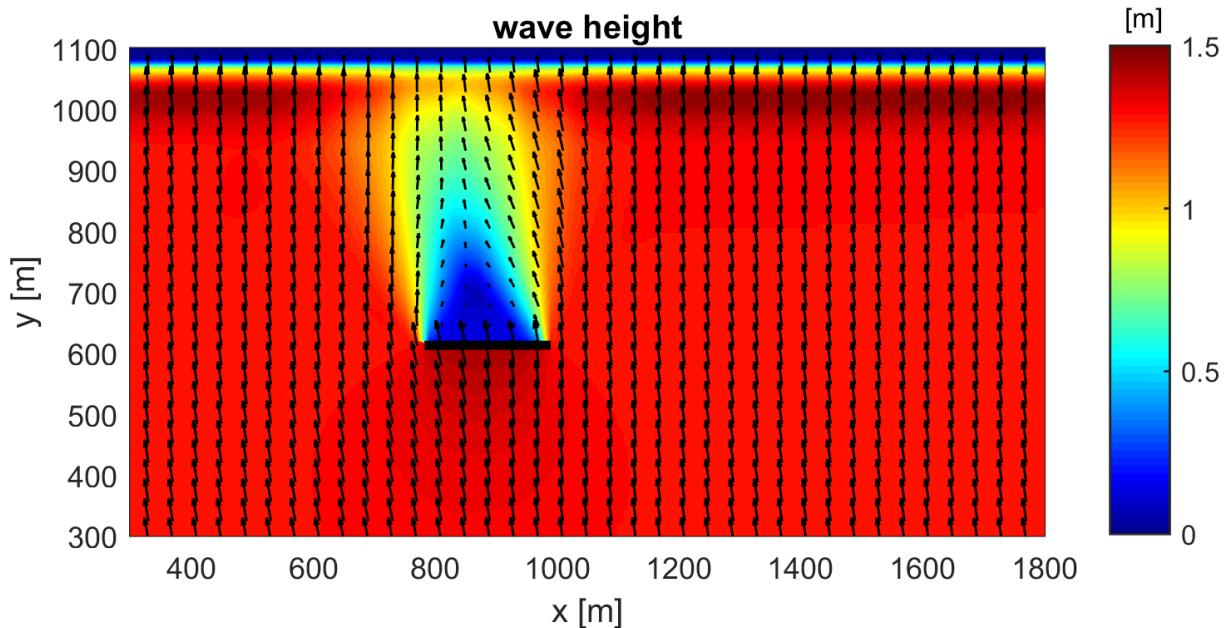


Figure 3.5.3 Computed wave heights and directions (based on SWAN-model); $H_{s,o} = 1.25$ m

Figure 3.5.3 shows the computed wave heights and directions in the lee of the breakwater. The significant wave height is strongly reduced in the lee of the breakwater.

Figure 3.5.4 shows the flow velocities in the lee of the breakwater. The wave-induced flow velocity is about 0.7 m/s at the upwave (right) side increasing to about 1 m/s in the lee of the breakwater. Circulation cells can be observed in the lee of the breakwater and at the downwave (left) side.

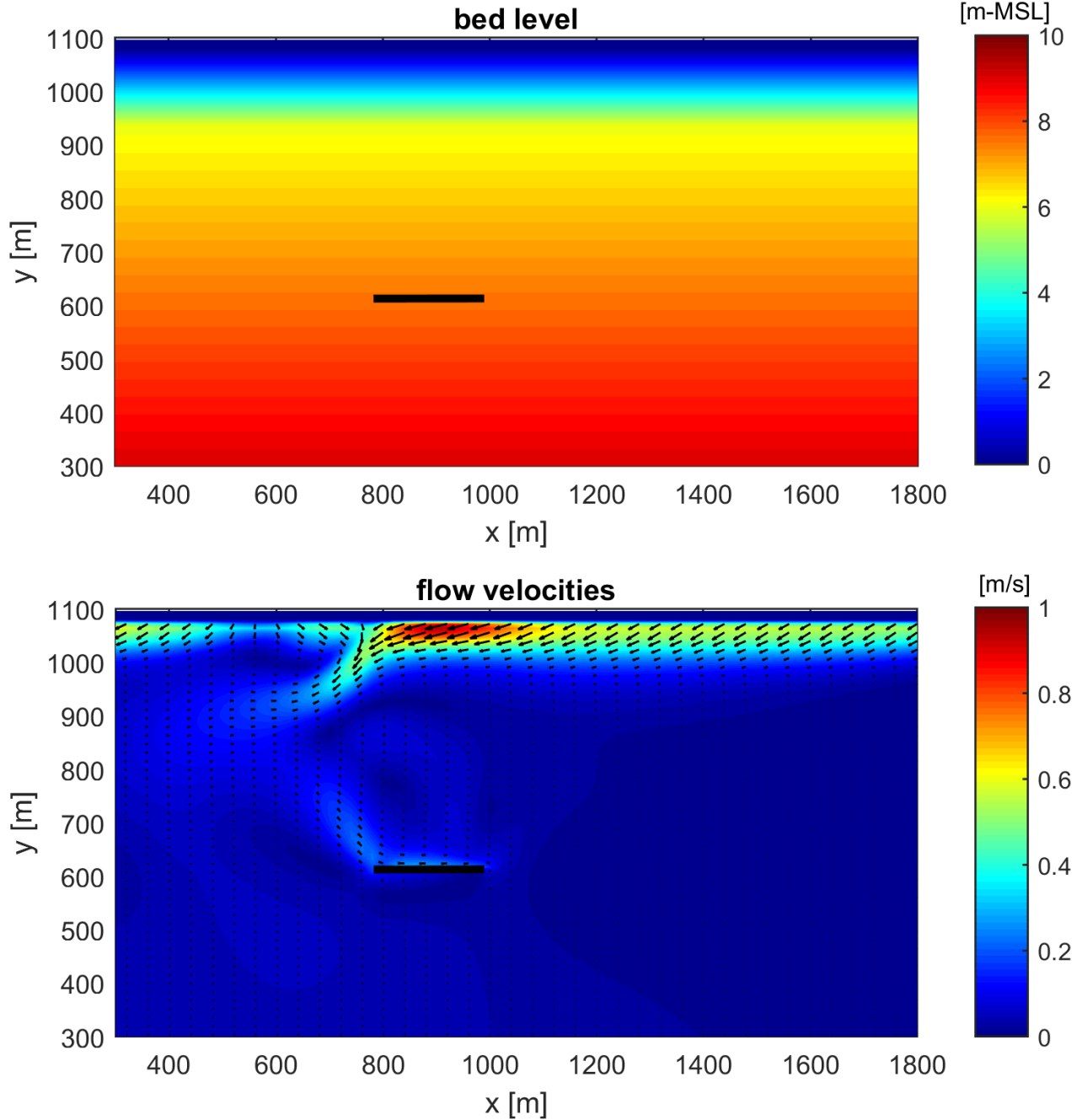


Figure 3.5.4 Computed flow velocities (based on DELFT3D-model); $H_{s,0} = 1.25$ m



Figure 3.5.5 shows the computed coastline changes after 5 years with the development of a salient in the lee of the breakwater.

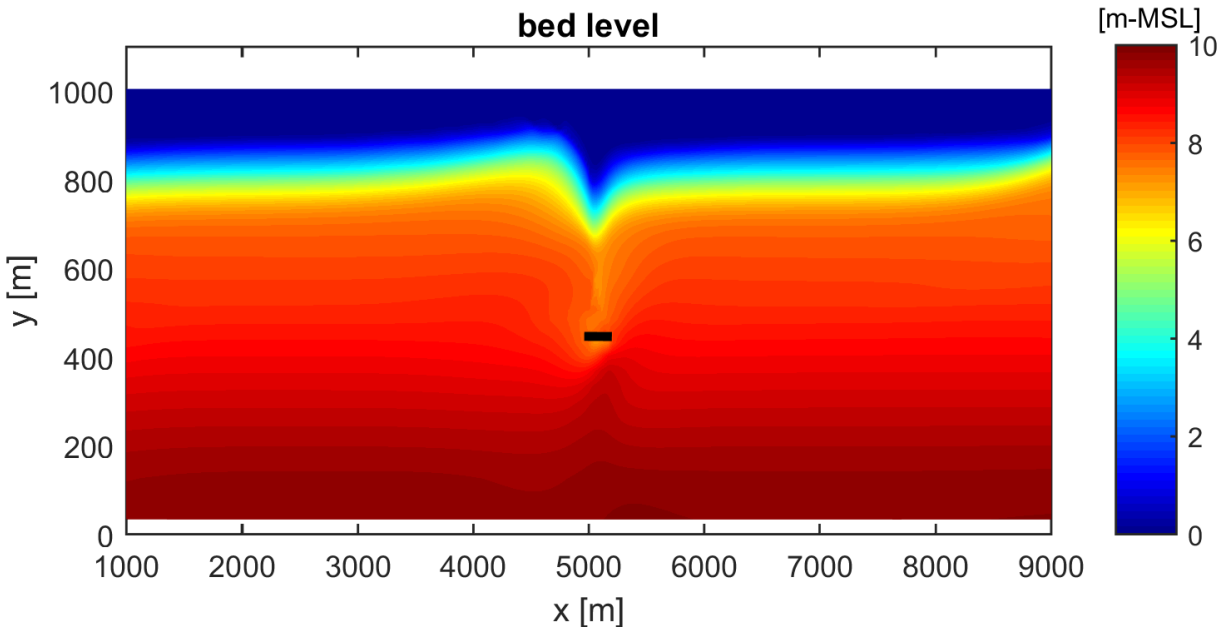


Figure 3.5.5 Computed coastline changes (based on DELFT3D-model); $H_{s,o} = 1.25$ m

LONGMOR-model

The LONGMOR 1D-model has been used to compute the coastline changes in the lee of the breakwater. The LONGMOR1D-model cannot accurately compute the longshore transport rates in the lee of the breakwater. Therefore, the longshore transport rates have been taken from the DELFT3D-model for one representative wave condition ($H_{s,o}=1.25$ m, $T_p=12$ s and wave incidence angle= 10°), see Figure 3.5.6. These values have been used to calibrate the longshore transport rates of the LONGMOR1D-model.

The results of Figure 3.5.6 shows the following phenomena:

- the longshore sand transport faraway from the structure is about $1000 \text{ m}^3/\text{day}$;
- the longshore sand transport increases to about $2500 \text{ m}^3/\text{day}$ (increase of factor 2.5) in the lee of the breakwater due to the generation of circulation velocities (setup differences);
- the longshore sand transport reduces to almost nil at a distance of about 100 m downdrift of the structure due to the strong reduction in wave height and current velocity;
- the longshore sand transport increases/re-adjusts to about $1000 \text{ m}^3/\text{day}$ over a distance of about 600 m (3 times the length of the structure) at the downdrift side.

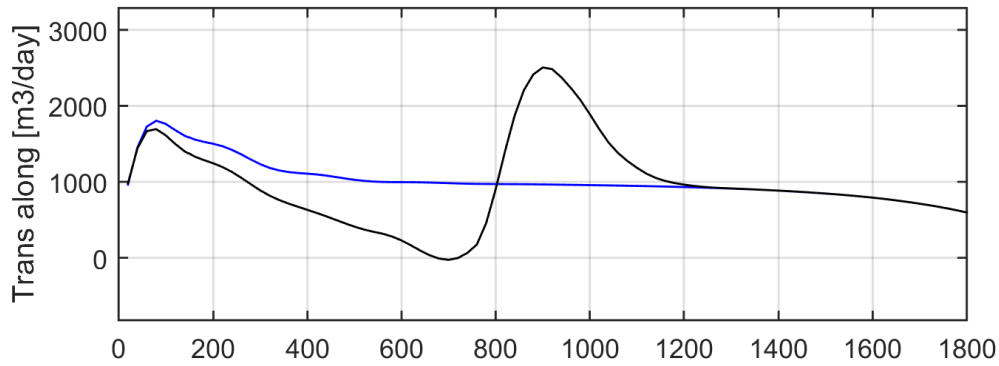


Figure 3.5.6 Computed longshore sand transport integrated over surf zone; location structure = 800-1000 m; $H_{s,o}=1.25$ m, $T_p=12$ s, wave incidence angle= 10° from southwest (right)

The input values of the LONGMOR1D-model is given in **Table 3.5.1**.

PARAMETER	VALUES
Offshore significant wave height	1.25 m during 200 days and 1.15 m during 165 days
Offshore wave angle to coast normal	10° and -10°
Peak wave period	12 s
Grid size and traject length	10 m; 10000 m
Time step and grid-'smoothing'	0.05 day; 0.001
Sand d_{50} , d_{90}	0.3; 0.6 mm
Slope beach-surf zone 0 tot -6 m MSL	1 to 33 (tan slope=0.03)
Breaker coefficient	0.7
Layer thickness of active zone	7 m (between +1 and -6 m to CD)
Longshore transport formula; Calibration coefficient	Van Rijn 2014; 1.05
Net longshore sand transport	100,000 m ³ /year
Angle of coastnormal to North	40 degrees
Tidal currents in surf zone	$V_{flood}=0$ m/s; $V_{ebb}=0$ m/s (no effect if both values are equal)
Beach nourishment volumes	0
Input files	congo1.inp;congo2.inp; congo3.inp; congo4.inp

Table 3.5.1 Input data of LONGMOR1D-model

The following cases have been distinguished:

- structure with 100% blocking of longshore transport;
- structure with reduced blocking (calibration based on results of DELFT3D-model);



Structure with 100% blocking

The most simple approach is to assume that the longshore sand transport is fully blocked (blocking of 100%) by the detached breakwater (as if the breakwater acts as a groin).

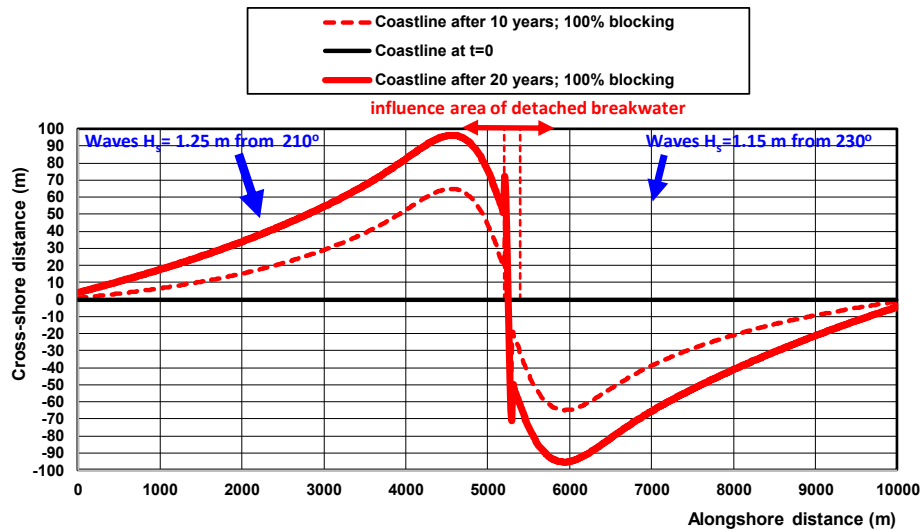


Figure 3.5.7 Computed coastlines of LONGMOR1D-model after 10 and 20 years in the case of a structure with 100% blocking; $LT=100,000 \text{ m}^3/\text{year}$

Figure 3.5.7 shows the computed coastlines after 10 and 20 years. The maximum coastline accretion is about 100 m at the updrift side of the structure. The accretion extends over an updrift distance of about 5 km. Severe erosion is present at the downdrift side.

Structure with reduced blocking

A detached breakwater is a structure which allows the passage of longshore sand transport in the lee of the structure. The reduction (blocking) of the longshore sand transport depends on the ratio of the structure length (L) and the distance (D) between the structure and the coastline.

Based on the DELFT3D-model results, the LONGMOR1D-model has been calibrated to give (for both wave directions 10° and -10°):

- longshore sand transport ($Q_{LT,x=0}$) is constant up to start of breakwater;
- increase of longshore transport to $1.5Q_{LT,x=0}$ at end of breakwater;
- decrease of longshore transport to $0.2Q_{LT,x=0}$ at 200 m beyond downdrift end of breakwater;
- increase of longshore transport to $Q_{LT,x=0}$ at 400 m beyond downdrift end of breakwater;
- longshore sand transport ($Q_{LT,x=0}$) is constant up to end of computational domain.

Figure 3.5.8 shows the computed coastlines after 10, 20 and 40 years. Minimal numerical smoothing ($<1\%$) has been applied. A salient is generated in the lee of the detached breakwater.

The maximum cross-shore extension of the salient is about 60 m after 10 years, which remains stable over a time scale of 40 years. The cross-shore extension is about 12% of the distance between the breakwater and the coast.

The alongshore length scale of the salient is about 600 to 700 m (3 times the length of the breakwater).

The coastal accretion updrift of the salient is about 15 m after 40 years; the maximum coastal recession is about 15 to 20 m on both sides of the structure after 40 years. The alongshore erosion scale is almost 3 km at the downdrift side.

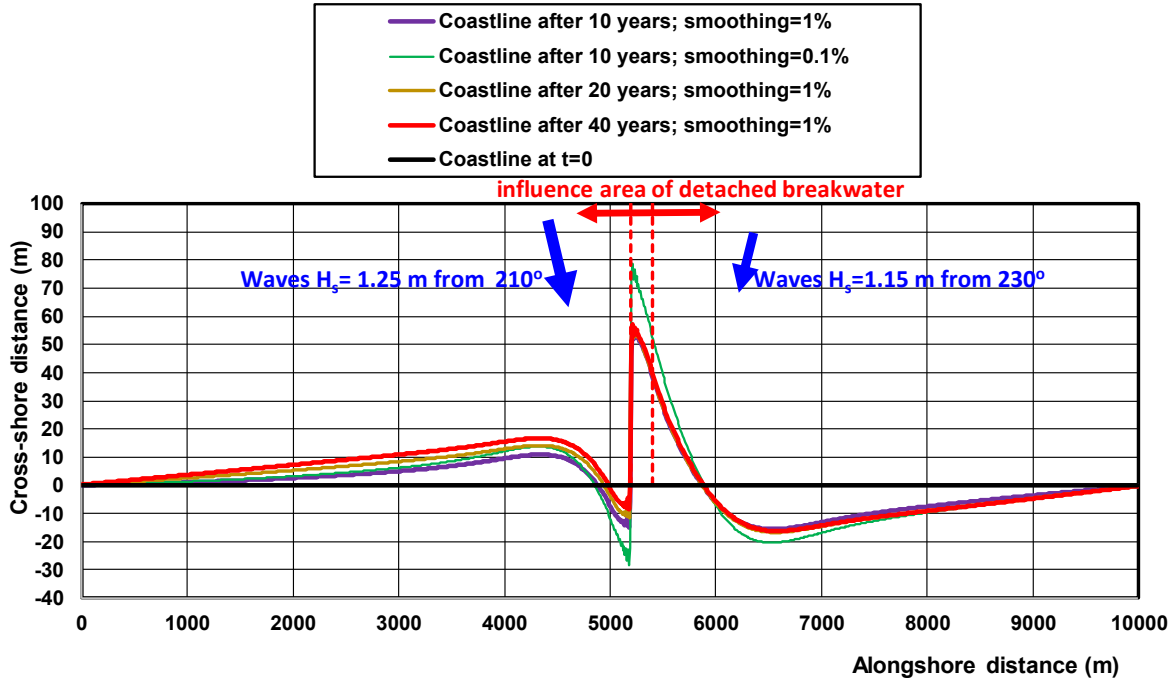


Figure 3.5.8 Computed coastlines of LONGMOR1D-model after 10, 20 and 40 years in the case of a detached breakwater with reduced blocking; $LT=100,000 \text{ m}^3/\text{year}$

Figure 3.5.9 shows similar computation results for a longshore transport rate of $200,000 \text{ m}^3/\text{year}$ (wave heights are 1.25 and 1.15 m; wave incidence angles are 20° and -20°). A much larger salient is generated in the lee of the detached breakwater. The maximum cross-shore extension of the salient is about 150 m after 40 years. The coastal accretion updrift of the salient is about 40 m after 40 years; the maximum coastal recession is about 40 m on both sides of the structure after 40 years. The alongshore erosion scale is almost 4 km at the downdrift side.

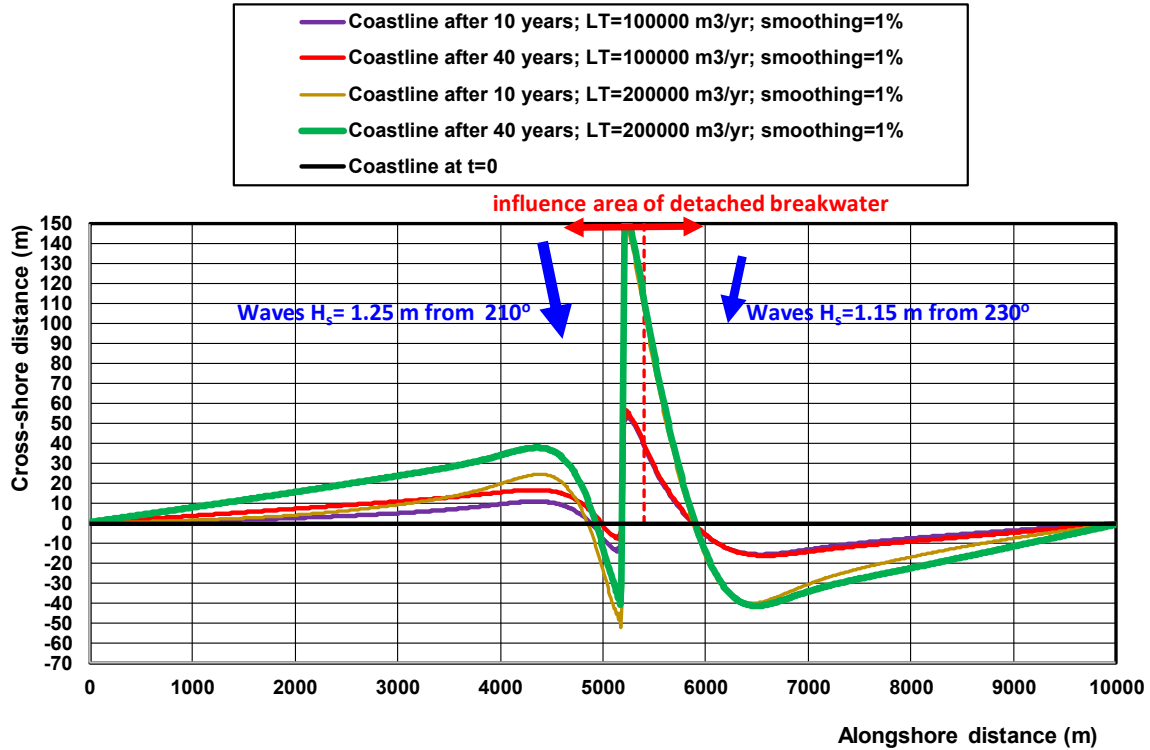


Figure 3.5.9 Computed coastlines of LONGMOR1D-model after 10, 20 and 40 years in the case of a detached breakwater with reduced blocking; $LT=100,000$ and $200,000 \text{ m}^3/\text{year}$



3.6 Design of long groyne near Soulac sur Mer, France

3.6.1 General

Since long the beaches between Négade and the inlet of the Garonne in France are eroding with rates of 5 to 10 m per year despite many coastal defense works (structures). The evacuation of the building Le Signal at the beach front of Soulac in January 2014 marks the severity of the erosion problems. In response to that, Barriquand groin at the north beach of Soulac was extended in 2014 to promote more deposition of sand at the beach. In 2018, the local authorities (Communauté de Communes Médoc Atlantique; CDC MA) have adopted a new strategy aimed at:

- reduction of the erosion vulnerability of the coast;
- maintenance and reinforcement of defense structures at the beaches of the urbanized areas;
- regular placements of beach sand to prevent beach erosion.

The objective of the present study is to propose a series of technical coastal protection measures for the coastal section between L'Amélie and the Barriquand-groin in the north of Soulac sur Mer. This coastal section consists of (see **Figure 3.6.1**):

- Les dunes de L'Amélie (1.5 km);
- La plage des Naiades (1 km);
- Les dunes de Boulevard (0.5 km);
- La Plage centrale jusqu'a l'épi Barriquand (1 km);
- Les brise-mers des Arros, des Huttes et des Cantines (3.1 km);
- Les dunes de Tout-Vent (0.6 km).



Figure 3.6.1 Coastal region between Point La Grave (north) and Point La Négade (south)

3.6.2 Longshore sand transport computations



Methods

Two methods have been used to compute the longshore sand transport at various locations along the coast between Négade and Barriquand., as follows:

- simplified LONGMOR-model; which computes the wave height and the wave incidence angle at the breaker line and, based on that, the longshore sand transport rate in the surf zone for a given annual offshore wave climate; three longshore sand transport equations are implemented (CERC, Kamphuis 1991 and Van Rijn); the model is valid for uniform shorelines with shore-parallel depth contours;
- detailed CROSMOR-model; which computes the wave heights, longshore and cross-shore currents and longshore and cross-shore sand transport rates along a bottom profile normal to the shore.

The basic input parameters of both models are given in **Table 3.6.1**.

Model	Parameters	Values
LONGMOR	1. Offshore depth (m to CD)	-20
	2. Tidal currents (m/s)	0
	3. Breaking coefficient= ratio of wave height and water depth at breakerline	0.5
	3. Median sand diameter (mm)	0.35
	4. Beach slope	0.01
CROSMOR	5. Fluid and sediment density (kg/m ³)	1020, 2650
	1. Offshore depth (m to CD)	-30
	2. Depth-averaged flood/ebb tidal currents at offshore boundary (m/s)	0.3; -0.3
	3. Tidal flood/ebb water levels to mean sea level (m)	1.7; -1.7
	4. Water depth at most landward grid point (m)	0.3
	5. Storm surge level (m)	0
	6. Number of Rayleigh-distributed wave classes	10
	7. Wave breaking	automatic
	8. Horizontal mixing coefficient (m ² /s)	0.1
	9. Sand diameter d ₅₀ , d ₉₀ (mm)	0.35; 0.7
	10. Bed roughness	automatic
	11. grid size (m)	2 to 50
12. Time step	automatic	

Table 3.6.1 General model input parameters

LONGMOR-model results

Figure 3.6.2 and **Table 3.6.3** show the computed longshore sand transport (LST) values of Kamphuis (1991) and Van Rijn (2014) as function of the shore normal angle varied in the range of 80° to 180°. The LT-equation of Bayram et al. (2007) has also been used (see Table 3.2.1), but the values are much smaller (factor 3 to 4) than the other LT-values.

The LST-values are based on the detailed wave climate with 59 wave classes of **Table 3.6.2**.

The shore normal angle to North is defined as the angle of the normal line from the sea to the beach.

The wave incidence angle is defined as the angle of the wave propagation vector to North. Three LST-values are shown: northgoing value, southgoing value and net value.

The LST-values predicted by the method of Van Rijn are higher (up to 50%) than those of the method of Kamphuis. The method of Van Rijn (2014) has also been used with the tidal current included (depth-averaged velocity of +0.3 and -0.3 m/s in the surf zone) resulting in much smaller net northgoing longshore sand transport values (compare red solid curve and dashed red curve) as the southgoing longshore sand transport is much higher due the southgoing tidal current.

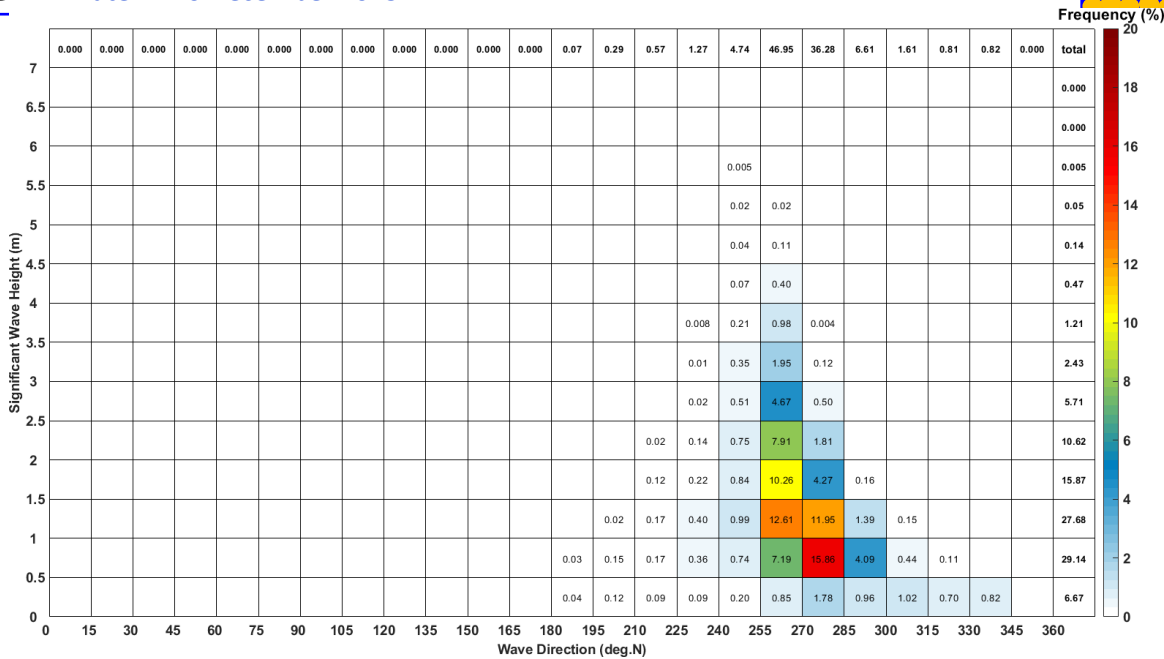
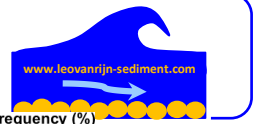


Table 3.6.2 Annual-averaged wave data (2009-2019) at -20 m of location Center

The results clearly indicate that the northgoing LST is strongly dominant for angles > 90° (north of Point Négade). The southgoing LST-values are only substantial for angles < 90° (south of Point Négade). The northgoing LST is maximum with a value of 1 to 1.5 million m³/year around an angle of 125° (close to Barriquand). It should be realized that the LST-values represent sand transport capacity values. The actual LST are most likely smaller due to the presence of structures and limited availability of sand.

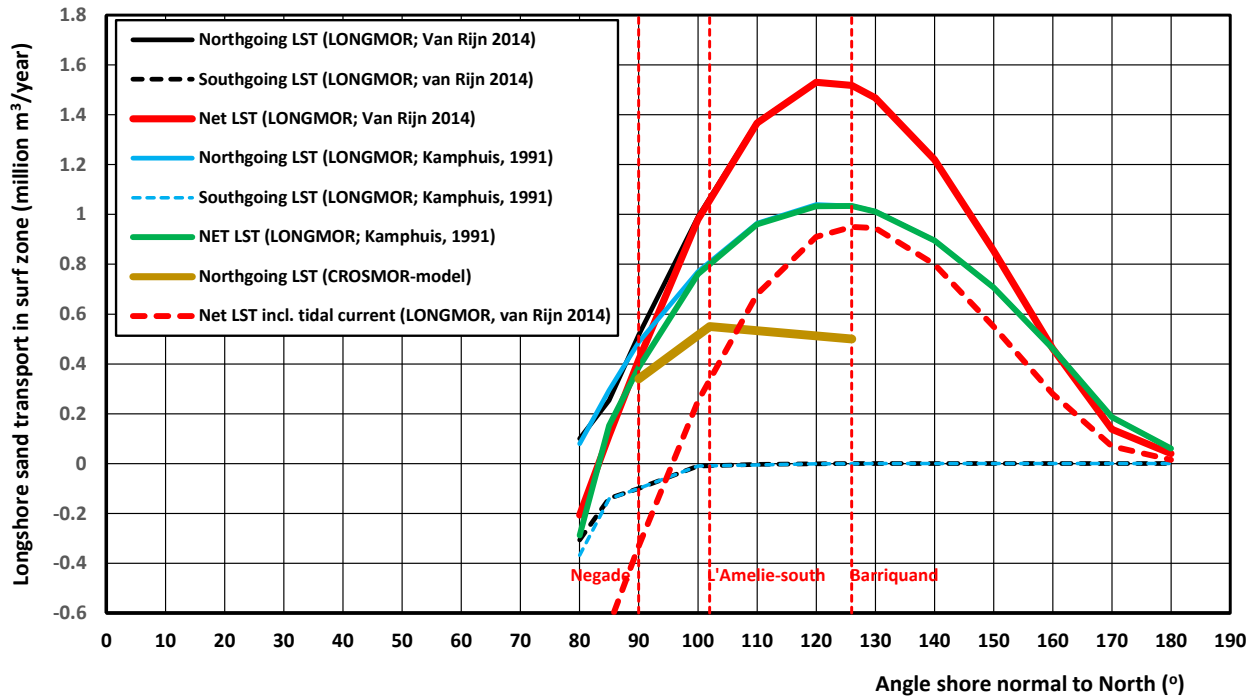


Figure 3.6.2 Longshore sand transport at locations north of Point Négade, LONGMOR; $d_{50}=0.35$ mm



Angle of shore normal (from sea to beach) to North (°)	Longshore sand transport (Mm ³ /year) excluding tidal current Van Rijn (2014)			Longshore sand transport (Mm ³ /year) Kamphuis (1991)			Longshore sand transport (Mm ³ /year) Bayram et al. (2007)		
	North going	South going	Net	North going	South going	Net	North going	South going	Net
80	0.1	-0.306	-0.206	0.08	-0.368	-0.288	0.035	-0.85	-0.05
85	0.253	-0.14	0.133	0.294	-0.142	0.152	0.085	-0.035	0.05
90	0.517	-0.1	0.417	0.487	-0.1	0.387	0.173	-0.022	0.151
100	0.99	-0.01	0.98	0.77	-0.01	0.76	0.32	-0.017	0.31
110	1.37	-0.003	1.367	0.965	-0.005	0.96	0.41	-0.0005	0.41
120	1.531	-0.0006	1.5304	1.04	-0.001	1.033	0.42	-0.0001	0.42
126	1.519	-0.0002	1.5182	1.034	-0.0005	1.0335	0.4	0	0.4
130	1.468	-0.0001	1.4679	1.012	-0.0002	1.0118	0.37	0	0.37
140	1.22	0	1.22	0.895	-0.0001	0.8949	0.275	0	0.275
150	0.855	0	0.855	0.707	0	0.707	0.166	0	0.166
160	0.462	0	0.462	0.462	0	0.462	0.075	0	0.075
170	0.138	0	0.138	0.187	0	0.187	0.018	0	0.018
180	0.04	0	0.04	0.06	0	0.06	0.0045	0	0.0045

Angle shore normal to beach: Négade \cong 90°; L'Amélie-south \cong 103°; Barriquand \cong 126°

Transport coefficient Bayram=(9+4H_{s,br}/(w_s T_p))10⁻⁵, w_s=0.06 m/s =settling velocity

Table 3.6.3 Longshore sand transport (millions m³/yr); north of Point Négade, LONGMOR; d₅₀=0.35 mm

CROSMOR-model results

To get a better understanding of the wave and sand transport parameters along cross-shore bottom profiles, the CROSMOR-model has also been used (Files: SBAR1; SBAR2; SLAM1; SNEG1, Soulac1). This model has been applied to the cross-shore bottom profiles of Barriquand-northwest, L'Amélie-north, L'Amélie-south and Négade. The wave climate is based on location Center (**Table 3.6.2**) for Barriquand-northwest and location South for L'Amélie-north, L'Amélie-south and Négade. Six to seven wave cases including 90% of the wave energy are considered, see **Tables 3.6.4** to **3.6.7**.

The wave and transport parameter are computed for both HW (+1.7 m above mean sea level) and LW (-1.7 m). The effect of the tide level on LST is small. Model runs with and without tidal currents have been made. The tide-averaged and depth-averaged current velocity during the flood/ebb phases of the tide are represented by values of +0.3 m/s (flood to north) and -0.3 m/s (ebb to south). The results of the model runs with tidal currents have been used to derive the total sand transport on the shoreface (between -20 m and -5 m; seaward of the surf zone) as the total LST minus the LST in the surf zone.

The computed longshore sand transport values are, as follows (see also **Figure 3.6.4**):

Barriquand profile

- northgoing longshore sand transport in the surf zone (width up to 250 m) is about 0.5 M m³/year (million m³/year);
- total northgoing longshore sand transport increases to approximately 1.2 M m³/year when the tidal current velocities are included;
- northgoing longshore sand transport in shoreface zone is about 0.7 M m³/year;
- southgoing longshore sand transport in surf zone is absent;



L'Amelie-north

- northgoing longshore sand transport in the surf zone is about 0.55 M m³/year (million m³/year);
- total northgoing longshore sand transport increases to approximately 0.92 M m³/year when the tidal current velocities are included;
- net northgoing longshore sand transport in shoreface zone is about 0.42 M m³/year;
- southgoing longshore sand transport in surf zone is absent;

L'Amelie-south

- northgoing longshore sand transport in the surf zone is about 0.55 M m³/year (million m³/year);
- total northgoing longshore sand transport increases to approximately 0.7 M m³/year when the tidal current velocities are included;
- net northgoing longshore sand transport in shoreface zone is about 0.25 M m³/year; southgoing transport is increasing but smaller than northgoing transport);
- southgoing longshore sand transport in surf zone is absent;

Négade

- northgoing longshore sand transport in the surf zone is about 0.34 M m³/year (million m³/year);
- total northgoing longshore sand transport is about 0.32 M m³/year when the tidal current velocities are included;
- northgoing and southgoing longshore sand transport in shoreface zone are almost equal (net transport is almost zero);
- southgoing longshore sand transport in surf zone is minor.

Figure 3.6.3 shows the cross-shore distribution of wave height, longshore current velocity and sand transport along the Barriquand-profile for Case WSW4 during HW and LW of **Table 3.6.4**. The longshore current velocity at the offshore boundary is set to 0.3 m/s (flood) to north during HW and -0.3 m/s to south (ebb) during LW.

Typical features are:

- nearshore wave height is somewhat smaller during LW due wave breaking effects;
- longshore current during LW is to south (negative values) on the shoreface and gradually decreases in landward direction due to bottom friction; maximum longshore current in the surf zone during LW is 0.35 m/s to north (current velocities change from south to north near the shore); maximum longshore current in the surf zone during HW is 0.55 m/s to the north;
- longshore sand transport on the shoreface is to the north during HW;
- longshore sand transport on the shoreface is also to the north during LW when the longshore current is to the south; this is caused by the wave asymmetry effect on the bed load transport generating a relatively strong north-going transport; the longshore transport on the shore face is to south when wave asymmetry effects are neglected;
- longshore sand transport in the surf zone with breaking waves is relatively high and always to the north as the waves come in from west-south-west

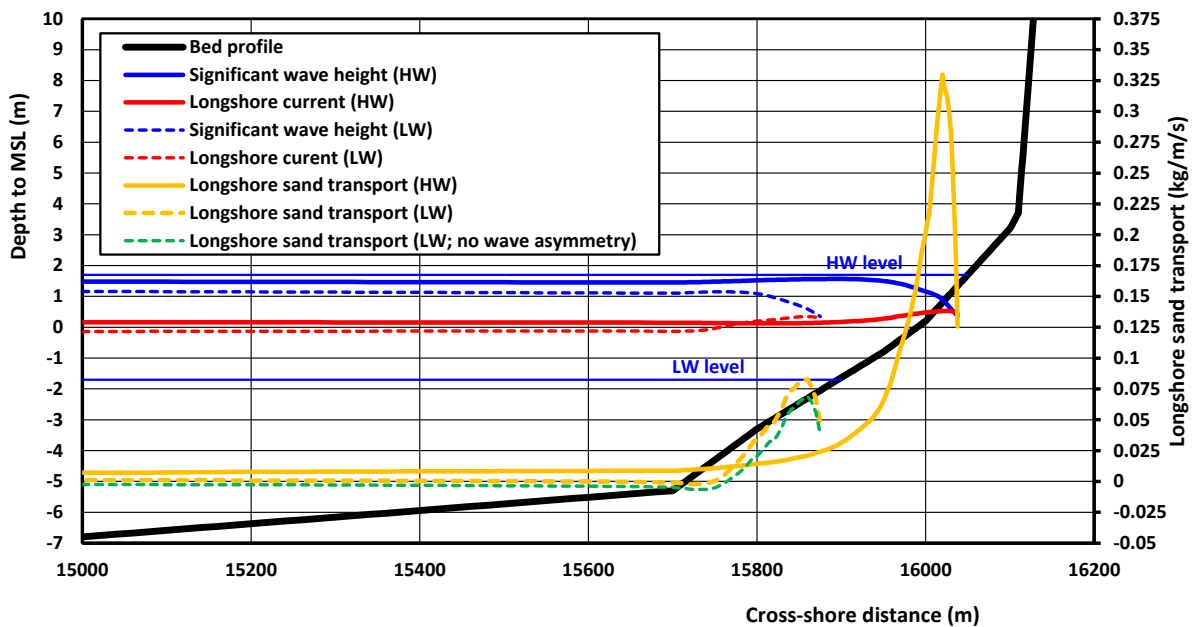
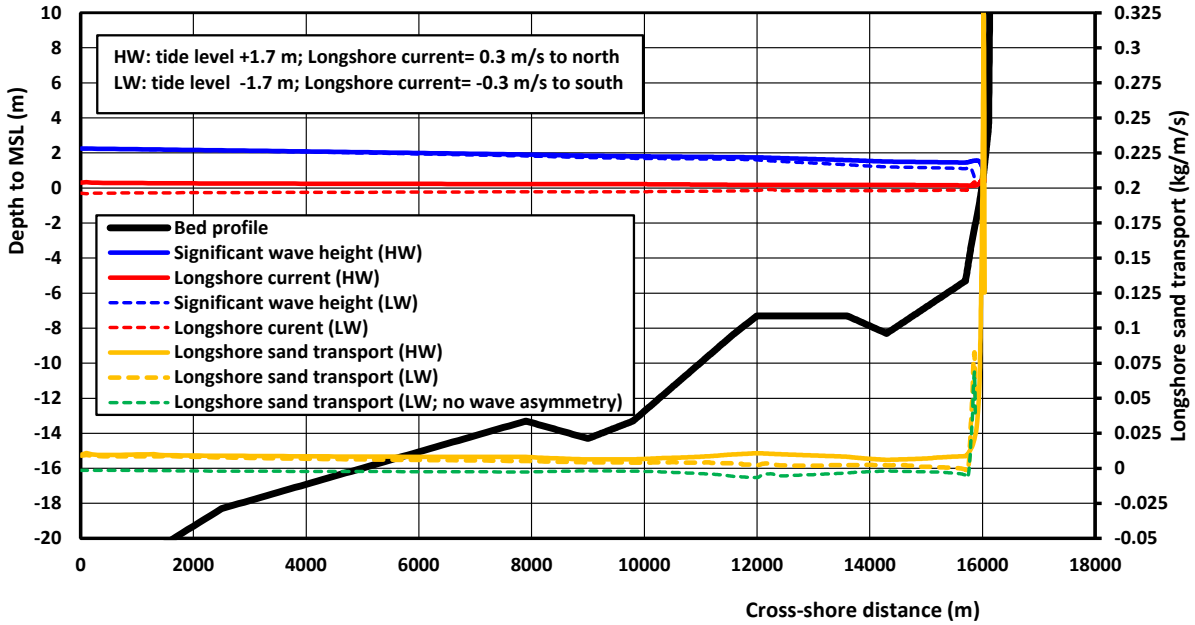


Figure 3.6.3 Computed wave height, longshore current velocity and longshore sand transport along cross-shore profile Barriquand-northwest; Case WSW4; $d_{50}=0.35$ mm; CROSMOR-model
Upper: deep water to shore profile; Lower: nearshore profile

Case	Offshore waves	Offshore wave	Per cen		Waves	Maximum longshore		Longshore sand transport ($m^3/year$)
------	----------------	---------------	---------	--	-------	-------------------	--	---



	H _s (m) T _p (s) α (°)	incidence angle (°) to shore normal	tage occurrence p (%)	Tide level and longshore current velocity at offshore boundary	at breaker line H _{s,br} (m) α _{br} (°)	and cross-shore current (m/s)	Surf zone width (m)	+=northgoing -=southgoing	
								Excluding tidal current	Including tidal current
W1	0.75; 7; 275 (95)	31	27	HW +1.7 m; v=0.3 m/s	0.58; 9	0.15; -0.05	40	1,200	6,000
				LW -1.7 m; v=-0.3 m/s	0.4; 8	0.05; -0.03	40	1,000	-5,000
W2	1.25; 9; 272 (92)	34	27	HW +1.7 m; v=0.3 m/s	0.9; 11	0.3; -0.1	70	10,000	33,000
				LW -1.7 m; v=-0.3 m/s	0.6; 9	0.15; -0.05	60	10,000	5,000
W3	1.75; 10; 268 (88)	38	15	HW +1.7 m; v=0.3 m/s	1.2; 14	0.4; -0.2	110	21,000	55,000
				LW -1.7 m; v=-0.3 m/s	0.8; 11.5	0.25; -0.1	100	21,000	17,000
WSW4	2.25; 12; 265 (85)	41	10	HW +1.7 m; v=0.3 m/s	1.5; 17	0.55; -0.25	190	45,000	150,000
				LW -1.7 m; v=-0.3 m/s	1.1; 15	0.35; -0.15	150	48,000	84,000
WSW1	3.0; 13; 262 (82)	44	8	HW +1.7 m; v=0.3 m/s	2.05; 20	0.7; -0.35	280	106,000	367,000
				LW -1.7 m; v=-0.3 m/s	1.6; 16	0.45; -0.2	160	110,000	195,000
WSW2	3.75; 14; 262 (82)	44	2	HW +1.7 m; v=-0.3 m/s	2.65; 21	0.9; -0.4	290	60,000	180,000
				LW -1.7 m; v=-0.3 m/s	1.8; 16	0.6; -0.25	170	63,000	83,000
Total								0.5 Mm³ to north	1.22 Mm³ to north; 0.005 Mm³ to south

α_o= offshore wave incidence angle to North; angle shore normal from beach to sea=306° (126°)

Tidal current positive = to north; Tidal current negative= to south

Table 3.6.4 Computed longshore sand transport at Barriquand-northwest profile; d₅₀=0.35 mm; CROSMOR

Case	Offshore waves H _s (m) T _p (s) α (°)	Offshore wave incidence angle (°) to shore normal	Percentage occurrence p (%)	Tide level and longshore current velocity at offshore boundary	Longshore sand transport (m ³ /year)	
					+=northgoing -=southgoing	Excluding tidal current
WNW1	0.75; 7; 275 (95)	31	31	HW +1.7 m; v=0.3 m/s	1,800	7,300
				LW -1.7 m; v=-0.3 m/s	1,800	-4,500
WSW1	0.9; 9; 265 (85)	41	26	HW +1.7 m; v=0.3 m/s	11,000	36,000
				LW -1.7 m; v=-0.3 m/s	14,000	-500
WSW2	1.25; 10; 263 (83)	43	15	HW +1.7 m; v=0.3 m/s	25,000	68,000
				LW -1.7 m; v=-0.3 m/s	35,000	22,000
WSW3	1.6; 12; 260 (80)	46	10	HW +1.7 m; v=0.3 m/s	55,000	159,000
				LW -1.7 m; v=-0.3 m/s	79,000	82,000
WSW4	2.0; 13; 260 (80)	46	5	HW +1.7 m; v=0.3 m/s	67,000	172,000
				LW -1.7 m; v=-0.3 m/s	80,000	97,000
WSW5	2.35; 14; 260 (80)	46	2	HW +1.7 m; v=-0.3 m/s	52,000	113,000
				LW -1.7 m; v=-0.3 m/s	76,000	67,000
WSW6	3.05; 15; 255 (75)	51	0.5	HW +1.7 m; v=-0.3 m/s	33,000	55,000
				LW -1.7 m; v=-0.3 m/s	45,000	39,000
Total					0.52 Mm³ to north	0.92 Mm³ to north; 0.005 Mm³ to south

α_o= offshore wave incidence angle to North; angle shore normal from beach to sea=306° (126°)

Table 3.6.5 Computed longshore sand transport at L'Amelie north profile; d₅₀=0.35 mm; CROSMORI

Case	Offshore waves H _s (m)	Offshore wave incidence	Percentage occurrence	Tide level and longshore current	Longshore sand transport (m ³ /year) +=northgoing
------	-----------------------------------	-------------------------	-----------------------	----------------------------------	--



	T _p (s) α (°)	angle (°) to shore normal	rence p (%)	velocity at offshore boundary	-southgoing	
					Excluding tidal current	Including tidal current
WNW1	0.75; 7; 275 (95)	7	31	HW +1.7 m; v=0.3 m/s	1,200	6,000
				LW -1.7 m; v=-0.3 m/s	1,500	-4,000
WSW1	0.9; 9; 265 (85)	17	26	HW +1.7 m; v=0.3 m/s	8,500	28,000
				LW -1.7 m; v=-0.3 m/s	15,000	-10,000
WSW2	1.25; 10; 263 (83)	19	15	HW +1.7 m; v=0.3 m/s	20,000	61,000
				LW -1.7 m; v=-0.3 m/s	30,000	6,600
WSW3	1.6; 12; 260 (80)	22	10	HW +1.7 m; v=0.3 m/s	50,000	140,000
				LW -1.7 m; v=-0.3 m/s	77,000	39,000
WSW4	2.0; 13; 260 (80)	22	5	HW +1.7 m; v=0.3 m/s	60,000	145,000
				LW -1.7 m; v=-0.3 m/s	93,000	53,000
WSW5	2.35; 14; 260 (80)	22	2	HW +1.7 m; v=-0.3 m/s	45,000	97,000
				LW -1.7 m; v=-0.3 m/s	65,000	40,000
WSW6	3.05; 15; 255 (75)	27	0.5	HW +1.7 m; v=-0.3 m/s	33,000	52,000
				LW -1.7 m; v=-0.3 m/s	45,000	32,000
Total					0.55 Mm³ to north	0.7 Mm³ to north; 0.014 Mm³ to south

α_o= offshore wave incidence angle to North; angle shore normal from beach to sea=282° (102°)

Tidal current positive = to north; Tidal current negative= to south

Table 3.6.6 Computed longshore sand transport at L'Amelie south profile; d₅₀=0.35 mm; CROSMOR

Case	Offshore waves H _s (m) T _p (s) α (°)	Offshore wave incidence angle (°) to shore normal	Percent occurrence p (%)	Tide level and longshore current velocity at offshore boundary	Longshore sand transport (m ³ /year)	
					+northgoing	-southgoing
					Excluding tidal current	Including tidal current
WNW1	0.75; 7; 275 (95)	-5	31	HW +1.7 m; v=0.3 m/s	-1,500	1,600
				LW -1.7 m; v=-0.3 m/s	-600	-5,000
WSW1	0.9; 9; 265 (85)	5	26	HW +1.7 m; v=0.3 m/s	8,500	20,000
				LW -1.7 m; v=-0.3 m/s	4,900	-14,000
WSW2	1.25; 10; 263 (83)	7	15	HW +1.7 m; v=0.3 m/s	17,000	39,000
				LW -1.7 m; v=-0.3 m/s	12,000	-20,000
WSW3	1.6; 12; 260 (80)	10	10	HW +1.7 m; v=0.3 m/s	36,000	83,000
				LW -1.7 m; v=-0.3 m/s	29,000	-8,000
WSW4	2.0; 13; 260 (80)	10	5	HW +1.7 m; v=0.3 m/s	39,000	86,000
				LW -1.7 m; v=-0.3 m/s	34,000	1,000
WSW5	2.35; 14; 260 (80)	10	2	HW +1.7 m; v=-0.3 m/s	23,000	48,000
				LW -1.7 m; v=-0.3 m/s	21,000	2,000
WSW6	3.05; 15; 255 (75)	15	0.5	HW +1.7 m; v=-0.3 m/s	18,000	30,000
				LW -1.7 m; v=-0.3 m/s	19,000	10,000
Total					0.34 Mm³ to north	0.32 Mm³ to north; 0.047 Mm³ to south

α_o= offshore wave incidence angle to North; angle shore normal from beach to sea =270° (90°)

Table 3.6.7 Computed longshore sand transport at Négade profile; d₅₀=0.35 mm;Crosmorl

Best estimate of longshore sand transport

Information of the north-going longshore sand transport (LST) from earlier studies shows values between 0.1 and 0.6 Mm³/year.



The results of the LONGMOR and CROSMOR-models indicate values in the range of 0.3 to 1.5 Mm³/year in the surf and shoreface zone between Négade and Barriquand. The LST values of the CROSMOR-model are more realistic than the values of the LONGMOR-model, as the actual cross-shore bottom profile is taken into account. The CROSMOR-model also produces LST-values in the shoreface zone.

Based on this, the best estimate of the LST in the surf and shoreface zones are shown in **Figure 3.6.4** and in **Table 3.2.8**. The north-going LST in the surf zone increases from south to north due to an increasing wave incidence angle with respect to the coastline angle. South of Négade is a point of zero LST (divergence point or null point). The maximum LST of about 0.6 Mm³/year is in good agreement with the annual erosion volume of about 0.7 Mm³/year between Négade and Le Signal.

It should be realized that the values given in Figure 3.6.4 for the surf zone are sand transport capacity values in conditions with unlimited supply of sand (long and straight beaches; wide and high beaches; multiple breaker bars).

The coastal section of Soulac and adjacent beaches has a northern boundary at the inlet and a southern boundary at Négade, where the longshore sand transport is almost zero (null point). The total length of this coastal section is about 11 km. Most of the sand supply comes from dune erosion in two regions: Négade-L'Amelie (1.5 km) and L'Amelie-Camping LS (1.5 km). The actual net longshore sand transport at Soulac beach is unknown, but is less than the longshore sand transport capacity and is estimated to be about 300,000 ± 150,000 m³/year.

In the future, the longshore sand transport at Soulac beach may be substantially smaller if measures (dune revetments) are taken to reduce the dune erosion between Négade and Camping Les Sables.



Figure 3.6.4 Net annual longshore sand transport values in shoreface zone (seaward of -5 m depth) and in surf zone (landward of -5m depth line)

Coastal sand transport	Coastal section L'Amelie to Soulac sur Mer		
	Between LAT and HAT (active layer ≈ 5 m)	Between LAT and -5 m CDL	Between -5 m and -25 m CD



Net annual longshore sand transport (NALT) excluding tidal currents (m ³ /year)	lower limit-upper limit 100.000-200.000	100.000-200.000	<100.000
Net annual longshore sand transport (NALT) including tidal currents (m ³ /year)	150.000-300.000	150.000-300.000	300.000-600.000

Table 3.6.8 Best estimates of longshore sand transport in coastal zone between L'Amelie and Soulac sur Mer (sand 0.35 mm); (MSL= mean sea level; LAT \cong 2.5 m below MSL; HAT \cong 2.5 m above MSL)

3.6.2 Coastline hindcast 2014-2021

The LONGMOR-model has been used to hindcast the coastline changes between 2014 and 2021 (5 years), which is the period after extension (with 80 m) of the Barriquand-groin in 2014 (**Figure 3.6.5**). The coastline is defined as the MSL-line (MSL=Mean Sea Level). The model domain extends over about 6 km south of the Barriquand-groin. The tip of the Barriquand-groin is landward of LAT-line (about 2.5 m below MSL).

The model input data are given in **Table 3.6.9**. The angle between the main wave direction and the shore normal varies between 15° (L'Amélie) and 30° (Barriquand).

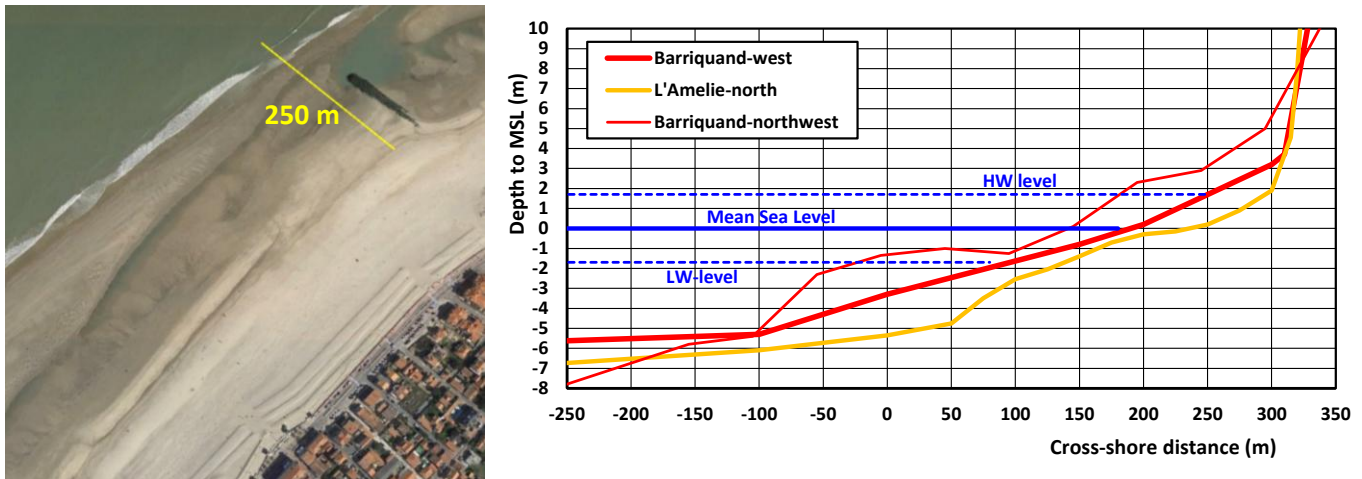


Figure 3.6.5 Width of surf zone near Barriquand-groin seaward of MSL line

Preliminary model runs

Preliminary model runs have been performed based the simplified coastline (2014) derived from Google Earth imagery. The two most important parameters are the net annual langshore sand transport (NALT) and the percentage of bypassing sand transport (BPP) over and along the tip of the groin. The NALT is asumed to be in the range of 150,000 m³/year landward of LAT-line (active layer=5 m) to 500.000 m³/year landward of -5 m depth line below MSL (active layer of 10 m), based on a (separate) detailed study of longshore sand transport for representative wave conditions and tidal currents. The BPP is estimated to be in the range of 40% to 75%, as the existing groin is situated landward of the LAT depth contour, whereas the surf zone extends to the -5 m depth contour. Furthermore, sand will be carried over the groin during storm conditions.

Preliminary model runs have been made for four cases:

- Case A: NALT=300,000 m³/year and BPP=60%; offshore wave incidence angle=30°; Layer= 10 m;
- Case B: NALT=300,000 m³/year and BPP=60%; offshore wave incidence angle=15°; Layer= 10 m;
- Case C: NALT=500,000 m³/year and BPP=75%; offshore wave incidence angle=30°; Layer= 10 m;
- Case D: NALT=150,000 m³/year and BPP=60%; offshore wave incidence angle=30°; Layer= 5 m.



The results of Case A to D are shown in **Figure 3.6.6**.

Case A to D yield similar results. The maximum accretion over 5 years close to the groin is about 60 m, which is slightly less than the extension (80 m) of 2014. The total sand deposition volume of Case D is about 210.000 m³ over 5 years

Summarizing, it is noted that similar results can be obtained by different settings of the (many) free input parameters inherent of a relatively simple 1D-model approach. Based on these results, the net longshore sand transport at Soulac is estimated to be of the order of 200,000 ± 50,000 m³/year landward of the LAT-line.

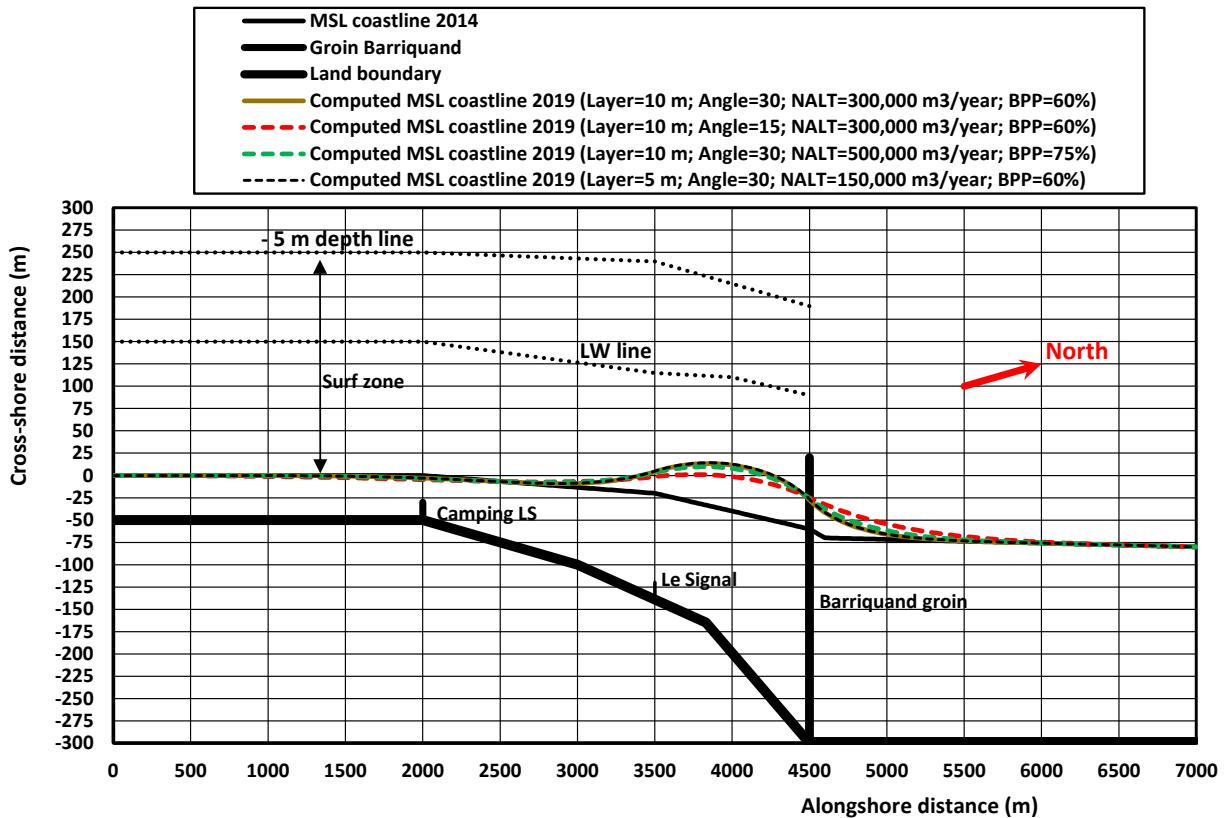


Figure 3.6.6 Computed coastline changes in region Soulac sur Mer 2014-2019; LONGMOR-model

PARAMETER	VALUES
Offshore significant wave height	1.5 m (100% of the time)
Offshore wave angle of main wave direction	15°; 30°
Peak wave period	8 s
Grid size and domain length	20 m; 4500 m
Time step and grid-‘smoothing’	0.01 day



Sand d_{50} , d_{90}	0.35; 1 mm
Slope beach-surf zone 0 tot -5 m MSL	1 to 50 (tan slope=0.02)
Breaker coefficient	0.7
Layer thickness of active zone	10 m (between -5 m and +5 m to MSL) 5 m (between LAT and HAT)
Longshore transport equation; Calibration coefficient K	Van Rijn 2014; K=variable
Net annual longshore transport (NALT) landward of LAT and bypassing percentage	NALT=200,00-300,000 m ³ /year; BPP=40%-60%
Net annual longshore transport (NALT) landward of -5 m depth and bypassing percentage	NALT=400,000 -600,000 m ³ /year; BPP=60%-75%
Angle of coast normal to North (from beach to sea)	285 to 305 degrees
Tidal currents in surf zone	$V_{flood}=0$ m/s; $V_{ebb}=0$ m/s (no effect if both values are equal)
Beach nourishment volume	based on Table 3.3.2
Input files	Soul1.inp (preliminary runs) Soul1d.inp (detailed calibration runs)

Table 3.6.9 *Input data of LONGMOR-model; Soulac sur Mer.*

Detailed calibration runs

The detailed coastlines (MSL, HAT, LAT, 5 m depth) of 2014, 2017 and 2020 supplied by the client are shown in **Figure 3.6.7**. The origin ($x=0$) is the groin north of L'Amélie. The model was calibrated by varying the K-coefficient of the longshore sand transport in the active layer of 5 m (between LAT and HAT). Detailed model runs have been made with and without local sand replacements (excavation and dumping of beach sand. The sand replacements were done by 7 trucks carrying 15 m³ of sand each working 6 hours a day (3 hours before and after low tide). Sand was extracted close to the Barriquand-groin and dumped near Camping LS. Production was 10,000 m³ per week and maximum 60,000 m³ over a period of 6 weeks in spring (March, April, May). In total, about 200,000 m³ of sand has been replaced between 2018 and 2021.

Figure 3.6.7 also shows hindcasted MSL-coastlines between 2014 and 2021 excluding and including local sand replacements based on the values from **Table 3.6.10**. Very reasonable agreement can be observed between the predicted MSL-coastline of September 2021 (including sand replacements) and measured MSL-coastline of May 2020.

Major erosion (about 300,000 m³ over 7 years with sand replacements) occurs in the section between L'Amélie and Camping LS, which is caused by the change of the coastline north of L'Amélie with respect to the coastline south of L'Amélie resulting in a significant increase of NALT.

Deposition of sand (about 600,000 m³ over 7 years without sand replacements) prevails between Le Signal and Barriquand-groin ($x=2200$ to $x=3700$ m). The deposition north of the Barriquand-groin is about 125,000 m³ over 7 years due to bypassing processes. The computed erosion volume in the section north of L'Amélie between $x=0$ and $x=2200$ m is about 300,000 m³ over 7 years. The net deposition volume between $x=0$ and $x=6000$ m is about $600,000+125,000-300,000=425,000$ m³ over 7 years or about 60,000 m³/year which is about equal to the difference (170,000-110,000 m³/year) in longshore sand transport between $x=0$ and $x=6000$ m (**Figure 3.6.8**).

The maximum predicted accretion including sand replacement is about 100 m at $x=3500$ m. The MSL line is far seaward of the tip of the groin at that location ($x=3500$ m). The replacement of sand from section 3300-3800 m to section 1150-2300 m in the period 2018 to 2021 mitigates the erosion around Camping LS.

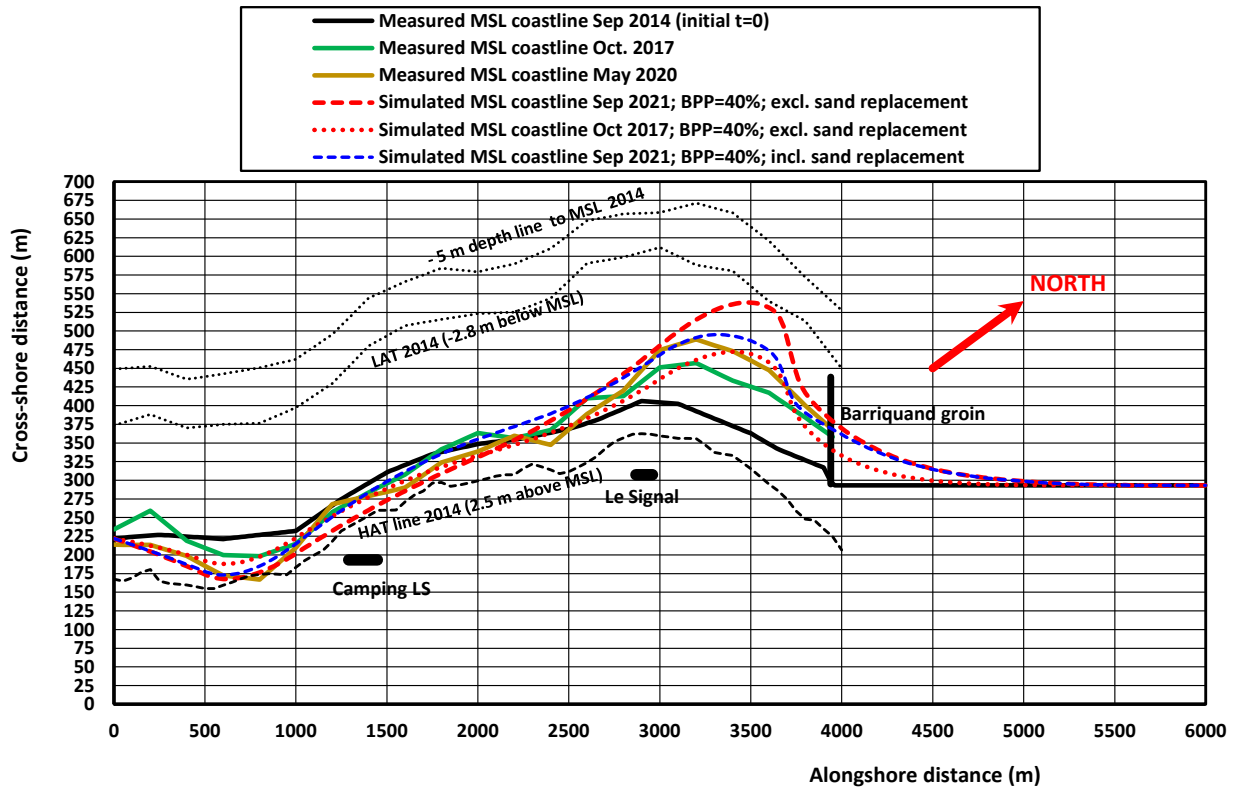


Figure 3.6.7 Computed coastline changes in region Soulac sur Mer 2014-2020; detailed calibration of LONGMOR-model

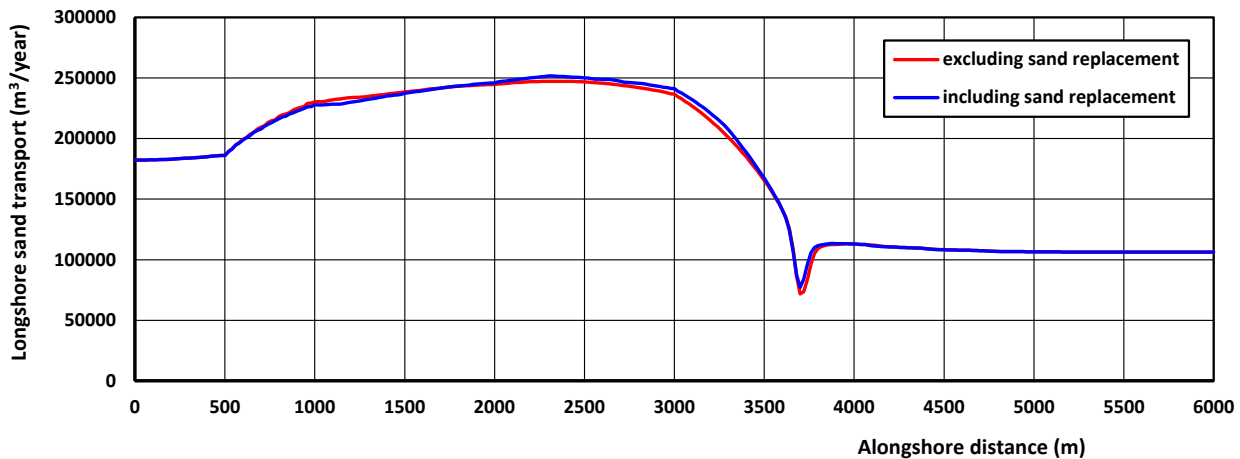


Figure 3.6.8 Computed longshore sand transport landward of the LAT-line; detailed calibration of LONGMOR-model

Figure 3.6.8 shows the net longshore sand transport (NALT) landward of the LAT-line and averaged over the period September 2014 to September 2021.

The NALT at the origin is about 170,000 m³/year which increases to 250,000 m³/year around Le Signal and decreases to 110,000 m³/year between Le Signal and Barriquand-groin (x=2500 to 4000 m). The bypassing longshore transport is about 110,000 m³/year, which is about 45% of the updrift value of 250,000 m³/year. The increase of NALT between x=0 and x=2200 m is caused by the change of the coastline north of L'Amélie with



respect to the coastline south of L'Amélie. The overall NALT-value over the length of the domain decreases by about 60,000 m³/year or a total net deposition volume about 420,000 m³ over 7 years.

Date	Volume (m ³)	Volume per unit length and time (m ³ /m/day)	Excavation location	Dumping location
October-November 2018 (60 days)	40,000	-1.33/0.83	x=3300-3800 m	x=1500-2300
	5,000	-0.17/0.55	x=3300-3800 m	x=2850-3000
April-May 2019 (60 days)	40,000	-1.33/0.83	x=3300-3800 m	x=1500-2300
May-June 2020 (60 days)	60,000	-2/0.87	x=3300-3800 m	x=1150-2300
April-May 2021 (60 days)	60,000	-2/0.87	x=3300-3800 m	x=1150-2300

Table 3.6.10 Excavation and dumping volumes of beach sand (- =extraction; +=dumping)

3.6.3 Design of groyne extension at Barriquand

Varions runs have been made for a longer groyne at Barriquand, see **Figure 3.6.9**.

Figure 3.6.10 shows the net longshore sand transport (NALT) landward of the LAT-line and averaged over the computation period.

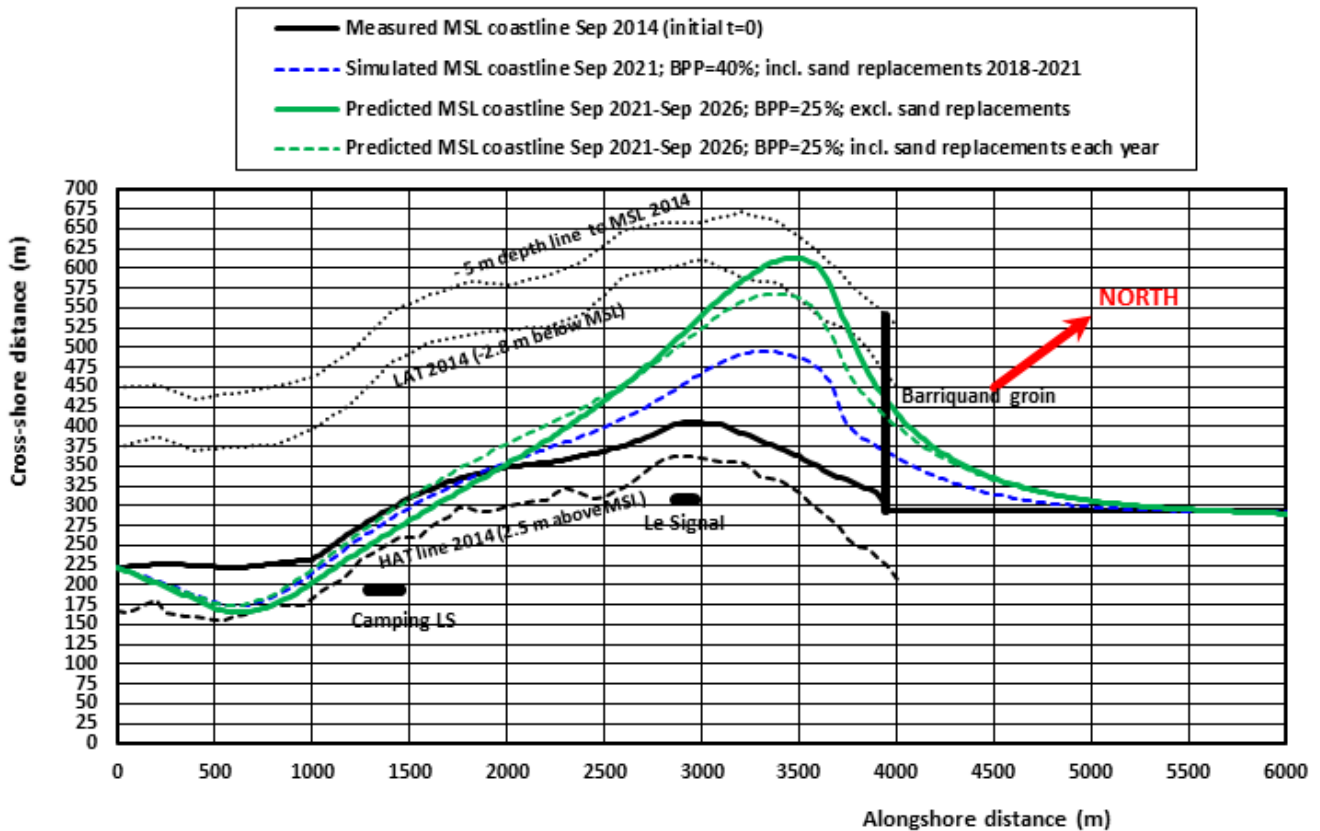


Figure 3.6.9 Computed coastline changes in region Soulac sur Mer 2014-2020; longer groyne

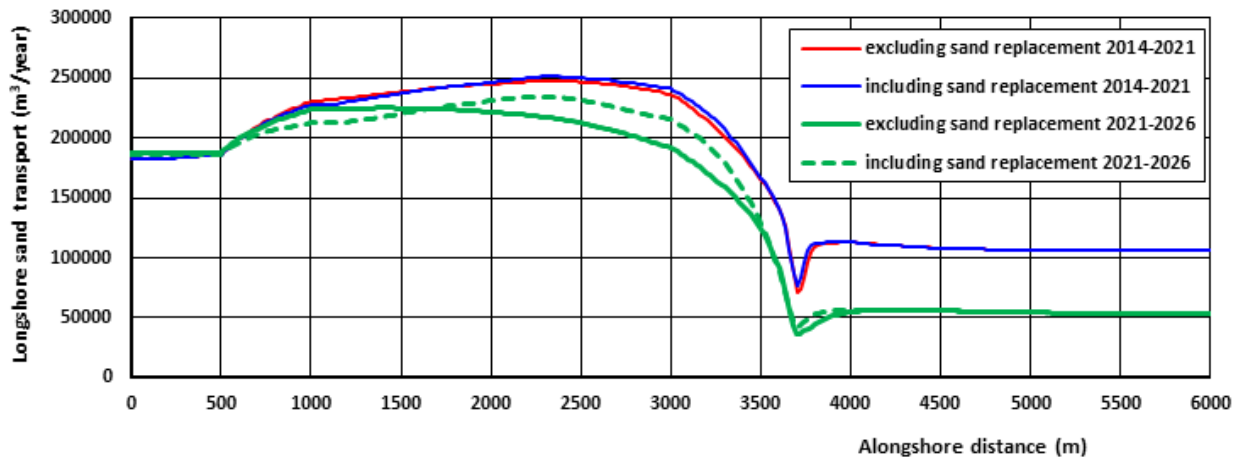


Figure 3.6.10 Computed longshore sand transport landward of the LAT-line; longer groyne

3.6.4 New groin at Boulevard Des Dunes

An alternative option (C) is a new groin at boulevard Des Dunes at about 2500 m from the origin. The detailed coastlines (MSL, HAT, LAT, 5 m depth) of 2014, 2017 and 2020 supplied by the client are shown in **Figure 3.6.11**. The origin ($x=0$) is the groin north of L'Amélie. The model was calibrated by varying the K-coefficient of the longshore sand transport in the active layer of 5 m (between LAT and HAT). The LONGMOR-model of LVRS Consultancy has been used to predict the coastline development between Camping LS and Barriquand-groin at Soulac-beach over a period of 10 to 15 years (2020-2035) without beach nourishment or sand replacements.

Three cases are considered, as follows:

- initial coastline May 2020; predicted coastline 2030
bypassing percentage Des Dunes-groin=85%;
bypassing percentage Barriquand groin=75%;
- initial coastline May 2020; predicted coastline 2030
bypassing percentage Des Dunes-groin=85%;
bypassing percentage Barriquand groin=90%;
- initial coastline May 2020; predicted coastline 2035
bypassing percentage Des Dunes-groin=70%;
bypassing percentage Barriquand groin=90%.

The input data and settings (based on calibration runs) are given in **Table 3.6.11**. The bypassing values are based on detailed computations of the Telemac-model system including the new groin and the Barriquand-groin.

PARAMETER	VALUES
-----------	--------



Offshore significant wave height	1.5 m (100% of the time)
Offshore wave angle of main wave direction	15°; 30°
Peak wave period	8 s
Grid size and domain length	20 m; 4500 m
Time step and grid-‘smoothing’	0.02 day; 0.005
Sand d_{50} , d_{90}	0.35; 1 mm
Slope beach-surf zone 0 tot -5 m MSL	1 to 50 (tan slope=0.02)
Breaker coefficient	0.7
Layer thickness of active zone	5 m (between LAT and HAT)
Longshore transport equation; Calibration coefficient K	Van Rijn 2014; K=variable
Net annual longshore transport (NALT) landward of LAT and bypassing percentage	NALT=200,00-300,000 m ³ /year; BPP at new DD-groin=70%-85%
Angle of coast normal to North (from beach to sea)	285 to 305 degrees
Tidal currents in surf zone	$V_{flood}=0$ m/s; $V_{ebb}=0$ m/s (no effect if both values are equal)
Beach nourishment volume	none
Input files	SoulDD1.inp

Table 3.6.11 *Input data of LONGMOR-model; Soulac sur Mer.*

Figure 3.6.11 shows predicted coastline for the three case of Option C.

Figure 3.6.12 shows the net longshore sand transport along the domain of 6 km. The total volume of sand trapped over the domain of 6000 m is 185,000-145,000= 40,000 m³ per year, or about 400,000 m³ over 10 years. This low trapping value is caused by the relatively high bypassing percentages

The results are, as follows:

- coastal accretion of about 300,000 m³ over 10 years southward of the new groin at Boulevard DD;
- erosion of sand of about 150,000 m³ over 10 years in the middle part between the new groin and the Barriquand-groin; accretion of about 150,000 m³ over 10 years at both ends of the compartment between the two groins; sand volume between groins is redistributed;
- coastal accretion of about 75,000 m³ over 10 years northward of the Barriquand-groin.

The accretion at south updrift side of new groin does not increase much in the period 2030 to 2035, because the coastline at the updrift side of the new groin becomes gradually normal to the incoming waves.

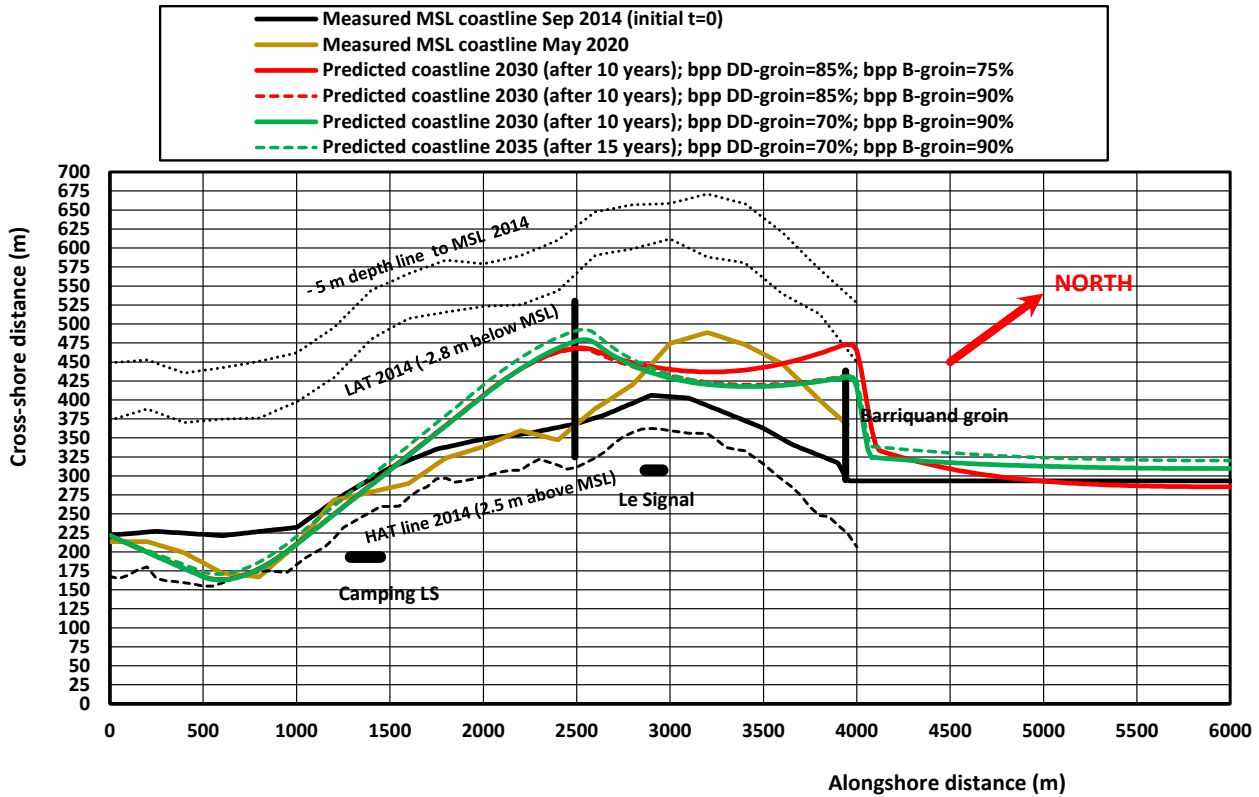


Figure 3.6.11 Predicted coastline development in period 2020-2035; Option C;
Net longshore sand transport at origin = 185,000 m³/year; LONGMOR-model (soulDD1.inp)

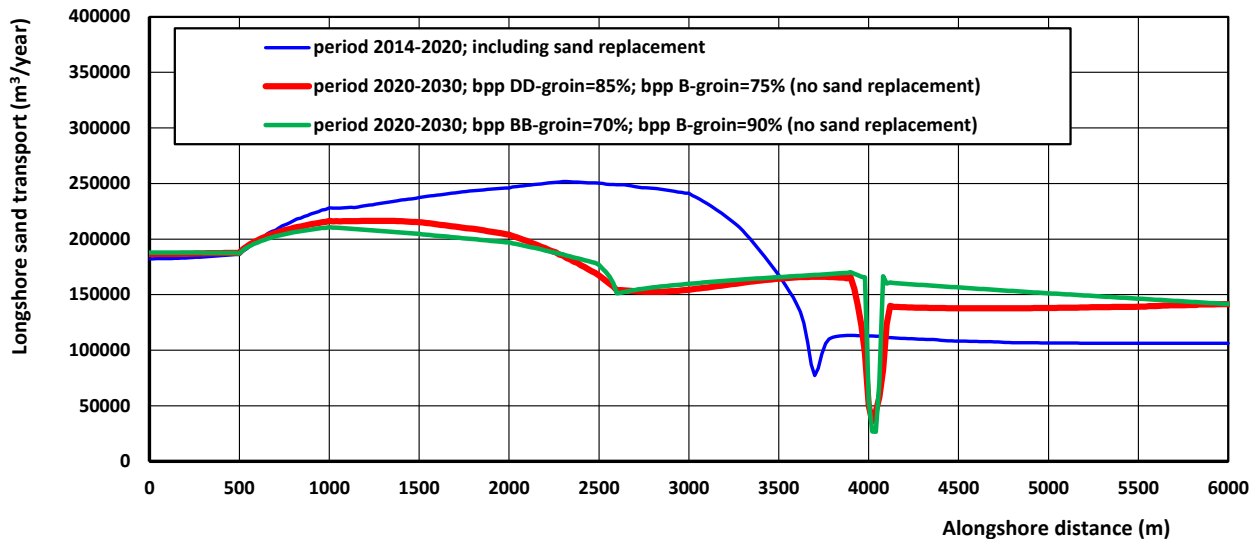


Figure 3.6.12 Computed annual-averaged longshore sand transport landward of the LAT-line; new dune



3.7 Design Abu Qir western bay type beach

The design of the Abu Qir land reclamation in Egypt includes the design of the Western beach, which is the focus of this report. Data are taken from the Report: Detailed Design Report Western Beach (5855-DI-ENG-RPT-000) prepared by Consultant Modimar, Italy (September-October 2025).

Coastline

The stability of the coastlines of the western beach is studied.

Initial coastlines are shown in **Figure 3.7.1**. The bathymetry inside the bay is shown in **Figure 3.7.2**.

Initial beach profiles are shown in **Figure 3.7.3**.

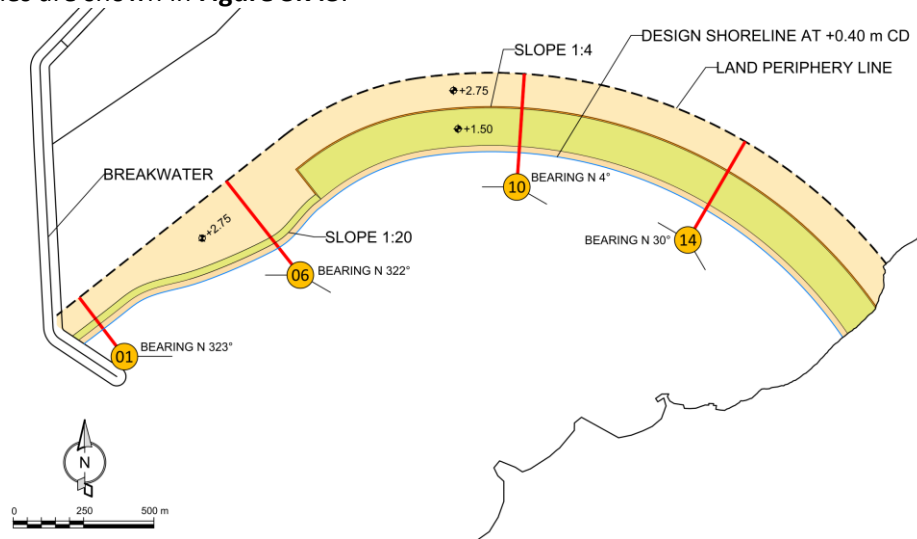


Figure 3.7.1 Coastline (initial)

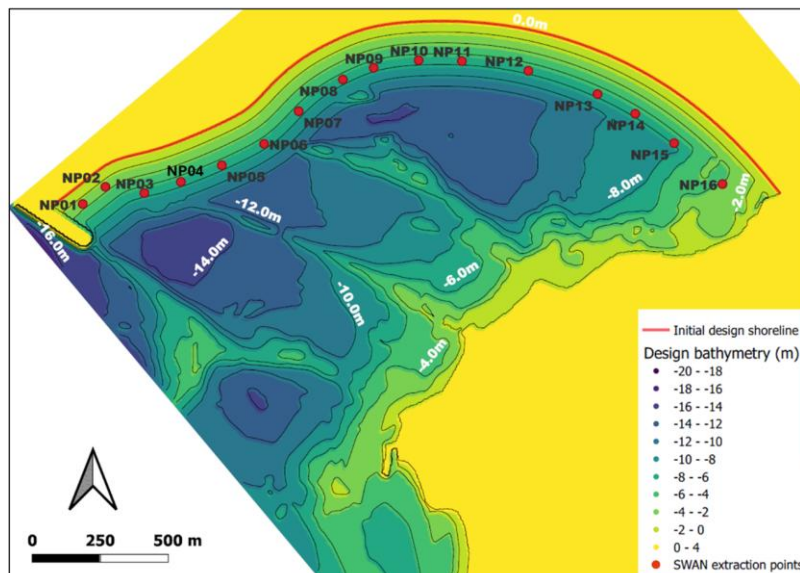


Figure 3.7.2 Bathymetry inside the bay

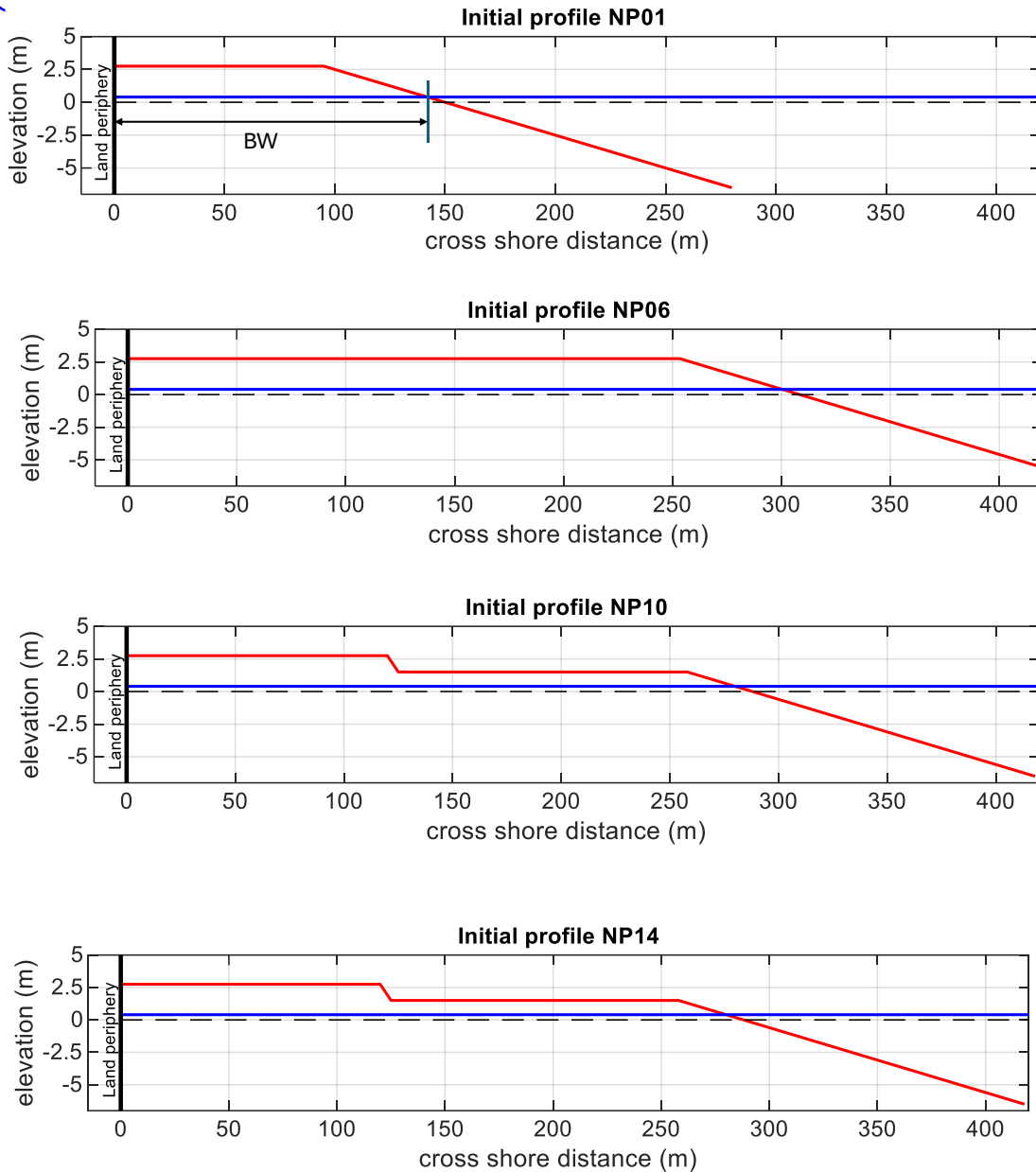


Figure 3.7.3 Initial beach profiles at four locations

Water levels

Chart datum is LAT (lowest Astronomical Tide). Mean sea level (MSL) is about 0.16 m above LAT and CD. HAT is about 0.14 m above MSL (0.3 m above LAT). Storm level is 0.6 to 1 m above MSL (extreme conditions).

Wave climate

Offshore wave data are available for the period 1979-2021.

The annual wave climate at point A (water depth of 35 m) is, as follows (Figure 3.7.4):

- waves are most frequent from NW: percentage of occurrence of 80%;
- waves < 0.5 m: percentage of about 25% (windless weather);
- Waves with $H_s > 0.5$ m and < 4 m from NW represent about 55%;
- Waves with $H_s > 4.0$ m, mostly from the north-west and west sectors during 0.5 % of the time;
- Wave height exceeded 12 hours per year $H_{s,12}$ is equal to 4.9 m;



- Most extreme storm in period 1979-2021 (about 40 years) occurred in December 2010: $H_s=6.14$ m, $T_p=12.5$ s, angle=280-320°; duration 96 hours (outside bay);
- Predicted storm wave height (point A) with return period of 10 years: $H_s=6$ m, $T_p=12$ s; angle=285°;
- Predicted storm wave height (point A) with return period of 100 years: $H_s=6.7$ m, $T_p=12.5$ s; angle=285°.

Waves from 300°+315°+330° at depth of 35 m (point A) are crudely represented together in **Table 3.7.1**.

H_s (m)	T_p (s)	Percentage of time (%)	Days
0.75	4	30	110
1.25	5	15	55
1.75	6	7	25
2.25	7	3	11
4.0	9	0.5	2
5.0	10	0.25	1
6.0	12	0.1	0.5

Table 3.7.1 Waves in point A at depth of 35 m outside bay area

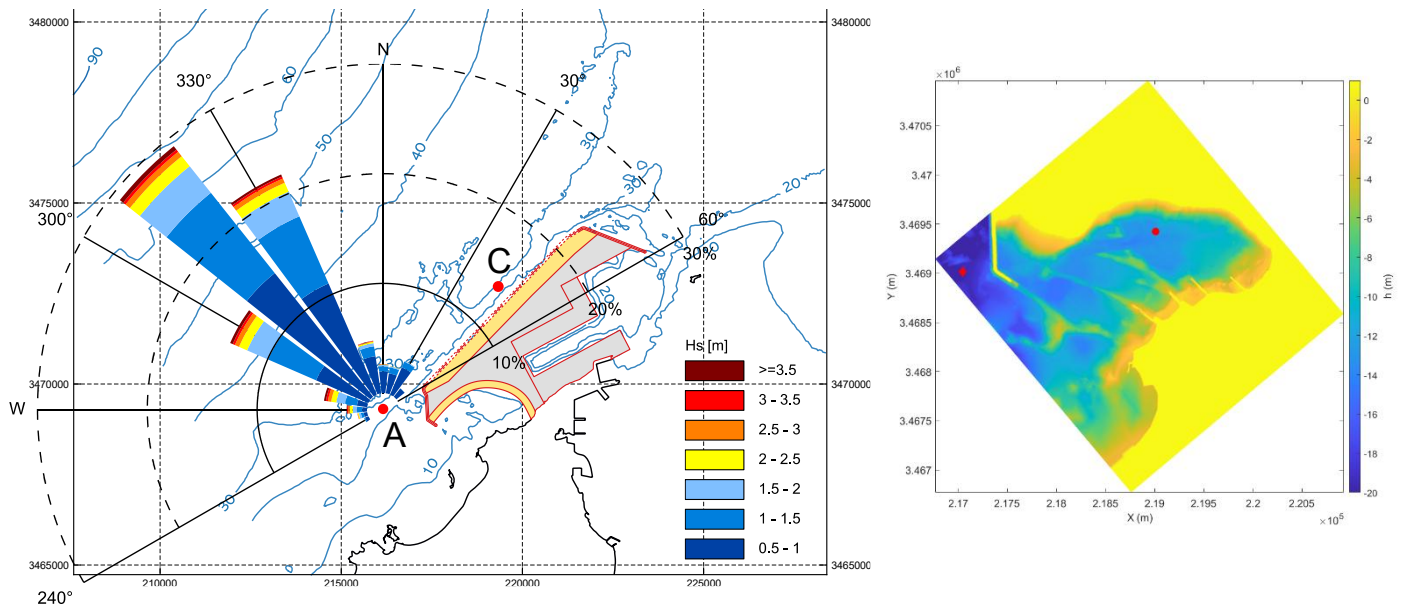


Figure 3.7.4 Wave rose in point A (west of breakwater; depth 35 m); wave bouys outside and inside bay

Measured wave data inside the bay are available from two wave bouys (period 1 January to 26 March 2025); one buoy at depth of -20 m just outside the bay and another buoy inside the bay at depth of -12 m (about 2 km from the outer buoy), see **Figure 3.7.4**. Analysis of the wave data shows $H_{s,inside} \cong 0.15 H_{s,outside}$. The most energetic event occurred in the period 5 to 7 February 2025 with $H_{s,max}=5.9$ m coming from 300° to 340°. Swan model results of the wave height are in reasonable agreement with the measured data at the location of the inside wave buoy.

Examples of wave computations of the SWAN-model are shown in **Figure 3.7.5**.

Circulation currents are most likely generated by differences in wave setup (breaking waves).

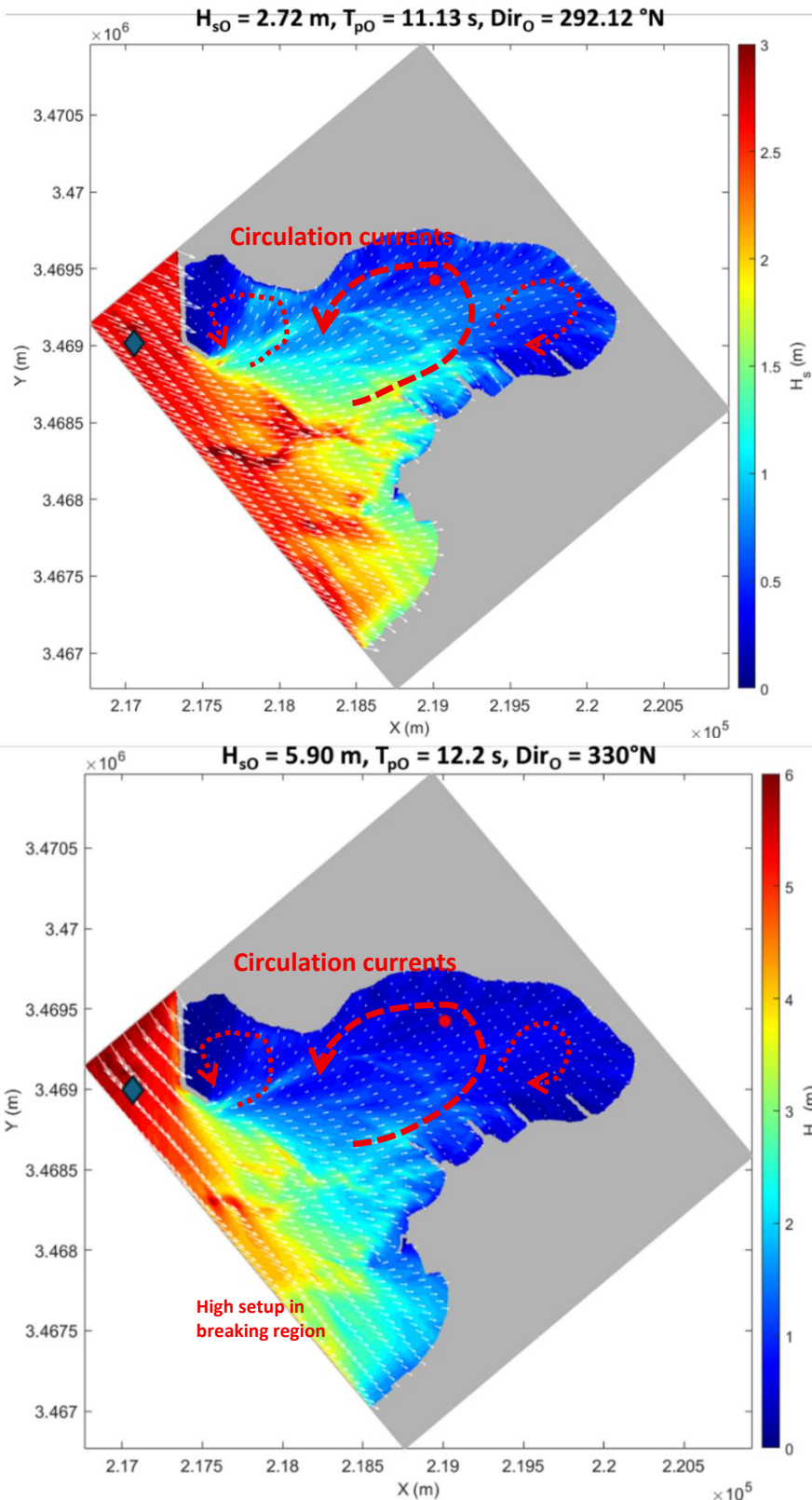
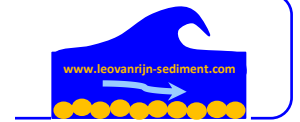


Figure 3.7.5 Examples of wave height and wave pattern computations based on SWAN-model
Wave roses based on the SWAN wave model results in the bay area are shown in **Figure 3.7.6**.
The wave data derived from the wave roses are given in **Table 3.7.2**.



Swan wave modelling results inside the bay at depth of -6.1 m due to a storm are also shown in **Table 3.7.2** (last column). The wave height at the bay entrance is $H_{s,0}=4.1$ m at depth of -12 m. The wave period is $T_p=14$ s. The water level is 0.62 m above CD. The highest wave height of $H_s=1.12$ m with incident angle of 247° to N (37° to shore normal) occurs in point NP14.

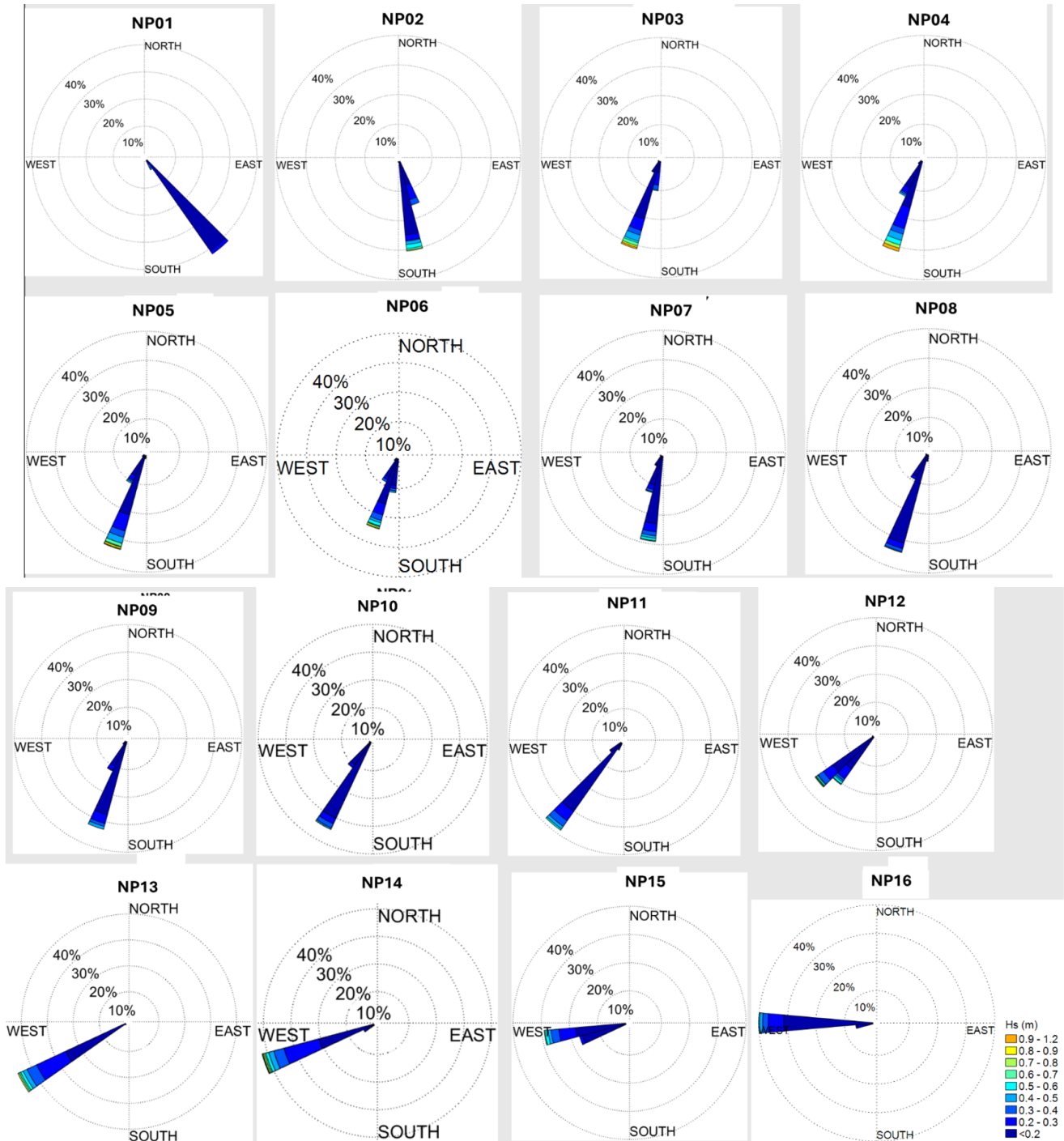


Figure 3.7.6 Wave roses based on SWAN model results



Location	Shore normal angle to N (°)	Wave incidence angle to N (°)	Wave angle to shore normal (°)	Wave angle to normal x-axis (°)	Wave height H _s (m)	Wave period T _p (s)	Duration (days)	Swan modelling results H _s (m) and wave incidence angle (°) to N
NP02	323	345	-22	+15	0.3	5	155	H _s =0.62; Angle=163
					0.6	6	11	
					1.0	7	0	
NP04	335	25	-50	-25	0.3	5	150	
					0.6	6	14	
					1.0	7	1	
NP06	322	25	-63	-25	0.3	5	150	0.86; 203
					0.6	6	15	
					1.0	7	1	
NP08	342	25	-43	-25	0.3	5	155	
					0.6	6	11	
					1.0	7	0	
NP10	4	30	-26	-30	0.3	5	155	0.79 227
					0.6	6	11	
					1.0	7	0	
NP12	20	50	-30	-50	0.3	5	155	
					0.6	6	11	
					1.0	7	0	
NP14	30	65	-35	-65	0.3	5	150	1.12; 247
					0.6	6	14	
					1.0	7	2	
					1.15	14	1	
NP16	40	90	-50	-90	0.3	5	155	
					0.6	6	11	
					1.0	7	0	

Table 3.7.2 Wave data inside bay based on SWAN-model results (derived from the wave roses of Figure 6)

Wave heights inside bay based on wave diffraction theory

The method of Kamphuis (1992) has been used to compute the K_d-factors in the diffraction zone, see Figure 3.7.7. The bay area is schematized as follows:

- the waves diffract around Point D (this part of the shore can be seen as a shore parallel structure);
- the incoming waves (from direction 315°) are almost perpendicular to the shore at point D;
- the K_d-factor =0.08 for line 80 making an angle of 80° to the normal line;
- the K_d-factor =0.24 for line 60 making an angle of 60° to the normal line.

Based on this, the wave height along the shore of the Bay area is set to (Table 3.7.3):

- section D-E: 15% of incoming wave height;
- section E-F: 25% of the incoming wave height;
- section F-G: 15% of the incoming wave height (shallow zone near main coast).

Incoming waves	Section D-E	Section E-F	Section F-G
----------------	-------------	-------------	-------------



			(Points NP01-NP10)		(NP10-NP14)		(NP14-NP16)	
H _s (m)	T _p (s)	Percentage of time (%)	H _s (m)	Angle to s.n. (°)	H _s (m)	Angle to s.n. (°)	H _s (m)	Angle to s.n. (°)
0.75	4	30 (110 days)	0.12	40	0.2	30	0.11	40
1.25	5	15 (55 days)	0.20	40	0.3	30	0.2	40
1.75	6	7 (25 days)	0.25	40	0.45	30	0.25	40
2.25	7	3 (10 days)	0.35	40	0.55	30	0.35	40
4.0	9	0.5 (2 days)	0.6	40	1.0	30	0.6	40
5.0	11	0.25 (1 day)	0.75	40	1.25	30	0.75	40
6.0	12	0.1 (0.5 day)	0.9	40	1.5	30	0.9	40

Table 3.7.3 Wave heights in diffraction zone in bay area (s.n.=shore normal; Sections in Figures 2 and 7)

Grain size

The beach fill will be made of well sorted medium-fine dredged sand with a $d_{10} \approx 0.10$ mm, $d_{50} \approx 0.22$ mm and $d_{90} = 0.73$ mm.

Computed net longshore sand transport (LONGMOR-modelling)

The computed net longshore sand transport values (LST) of the LONGMOR-model (Van Rijn, 2014) are given in **Table 3.7.4**.

The net LST-values are between 4,000 and 16,000 m³/year in clockwise direction.

Location	Net longshore sand transport (m ³ /year)	
	Wave climate based on SWAN-model	Wave climate based on diffraction theory
NP02	7,700	4,000
NP04	12,000	
NP06	7,800	
NP08	11,000	
NP10	9,800	16,000
NP12	10,5000	4,000
NP14	13,000	
NP16	11,400	

Table 3.7.4 Net longshore sand transport (LST) inside bay

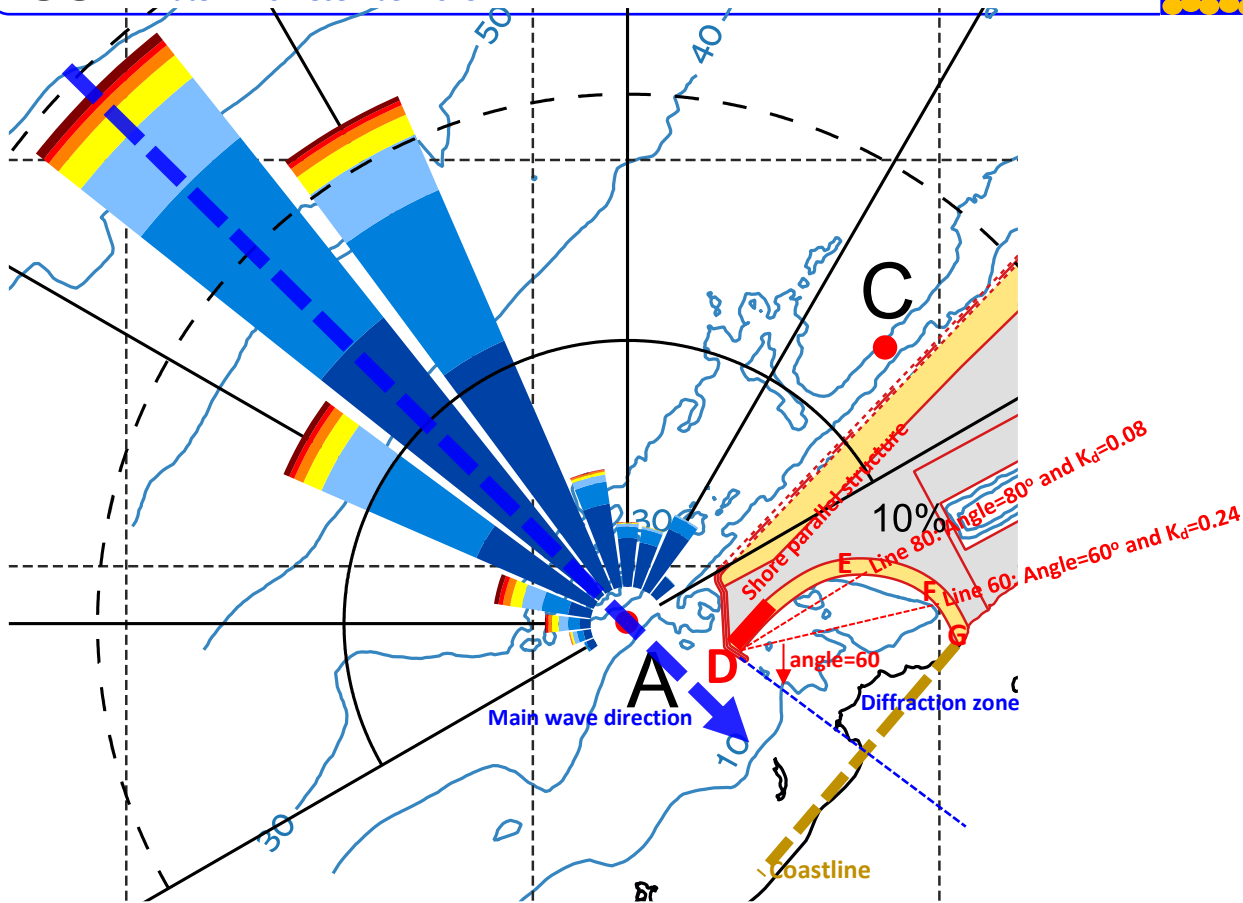


Figure 3.7.7 Computation of wave diffraction (method of Kamphuis) in bay area; annual conditions

Computed coastline changes by longshore processes (LONGMOR-modelling)

The 1D LONGMOR2025 coastline model (Tonnon et al., 2018; Van Rijn and Huisman, 2025) has been used to compute the coastline changes over 10 years (input file ABUW2n.inp). Using the input wave data, the net longshore sand transport (LST) is calibrated to give a maximum value of about 15,000 m³/year ($d_{50}=0.22$ mm), see Table 3.7.4. All wave input data are given in Table 3.7.5.

Longshore modelling results

Figure 3.7.8 shows the computed coastline after 10 years and the net LST (averaged over 10 years).

The maximum LST is about 14,000 m³/year in clockwise direction.

Recession occurs along the western section of the bay (see red circle) and accretion along the eastern section of the bay, where the coastline will tend to become normal to the incoming waves. Diffracted waves will smooth out the outcropping coastline (red circle) on the western side of the bay. The maximum coastline recession after 10 years is of the order of 55 m (NP06) at the western side of the bay. The maximum accretion after 10 years is about 40 m at the eastern side (NP14).

Based on the present results, the decadal maintenance is of the order of 100,000 m³ over 10 years.

It is noted that the accuracy of the predicted coastline in the western part of the bay is rather limited as the waves and associated transport processes are strongly affected by complex wave diffraction processes which are not very well known, particularly in the corner area of the breakwater. The present model settings are selected in such a way that sand accumulates in this area (curved beach segment).



General input parameters	Values
Beach sediment (d_{50}, d_{90} ; mm)	0.22; 0.73
Beach slope (-)	1 to 20
Breaking coefficient (-)	0.6
Thickness of active beach layer (m)	6
Grid size (m)	5
Time step (days)	0.01
Coastline smoothing parameter	0.0025
LST-equation	Van Rijn (2014)

Wave parameters	x-Locations along Western Bay					
	X=50 m NP02	X=475 m NP06	X=830 m NP08	X=1040m NP10	X=1500 m NP14	X=1725 m NP16
Water depth where wave parameters are given (m to CD)	-6	-6	-6	-6	-6	-6
Wave height H (m)	0.6	0.6	0.6	0.6	0.6	0.6
Wave period T (s)	6	6	6	6	6	6
Wave angle to x-axis θ (°)	10°	-25°	-25°	-30°	-65°	-90°
Duration (days per year)	365	365	365	365	365	365

Table 3.7.5 Input wave data of LONGMOR coastline model

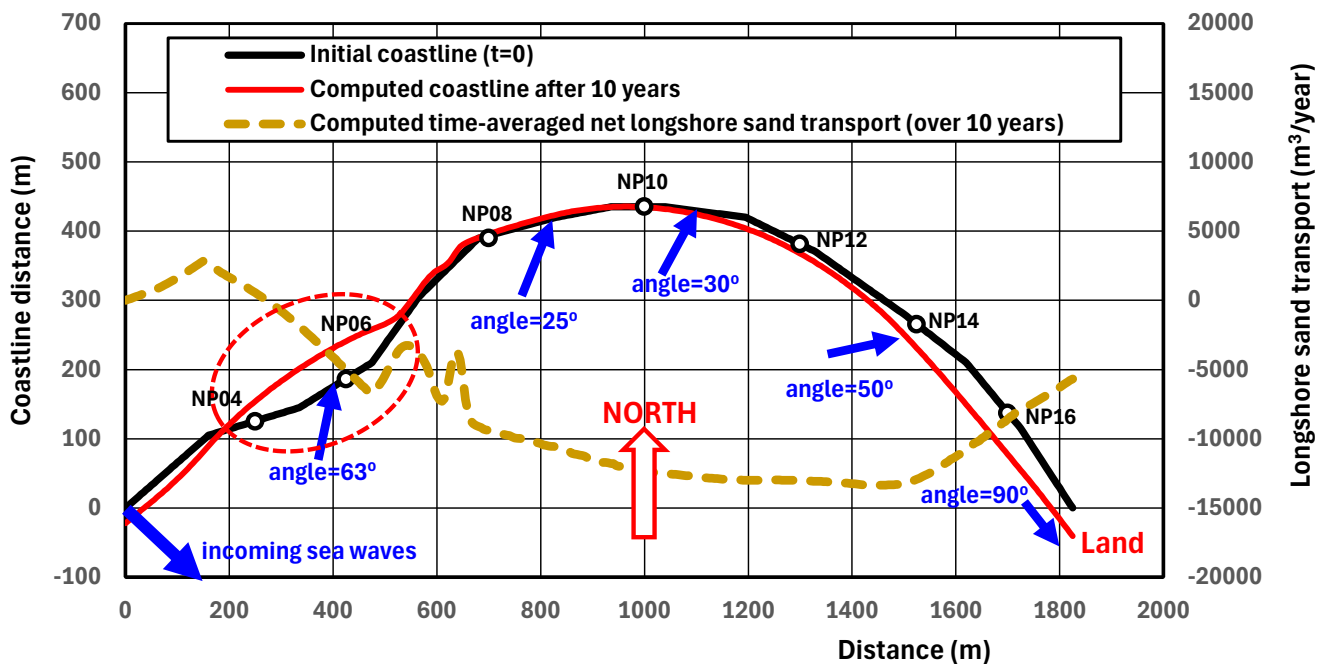


Figure 3.7.8 Computed coastline after 10 years and the net LST (averaged over 10 years)



4. References

- Kamphuis, J.W. 1991.** Alongshore sediment transport rate. *Journal of Waterway, Port, Coastal and Ocean Engineering*, Vol. 117, p. 624-640
- Kamphuis, J.W. 1992.** Short course on design and reliability of coastal structures. Chapter 9, Proc. 23rd ICCE, Venice, Italy.
- Shore Protection Manual, 1984.** CERC, Waterways Experiment Station, Vicksburg, USA
- Van Rijn, L.C., 1990, 2011.** Principles of fluid flow and surface waves in rivers, estuaries and coastal seas. www.leovanrijn-sediment.com.
- Van Rijn, L.C., 1993.** Principles of sediment transport in rivers, estuaries and coastal seas. www.leovanrijn-sediment.com.
- Van Rijn, L.C., 1998.** Principles of coastal morphology. www.leovanrijn-sediment.com.
- Van Rijn, L.C., 2002.** Longshore sand transport. Proc. 28th ICCE, Cardiff, U.K.
- Van Rijn, L.C., 2005, 2017.** Principles of sedimentation and erosion engineering in rivers, estuaries and coastal seas. www.leovanrijn-sediment.com
- Van Rijn, L.C., 2014.** A simple general expression for longshore transport of sand, gravel and shingle. *Coastal Engineering*, 90, 23-39
- Van Rijn, L.C., 2015.** Coastal erosion in lee zone of structure. www.leovanrijn-sediment.com